npj Biofilms and Microbiomes

https://doi.org/10.1038/s41522-026-00955-3

Article in Press

Cetobacterium somerae as a microbial correlate of improved muscle quality after intestinal microbiota transplantation in Yellow River carp (*Cyprinus carpio*)

Received: 17 November 2025

Accepted: 25 February 2026

Cite this article as: Cheng, L., Li, Y., Zhang, Y. *et al. Cetobacterium somerae* as a microbial correlate of improved muscle quality after intestinal microbiota transplantation in Yellow River carp (*Cyprinus carpio*). *npj Biofilms Microbiomes* (2026). https://doi.org/10.1038/s41522-026-00955-3

Lijiao Cheng, Yijie Li, Yujie Zhang, Chaobin Qin, Liping Yang, Xiao Yan & Guoxing Nie

Cetobacterium somerae as a microbial correlate of improved muscle quality after intestinal microbiota transplantation in Yellow River carp (*Cyprinus carpio*)

Lijiao Cheng [1], Yijie Li [1], Yujie Zhang [2], Chaobin Qin [1], Liping Yang [1], Xiao Yan [1], Guoxing Nie [*1]

1. College of Fisheries, Henan Normal University, No. 46 Jianshe Road, Xinxiang 453007, PR China

2. College of Life Sciences, Henan Normal University, No. 46 Jianshe Road, Xinxiang 453007, PR China

***Corresponding author**

***ORCID iD*:** 0000-0002-0758-9933 (https://orcid.org/0000-0002-0758-9933)

E-mail address: niegx@htu.cn (Guoxing Nie)

Mailing address: College of Fisheries, Henan Normal University, No. 46 Jianshe Road, Xinxiang 453007, PR China

Lijiao Cheng, chenglijiao@stu.htu.edu.cn

Yijie Li, liyijie200105@163.com

Yujie Zhang, zh2995206504@163.com

Chaobin Qin, qinchao88639501@163.com

Liping Yang, weedyung@163.com

Xiao Yan, yanxiaobangong@163.com

Abstract

Dietary faba bean enhances fish muscle quality but concurrently reduces growth performance. The gut microbiota critically modulates muscle growth and quality. However, the specific microbial taxa, metabolites and regulatory mechanisms responsible remain to be elucidated. This study established a differential gut microbiota model in faba-bean-fed Yellow River carp (*Cyprinus carpio*), used whole-intestinal microbiota transplantation (WIMT) to directly test its effect on muscle quality, and supplemented the key bacterium and its metabolite to confirm their contribution. After a 6-week faba bean diet, growth performance declined, whereas muscle texture improved ($P < 0.05$). This improvement was concomitant with a higher abundance of the genera *Aeromonas* and *Cetobacterium* in the gut. Following 8 weeks of daily WIMT from faba-bean-fed donors, Yellow River carp maintained normal growth performance ($P > 0.05$) and simultaneously showed improved muscle texture, characterized by more small-diameter fibers, lower fat content, and higher collagen levels ($P < 0.05$), recapitulating the donor's key muscle phenotype. Meanwhile, WIMT reshaped the gut microbiome composition and its metabolic profile, and the marker species *Cetobacterium somerae* and its metabolite acetic acid showed associations with improvements in muscle quality. Further *in vivo* validation indicated that *C. somerae* reduced fat deposition and improved muscle texture, an effect possibly linked to activation of the AMPK-PGC-1α-FoxO pathway, and its metabolite acetic acid mirrored these changes. This study reveals the direct impact of gut microbiota on muscle quality through WIMT in Yellow River carp, provides novel evidence of the fish gut-muscle axis, and offers a scientific basis for improving muscle quality.

Keywords Yellow River carp, Muscle quality, Gut-muscle axis, Whole-intestinal microbiota transplantation, Faba bean, *Cetobacterium somerae*

Introduction

The microorganisms present in the intestines are regarded as complex microecological systems within the body, maintaining a consistent symbiotic relationship with their host. In fish, the gut microbiota is highly diverse and fundamental to gut immunity, endocrine function, energy balance, nutritional status, and overall health maintenance[1]. Investigating the complex interplay between the gut microbiome and the fish's physiology is vital for enhancing fish health and refining aquaculture practices. Recognized as the largest metabolic organ in animals, skeletal muscle is crucial to maintaining overall health[2]. The pivotal role of gut microbiota in regulating host muscle health has been capturing increasing scientific attention in recent years. As the core mechanism for bidirectional communication between the gut microbiota and muscle, the "gut-muscle axis" has emerged as a focal point of current research[3, 4]. Despite the limitations of observational studies in directly establishing the causal relationship of the gut-muscle axis, fecal microbiota transplantation (FMT) and bacterial preparations can directly modulate the gut microbiota, thereby providing effective means to study the influence of microbiota on host organs[5]. FMT studies in mammalian mice provided direct evidence that the gut microbiota influences muscle performance and function[6, 7]. Additionally, trace elements and metabolites such as short-chain fatty acids (SCFAs) produced by intestinal microorganisms can reach muscle and modulate its growth, development, and metabolic functions[8]. Increasing evidence also suggests that gut microbiota may influence meat quality in poultry and livestock through the gut-muscle axis. For instance, oral transplantation of gut microbiota from Beijing high-quality meat chickens into commercial broilers

reportedly improved growth performance, reduced muscle drip loss and increased myofiber diameter[9]. Similarly, mice transplanted with intestinal microbiota from myostatin-deficient (*MSTN*$^{-/-}$) pigs exhibited selective hypertrophy of fast-twitch glycolytic myofibers, and this effect was mediated by the microbial metabolite valeric acid through activation of the Akt/mTOR pathway[10]. Overall, the findings indicate that the gut microbiota and its metabolites significantly contribute to muscle growth, function, and quality in animals.

In aquatic animals, fish in particular, muscle is the primary edible tissue whose growth, development, and metabolism govern energy homeostasis and overall growth performance, while also determining meat yield and muscle quality. For example, compared with low-yield rainbow trout (*Oncorhynchus mykiss*), the high-yield strain harbored a gut microbiota enriched in ketone body metabolism, pentose and glucuronate interconversions, and calcium signaling pathways, offering potential microbial markers for genetic selection[11]. Recirculating aquaculture-fasting strategy (RAS-F) elevated gut microbial diversity in bighead carp (*Aristichthys nobilis*), with key taxa (*Cetobacterium*, *Bacteroides*, and *Akkermansia*) boosting polyunsaturated fatty acids and umami amino acids, thereby improving fish quality[12]. In rice-fish symbiosis, rice flowering enhanced both the richness and variety of gut microbiota in tilapia (*Oreochromis niloticus*), which regulated amino acid and lipid metabolism through the gut microbiota-metabolism-muscle axis, improving tilapia's nutritional and muscle quality[13]. Similarly, common carp (*Cyprinus carpio*) in rice-fish symbiosis exhibited faster growth rates and improved nutritional composition and flavor, traits tightly associated with elevated intestinal SCFAs levels and mTOR pathway activation[14]. Dietary galacto-oligosaccharides or xylo-oligosaccharides improved the muscle texture of tilapia

by promoting myofiber development. This effect was linked to gut-microbiota-derived butyrate that modulated lipid metabolism[15]. Additionally, replacing 45% of dietary soybean meal with cottonseed protein concentrate increased the hardness of tilapia muscle and elevated intestinal butyrate, and *in vitro* assays confirmed butyrate's lipid-lowering effect[16]. A recent study on small yellow croaker (*Larimichthys polyactis*) demonstrated that direct dietary sodium acetate promoted muscle development via hyperplasia, characterized by reduced myofiber diameter and increased fiber number[17]. Independent work further revealed that valerate reduced myofiber size by suppressing myoblast proliferation and myotube differentiation via activation of the forkhead box O (FoxO) signaling pathway, thereby increasing the flesh hardness of tilapia[18]. In summary, the current research on aquatic animals indicates that gut microbiota and their SCFA metabolites play a significant role in promoting fish muscle growth and improving meat quality. Despite recent scientific interest, the role of gut microbiota in regulating muscle development and quality in aquatic animals remains an underexplored field. While the gut-muscle axis concept has emerged, robust evidence supporting its mechanisms is conspicuously absent. Current studies have largely stopped at identifying correlations rather than establishing causation, with insufficient experimental validation of how specific microbial communities or metabolites directly impact muscle development and quality characteristics.

The fine-grained muscle fibers of fish are easily digestible and rich in essential amino acids as well as polyunsaturated fatty acids[19]. These characteristics render fish a highly nutritious food source, widely acknowledged for its health benefits. With the increasing awareness of health among consumers, the quality of fish muscle has received greater attention and has consequently emerged

as a key determinant of its market value. In China's Yellow River Basin, the Yellow River carp (*Cyprinus carpio*) is a vital species for freshwater aquaculture. However, modern intensive farming practices have resulted in a decline in muscle quality, which is characterized by decreased firmness, a softer texture, and reduced mastication[20]. These changes have negatively impacted consumer experience and represent a significant bottleneck for the sustainable development of Yellow River carp. Feeding faba bean has recently emerged as a strategy to improve fish muscle firmness and texture quality, but it concurrently increases oxidative stress and compromises growth performance[20-22] while altering the intestinal microbiota[23, 24]. Related studies further demonstrated that a faba bean-supplemented diet altered the gut microbiota, influenced collagen deposition and myofibril reorganization, and significantly improved fish flesh texture[25]. Nevertheless, species-level shifts in the gut microbiota and the concomitant remodeling of its metabolites remain unclear, and causal evidence that core microbiota or their metabolites can drive meat-quality improvement is still lacking. Moreover, the underlying regulatory mechanisms remain to be elucidated. Therefore, to avoid the adverse effects of faba bean, it is imperative to elucidate the causal relationship between gut microbiota and muscle quality without faba bean and to develop microbiota-targeted nutritional strategies, thereby offering new insights for improving the muscle quality of Yellow River carp.

Previous studies revealed that traditional FMT selectively modified specific microbial populations due to differences in the source material and the transplantation process. In comparison, whole-intestinal microbiota transplantation (WIMT) more effectively restored the donor microbiota composition[26]. Study revealed that WIMT outperformed FMT in lessening the vulnerability of

dextran sulfate sodium (DSS)-induced germ-free (GF) mice to colitis[27]. Currently, no research exists in aquaculture directly utilizing WIMT to examine microbial regulation of muscle quality from the gut-muscle axis perspective. Based on the foregoing evidence, this study hypothesizes that: (1) Faba bean-based diet reshapes the gut microbiota and metabolite profile of Yellow River carp; (2) WIMT transmits the faba-bean-associated microbial and metabolite signatures and recapitulates the corresponding muscle-texture phenotype; (3) *Cetobacterium somerae* and its metabolite acetic acid are candidate factors potentially contributing to muscle-quality improvement in Yellow River carp. Therefore, this study established a divergent muscle-quality model in Yellow River carp by feeding either basal or faba-bean diets and subsequently compared the structural, functional, and metabolic profiles of the intestinal microbiota. WIMT was employed to screen for microorganisms and metabolites potentially associated with muscle phenotype, followed by *in vivo* supplementation with key strains and metabolites to validate their functionality. This study aims to elucidate the gut-muscle axis in fish and to provide a theoretical basis for microbiota-targeted enhancement of muscle quality in Yellow River carp.

Results

Faba bean feeding improved muscle quality and modified gut microbiota in Yellow River carp

Following a 6-week feeding trial (**Fig. 1A**), the FB group exhibited significantly reduced growth performance (lower final body weight and weight gain rate, WGR) and a markedly higher feed conversion ratio (FCR) than the CF group ($P < 0.05$; **Fig. 1B and 1C**; **Supplementary Table S1**).

Texture properties of raw and cooked muscle in the FB group exhibited markedly higher hardness, chewiness, cohesiveness, resilience, and gumminess ($P < 0.05$). Additionally, the shearing force of raw muscle and springiness of cooked muscle increased significantly ($P < 0.05$), while adhesiveness did not change significantly ($P > 0.05$). The findings indicated that 6 weeks of faba bean consumption significantly enhanced the muscle texture of Yellow River carp (**Fig. 1D**). The structure of muscle fibers is closely related to muscle texture. In the FB group, HE staining of Yellow River carp muscle showed that muscle fibers were loosely arranged, with a higher prevalence of small-sized fibers and larger inter-fiber spaces (**Fig. 1E**). Statistical analysis based on the minimum Feret diameter (MFD) showed a notably greater percentage of small-diameter fibers ($10 < MFD < 60$ μm), whereas the percentage of medium-diameter fibers ($60 \leq MFD < 120$ μm) decreased markedly relative to the CF group ($P < 0.05$). Additionally, the FB group exhibited significantly reduced muscle fiber density and proportion of total fiber area compared to the CF group ($P < 0.05$), which was likely associated with expansion of inter-fiber spacing and an increase in extracellular matrix (ECM) (**Fig. 1F**). Collagen content, which is closely associated with the characteristics of muscle texture, was assessed by measuring the total hydroxyproline (Hyp) content. The collagen content in the FB group was 1.88 times more than in the CF group ($P < 0.05$; **Fig. 1G**). Moreover, muscle composition analysis indicated that the FB group exhibited significantly lower crude fat and crude protein than the CF group ($P < 0.05$), whereas dry matter content showed no significant difference ($P > 0.05$; **Fig. 1H**).

To explore alterations in the gut microbiome of Yellow River carp after a faba bean diet, we performed 16S rRNA gene amplicon sequencing of intestinal contents. Raw sequence data were

deposited in the NCBI Sequence Read Archive (SRA) under BioProject ID PRJNA1311008. For the Alpha diversity indices, the FB group exhibited significantly lower species richness (chao1 and observed species) ($P < 0.05$; **Fig. 2A**). The Non-metric Multidimensional Scaling (NMDS) analysis showed a significant separation between CF and FB group sample points (**Fig. 2B**). The clustering heatmap indicated that the FB group exhibited high relatively abundances of *Aeromonas*, *ZOR0006*, *Cetobacterium*, and *Atopobium* (**Fig. 2C**). Correlation heatmap analysis revealed a positive association between *ZOR0006* and *Cetobacterium* with the total collagen content, as well as the hardness and chewiness of both raw and cooked muscle ($P < 0.05$; **Fig. 2D**), indicating a potential link to muscle quality traits.

Whole-intestine microbiota transplantation improves muscle quality while maintaining growth performance and oxidative balance in recipient Yellow River carp

Following the completion of the WIMT experiment (**Fig. 3A**), the growth performance was first assessed. The results showed the PCFB group had notably reduced growth compared to the CG group ($P < 0.05$), while the WIMT group maintained normal growth levels ($P > 0.05$; **Fig. 3C and 3D**; **Supplementary Table S2**). Serum biochemical indicators are essential in evaluating fish health. Compared with the CG group, the PCFB group exhibited significantly lower serum Alb, TG, HDL-C and LDL-C levels and markedly higher AST/GOT and ALT/GPT activities ($P < 0.05$). Notably, the WIMT group showed significant reductions only in TG and LDL-C ($P < 0.05$), whereas the remaining parameters did not differ significantly ($P > 0.05$; **Supplementary Fig. S1**). Serum antioxidant assays revealed that the PCFB group exhibited a lower GSH/GSSG ratio and

T-SOD activity, together with higher GSH-Px activity, H_2O_2 and MDA levels, than the CG group ($P < 0.05$), whereas the WIMT group showed elevated T-AOC ($P < 0.05$) without significant changes in any other parameter ($P > 0.05$; **Fig. 3E**). Muscle enzyme assays revealed a trend similar to that in serum, with T-AOC significantly lower in the PCFB group ($P < 0.05$). In contrast, the WIMT group exhibited marked increases in both GSH/GSSG ratio and T-SOD activity ($P < 0.05$; **Fig. 3F**). Further muscle gene-expression analyses showed that, relative to the CG group, PCFB group exhibited significantly lower superoxide dismutase (*sod*) and catalase (*cat*) gene mRNA levels, whereas glutathione peroxidase 1 (*gpx1*) and nuclear factor-erythroid 2-related factor 2 (*nrf2*) expression was up-regulated ($P < 0.05$). In the WIMT group, only *sod* gene expression was elevated ($P < 0.05$), with no significant changes in the other examined genes ($P > 0.05$; **Fig. 3G**). The muscle texture analysis revealed that, in both the WIMT and PCFB groups, the hardness, chewiness, gumminess, and shearing force of both raw and cooked meat, as well as the springiness of cooked meat, were significantly increased ($P < 0.05$; **Fig. 3H**). Overall, these data indicated that WIMT enhanced muscle texture and maintained growth performance and oxidative balance in Yellow River carp.

Which phenotypic indicators contribute to the enhancement of muscle texture characteristics? Masson staining of muscle tissue sections showed that, compared to the CG group, the WIMT and PCFB groups displayed largely comparable muscle fiber traits, characterized by loosely arranged muscle fibers and an increase in collagen fibers (stained blue) (**Fig. 4A**). Additional statistical examination showed that within the WIMT and PCFB groups, there was a notable rise in the percentage of small-diameter muscle fibers ($10 < MFD < 60$ μm), while the share of large-diameter

muscle fibers (120 ≤ MFD < 180 μm), mean MFD, and muscle fiber area percentage all significantly decreased ($P < 0.05$). However, no significant variation was detected in muscle fiber density ($P > 0.05$; **Fig. 4B**). Analysis of collagen content revealed that, in comparison with the CG group, both total collagen and insoluble collagen were markedly elevated in the WIMT and PCFB groups, while collagen solubility declined noticeably. Additionally, the PCFB group demonstrated markedly higher soluble collagen levels ($P < 0.05$; **Fig. 4C**). Muscle composition analysis revealed that, compared with the CG group, the WIMT group showed no noteworthy variation in dry matter or crude protein levels ($P > 0.05$). However, there was a marked drop in crude fat content ($P < 0.05$; **Fig. 4D**). To further explore the potential mechanisms by which WIMT enhances muscle quality, RNA sequencing (RNA-seq) analysis was used to examine the gene expression profiles in the muscles of Yellow River carp. Raw sequence data were deposited in the NCBI SRA under BioProject ID PRJNA1344608. Compared to the CG group, the PCFB group exhibited downregulated 2059 genes and upregulated of 2459 genes (**Fig. 4E**). In contrast, the WIMT group showed downregulation of 132 genes and upregulation of 289 genes (**Fig. 4F**). KEGG pathway analysis of the differentially expressed genes (DEGs) showed that, within the PCFB group, the most prominently enriched pathways were those related to cytoskeleton, motility and cell adhesion, included motor proteins, ECM-receptor interaction, tight junction, and adherens junction (**Fig. 4G**). In the WIMT group, oxidative phosphorylation and the citrate cycle (TCA cycle), core mitochondrial energy pathways, were most enriched, along with the nuclear energy regulator PPAR signaling (**Fig. 4H**). In both comparisons (PCFB vs CG and WIMT vs CG), the mitophagy-animal and adipocytokine signaling pathways central to energy sensing and mitochondrial quality

control were consistently enriched (**Supplementary Table S3**). Further quantitative PCR validation showed that, compared with the CG group, the expression levels of key autophagy-related genes microtubule-associated protein 1 light chain 3 type Ⅱ (*map1lc3b*) and autophagy related 16 (*atg16*), along with the lipid-metabolic genes adipose triglyceride lipase (*atgl*), carnitine palmitoyltransferase 1 (*cpt1*) and peroxisome proliferator-activated receptor alpha (*pparα*), were significantly up-regulated in both the PCFB and WIMT groups ($P < 0.05$; **Fig. 4I**). More importantly, the expression levels of 5'-AMP-activated protein kinase catalytic subunit alpha-1 (*ampkα1*), 5'-AMP-activated protein kinase catalytic subunit alpha-2 (*ampkα2*), peroxisome proliferator-activated receptor gamma coactivator 1-alpha (*pgc-1α*) and forkhead box O3 (*foxo3*), core genes for energy homeostasis and mitochondrial quality control, were all significantly increased ($P < 0.05$; **Fig. 4J**). Collectively, WIMT reduced the fibre area percentage and crude fat content, raised the proportion of small-diameter muscle fibres, elevated collagen content, and up-regulated AMPK-PGC-1*α*-FoxO-related gene expression, while also enriching the mitophagy-animal and adipocytokine signalling pathways.

Whole-intestine microbiota transplantation has no significant adverse effects on gut health in recipient Yellow River carp

Intestinal health and structural integrity contribute to the healthy growth of muscles in Yellow River carp. The total intestinal length measurements revealed that the PCFB group exhibited the shortest intestines ($P < 0.05$), whereas the WIMT and CG groups showed no statistically significant difference ($P > 0.05$; **Fig. 5A and 5C**). Further HE staining revealed that, relative to the CG group,

the PCFB group had shorter and sparser intestinal villus and a thinner muscular layer ($P < 0.05$). In contrast, the WIMT group displayed no significant alterations ($P > 0.05$; **Fig. 5B and 5D**). Detection of LPS revealed that intestinal LPS levels were significantly elevated in both the PCFB and WIMT groups compared to the CG group. However, serum LPS was markedly increased only in the PCFB group ($P < 0.05$), with no statistically significant difference observed between the WIMT and CG groups ($P > 0.05$; **Fig. 5E**). Analysis of intestinal immunity and barrier-related genes revealed that the PCFB group exhibited significant upregulation of pro-inflammatory factors tumor necrosis factor-α (*tnf-α*), interleukin-1β (*il-1β*), interleukin-6 (*il-6*), interleukin-8 (*il-8*), and nuclear factor-κB (*nf-κb*) relative to the CG group, while anti-inflammatory factors interleukin-10 (*il-10*), transforming growth factor-β (*tgf-β*) and barrier genes claudin (*cldn*), occludin (*ocln*), zonula occludens-1 (*zo-1*), and lysozyme (*lyz*) showed significant downregulation ($P < 0.05$). Conversely, the WIMT group exhibited significant downregulation of *li-6* gene expression ($P < 0.05$), with no significant changes in the expression of other immune-related genes ($P > 0.05$). Additionally, barrier function genes (*cldn*, *ocln*, and *zo-1*) were significantly upregulated ($P < 0.05$; **Fig. 5F**). In summary, the findings revealed that the PCFB group exhibited compromised intestinal structural integrity and impaired barrier function. In contrast, WIMT not only failed to compromise intestinal structural integrity but also appeared to enhance barrier function.

Antibiotic pretreatment reduces background intestinal microbiota diversity in recipient Yellow River carp

To enhance WIMT efficiency, a short-term mixed broad-spectrum antibiotic pretreatment was administered between week 4 (before antibiotic treatment, BA group) and week 6 (after antibiotic

treatment, AA group) of the feeding period. Raw 16S rRNA amplicon sequences are available in the NCBI SRA database under BioProject ID PRJNA1310288. As shown in **Fig. 6A**, antibiotic treatment markedly decreased gut microbiota α-diversity, as evidenced by the notable decline in the shannon, chao1, and observed_species indices ($P < 0.05$). The results of the clustering analysis at the phylum level indicated that the BA group and the AA group formed distinct branches (**Fig. 6B**). After antibiotic treatment, *Proteobacteria* and *Cyanobacteria* exhibited a marked rise in relative abundance, whereas the relative abundance of *Actinobacteria*, *Chloroflexi* and *Firmicutes* significantly decreased ($P < 0.05$; **Fig. 6C**). Overall, antibiotic treatment resulted in a significant decline in species richness and evenness within the gut microbial community, while also inducing notable changes in its structural composition. Subsequent measurements of serum biochemical indicators revealed that the AA group had significantly higher AST/GOT and ALT/GPT levels compared to the BA group ($P < 0.05$), while other measures remained unchanged ($P > 0.05$; **Fig. 6D**), suggesting potential liver function impairment in Yellow River carp following short-term antibiotic treatment.

Whole-intestinal microbiota transplantation significantly increases the abundance of the core intestinal bacterium *Cetobacterium somerae*

Raw 16S rRNA amplicon sequences are available in the NCBI SRA database under BioProject ID PRJNA1310847. After completing the 8-week WIMT, the analysis of gut microbiota alpha-diversity demonstrated that the PCFB group had notably lower shannon, chao1, and observed species indices than the CG group ($P < 0.05$), while the WIMT group did not display any

significant differences ($P > 0.05$). Furthermore, the PCFB group had a relatively lower simpson index and a higher good's coverage index ($P > 0.05$; **Fig. 7A**). The NMDS analysis revealed that the PCFB and WIMT groups were more similar to each other and distinctly separated from the CG group. This suggested that the microbial community structures of the PCFB and WIMT groups were somewhat similar, while both differed greatly from that of the CG group (**Fig. 7B**). The analysis of species composition at the phylum level revealed that *Pseudomonadota*, *Fusobacteriota*, *Bacillota*, and *Actinomycetota* were the dominant phyla in each experimental group (abundance > 10%). Relative to the CG group, the PCFB and WIMT groups showed a marked rise in *Fusobacteriota* abundance. Moreover, the PCFB group showed a notable increase in *Bacillota* relative abundance. Conversely, the relative abundance of *Pseudomonadota*, *Actinomycetota*, *Cyanobacteriota*, *Bacteroidota*, *Thermodesulfobacteriota*, *Verrucomicrobiota*, *Kiritimatiellota*, *Campylobacterota* and *Acidobacteriota* were significantly reduced ($P < 0.05$; **Fig. 7C**; **Supplementary Table S4**). At the genus level, the PCFB and WIMT groups exhibited a significant increase in the relative abundance of *Cetobacterium* and *Kluyvera*, whereas *Photobacterium*, *Actinoplanes*, *Desulfovibrio*, *Pseudomonas*, *Xenorhabdus*, *Aphanocapsa*, and *Burkholderia* exhibited a significant decline. Concurrently, the WIMT group also showed a significant elevation in *Shewanella*, *Kluyvera*, and *Streptococcus*. ($P < 0.05$; **Fig. 7D**; **Supplementary Table S5**). The species composition heatmap and significant difference analysis further revealed notable variations at the species level. The results revealed a significant increase in LPS-producing *Citrobacter freundii* in the PCFB group, alongside a marked rise in *C. somerae* and a concurrent decline in *Desulfovibrio* sp. UIV in both the PCFB and WIMT groups ($P < 0.05$;

Fig. 7E). Further random forest analysis results once again confirmed that *C. somerae* is a potential biomarker species for the PCFB and WIMT groups (**Fig. 7F**).

Whole-intestine microbiota transplantation reshapes the microbial function in recipient Yellow River carp

Functional prediction analysis is essential for revealing microbial functions associated with muscle quality. The PCA results showed distinct separation between the PCFB and WIMT samples and those of the CG group along the PC1 axis, suggesting significant differences in their metabolic pathway profiles. This finding indicated that WIMT significantly influenced the gut microbiota function of Yellow River carp, shifting its metabolic profile toward that of the donor (PCFB group) microbiota (**Fig. 8A**). The Bugbase functional prediction analysis revealed that the phenotype of the CG group predominantly comprised aerobic and facultatively anaerobic, gram-positive bacteria, which exhibited lower potential pathogenicity and stress tolerance. In contrast, the PCFB and WIMT groups were primarily composed of anaerobic, Gram-negative bacteria, which demonstrated greater stress tolerance and a stronger ability to form biofilms. Additionally, the PCFB group displayed a higher prevalence of mobile elements and an increased potential for pathogenicity (**Fig. 8B**). To comprehensively understand the functional changes within microbial communities and the interactions between hosts and microbes, differential analysis of metabolic pathways in the gut microbiota was conducted across different experimental groups. The annotation results based on the MetaCyc database indicated that the Biosynthesis, and Generation of precursor metabolite and energy (Level 1) were the most significant differential metabolic

pathways in the gut microbiota. In both the PCFB vs CG and WIMT vs CG comparison groups, there was a pronounced enrichment in pathways associated with Fatty acid and lipid biosynthesis (PWY-5667, PWY0-1319), Nucleoside and nucleotide biosynthesis (PWY-7229, PWY-5686), Amino acid biosynthesis (PWY-5104, PWY-5103, PWY-2942, BRANCHED-CHAIN-AA-SYN-PWY), Carbohydrate biosynthesis (CALVIN-PWY), and the Pentose phosphate pathways (NONOXIPENT-PWY). These pathways could significantly regulate host metabolism and muscle quality (**Fig. 8C**; **Supplementary Table S6**). Further analysis based on the KEGG database indicated that in both comparison groups, the function of Cell motility (Bacterial chemotaxis, ko02030) was significantly reduced. In contrast, several pathways were significantly enriched, including Metabolism of other amino acids (ko00471, ko00473), Carbohydrate metabolism (ko00030, ko00660), Glycan biosynthesis and metabolism (ko00550), Metabolism of cofactors and vitamins (ko00780), Biosynthesis of other secondary metabolites (ko00521), among others. Additionally, the Lipopolysaccharide biosynthesis pathway (ko00540) was significantly enriched in the PCFB group (**Fig. 8D**; **Supplementary Table S7**). In summary, WIMT reshaped the gut microbiota function of the recipient Yellow River carp. This finding not only underscored the essential role that gut microbiota play in maintaining overall health but also provided insights into the potential mechanisms through which these microorganisms influence muscle physiological functions in Yellow River carp.

Whole-intestinal microbiota transplantation significantly altered the metabolite profile of the gut microbiota in recipient Yellow River carp

Analyzing the changes in gut microbiota metabolites following WIMT provides critical insights into the mechanisms of microbe-host interaction. The raw data from the targeted metabolomics analysis of SCFAs in this study were deposited in the OMIX database of the National Genomics Data Center (NGDC), with OMIX IDs OMIX012256 (intestinal contents) and OMIX012255 (culture supernatant of *C. somerae* CFH_001, CS-CS). As shown in **Fig. 9A**, acetic acid was the predominant SCFA detected in the intestinal contents. Moreover, the PCFB and WIMT groups exhibited notably higher levels of acetic acid than the CG group, and the WIMT group showed significant increases in butyric acid and valeric acid levels ($P < 0.05$). Considering the potential link between these changes in SCFAs levels and *C. somerae*, the SCFAs content in the CS-CS was further analyzed. Results indicated that acetic acid had the highest concentration (24.32 ± 1.05 mg/g), followed by propionic acid (0.68 ± 0.03 mg/g) and butyric acid (0.32 ± 0.01 mg/g). These findings suggested that *C. somerae* CFH_001 produced these metabolites during its growth (**Fig. 9B**). To further clarify the shifts in gut microbiota metabolites after WIMT, LC-MS non-targeted metabolomics analyzed metabolites in the intestinal contents of the WIMT and CG groups. The raw data were deposited in the MetaboLights database with the identifier MTBLS13128. Results showed that 707 metabolites were detected in positive ion mode (**Fig. 9C**) and 344 metabolites in negative ion mode (**Fig. 9D**), with lipids, lipid-like molecules, organic acids and their derivatives identified as the predominant categories. The volcano plots revealed that, compared with the CG group, the WIMT group exhibited 174 differentially regulated metabolites in positive ion mode (79 upregulated and 95 downregulated) (**Fig. 9E**) and 68 in negative ion mode (32 upregulated and 36 downregulated) (**Fig. 9F**). PCA analysis showed that the CG and WIMT groups were

distinctly separated along the PC1 axis in both ion modes, which indicated that significant alterations occurred in the gut microbiota metabolite profile following WIMT (**Fig. 9G and 9H**). Further analysis of the 10 most increased differential metabolites in both ion modes revealed that amino acids and their derivatives were the most diverse and significantly more abundant in the WIMT group (including L-Pyroglutamic acid, D-(-)-Glutamine, DL-Glutamine, 2-Methylglutaric acid, L-Glutathione oxidized, among others). The relative abundances of polyphenolic compounds, sugars and their derivatives, and other metabolites was also markedly elevated (**Fig. 9I and 9J**). Metabolites from gut microbiota influence host physiology by regulating diverse metabolic pathways. Further KEGG functional enrichment analysis revealed the impact of gut microbiota on the metabolic activities of Yellow River carp following WIMT. The WIMT group exhibited notable enhancement of various metabolic pathways in the positive ion mode, including pyrimidine metabolism, glutathione metabolism, biosynthesis and metabolism of amino acids (**Fig. 9K**). Under negative ion mode, pathways such as cysteine and methionine metabolism, ABC transporters, phenylalanine, tyrosine, and tryptophan biosynthesis were also significantly enriched (**Fig. 9L**). In summary, the results demonstrated that following WIMT, the gut microbiota metabolite profile underwent significant changes. Specifically, the levels of SCFAs (such as acetic acid), amino acids and their derivatives, among others, were significantly increased, and metabolic pathways related to amino acids, material transport, and carbohydrate metabolism were notably enriched.

Supplementing with *Cetobacterium somerae* CFH_001 and sodium acetate significantly

improved muscle texture in Yellow River carp

Subsequently, the regulatory effects of supplemented *C. somerae* and its most divergent metabolic product acetic acid on the muscle texture of Yellow River carp were systematically validated. To mimic the intestinal inflammation caused by feeding faba beans, an LPS induced inflammatory stress model was employed to further assess the capability of *C. somerae* to maintain muscle quality under inflammatory conditions. Core indices including muscle proximate composition, collagen content, and textural properties were the primary focus of the study. Following an 8-week feeding trial (**Fig. 10A**), under normal conditions, muscle proximate composition showed that, relative to the CG group, the CS and SA groups had comparable dry matter ($P > 0.05$), lower crude fat, and higher crude protein and total collagen ($P < 0.05$). Under inflammatory conditions, dry matter was elevated in both the LPS and CS-LPS groups relative to the CG-PBS group, while crude fat and crude protein declined in the LPS group and total collagen increased significantly in the CS-LPS group ($P < 0.05$; **Fig. 10B**). Textural analysis showed that both CS and SA groups exhibited significantly higher hardness and chewiness in raw muscle compared with the CG group ($P < 0.05$). In cooked muscle, the CS group displayed concurrent increases in hardness, chewiness, and gumminess, whereas the SA group showed elevated chewiness but reduced cohesiveness and resilience ($P < 0.05$). Relative to CG-PBS, the CS-LPS group demonstrated significantly greater hardness and gumminess in both raw and cooked muscle, along with an increase in cooked-muscle chewiness ($P < 0.05$; **Fig. 10C**). Molecular-level findings further demonstrated that *C. somerae* significantly upregulated genes associated with muscle autophagy (*map1lc3b*, *atg16*), lipid

metabolism (*atgl*, *cpt1*, *pparα*), and the AMPK-PGC-1α-FoxO pathway (*ampkα1*, *pgc-1α*, *foxo3*) under both normal and inflammatory conditions. Notably, sodium acetate supplementation produced an equivalent activating effect ($P < 0.05$; **Fig. 10D and 10E**). Collectively, phenotypic and molecular analyses showed that *C. somerae* activated AMPK-PGC-1α-FoxO pathway-related gene expression, leading to reduced muscle fat deposition and improved muscle texture, changes that were recapitulated by its metabolite acetic acid. Consequently, supplementation with *C. somerae* (or sodium acetate) presented a promising strategy for maintaining and enhancing the muscle quality of Yellow River carp.

Discussion

The Yellow River carp, endemic to China's Yellow River Basin, faces developmental challenges linked to softened texture and reduced firmness of muscle, necessitating innovative remediation strategies. In this study, a six-week faba bean diet significantly enhanced Yellow River carp muscle texture and markedly increased hardness and chewiness. Concurrently, the gut microbiota underwent significant changes, in which the unclassified genus *ZOR0006* and *Cetobacterium* positively correlated with muscle-quality indices. In the whole-intestinal microbiota transplantation (WIMT) experiment with faba bean-fed donors, results indicated that the transplanted gut microbiota might activate the AMPK-PGC-1α-FoxO signaling cascade through the gut-muscle axis. This regulation of mitophagy-animal and adipocytokine signaling pathways significantly enhanced the muscle quality of Yellow River carp. Notably, *C. somerae* and its metabolic product acetic acid were identified as the key factors associated with this beneficial

effect. *In vivo* supplementation assays provided further evidence that *C. somerae* and acetic acid notably improved the muscle quality of Yellow River carp (**Fig. 11**). This study provides novel evidence for the gut-muscle axis in fish and establishes a theoretical basis for innovative strategies to improve muscle quality through gut microbiota.

In the field of aquaculture, fish products of superior quality are increasingly favored by consumers. This shift in consumer demand has positioned the improvement of fish quality as a pivotal focus area in nutrition research. The muscle texture of fish directly influences consumers' perception of mouthfeel and is a critical factor that consumers consider when purchasing and consuming fish. Texture characteristics are closely associated with several key factors, including the diameter and density of muscle fibers, collagen content, and fat content in muscle[28, 29]. Extensive studies indicate that a smaller diameter coupled with a higher density of muscle fibres confers greater firmness and chewiness to fish flesh[29]. Collagen, the main structural protein of muscle connective tissue and extracellular matrix, increases fish flesh hardness and chewiness in direct proportion to its content[30]. Fish with higher fat content generally exhibit lower muscle hardness[31]. These characteristics collectively influence the overall quality of fish meat by affecting its texture. Feeding fish a faba bean-based diet led to a widespread increase in flesh firmness, primarily attributable to elevated collagen content, reduced muscle fiber diameter and widened intercellular spaces. Many studies noted a concurrent rise in fiber density[22, 32, 33]; however, some observed unchanged density despite fiber thinning[20], or even thicker fibers with lower density[25]. Similarly, while most experiments indicated a decrease in muscle fat content[20, 22], there were also reports of the opposite effect[25, 32]. Such inconsistencies suggest that the enhancement of muscle hardness

under broad bean feeding is a complex interplay of factors, including increased collagen cross-linking, lipid deposition, and muscle fiber morphological changes, rather than a result solely determined by a single variable. The results of this study indicated that a 6-week diet of faba bean significantly enhanced the muscle texture of Yellow River carp. This was evidenced by an increased proportion of small-diameter muscle fibers, a reduced muscle fiber density and total area percentage, elevated total collagen content, and decreased crude fat content. These findings suggest that the observed increase in muscle hardness is likely attributable primarily to an increased proportion of small-diameter myofibers, enhanced collagen cross-linking, and reduced muscle fat rather than to changes in myofiber number alone.

Microbes play a crucial role in the host's nutrient metabolism. Following faba bean feeding, how did the gut microbiota structure of Yellow River carp change? Previous research demonstrated that feeding grass carp (*Ctenopharyngodon idellus*) faba bean induced an imbalance in their gut microbiota, marked by a decline in advantageous bacteria like *Fusobacteriaceae* and a rise in potentially pathogenic taxa such as *Proteobacteria*. Interestingly, *Acinetobacter* within the *Moraxellaceae* family was identified as a contributor to alterations in the gut microbial community structure and could have potentially served as a biomarker, shedding light on the mechanism of muscle quality improvement induced by faba bean feeding in grass carp[24]. In recent years, studies showed that feeding tilapia with faba bean-based diets altered the gut microbiota, characterized by increased *Rhodobacter*, *Akkermansia*, and *Propionibacteriaceae*. These changes affected muscle collagen accumulation and myofibril remodeling by modulating lipopolysaccharide (LPS) and reactive oxygen species (ROS) associated signaling pathways[25]. An in-depth characterization of

the structural and functional shifts in the gut microbiota induced by faba bean consumption in Yellow River carp opened new avenues for muscle-quality improvement. The study revealed that after six weeks of continuous feeding, the FB group experienced a notable drop in gut microbiota α-diversity, along with significant alterations in the overall microbiota composition, marked by increased levels of the genera *Aeromonas*, unclassified *ZOR0006*, *Cetobacterium*, and *Atopobium*. The increased relative abundance of potential pathogenic bacteria, like *Aeromonas* and *Atopobium*, may result from anti-nutritional factors in faba beans, which disrupt the balance of the gut microbiota and alter the microbial composition. The unclassified bacterium *ZOR0006* within the phylum *Firmicutes* had been detected exclusively in fish to date. Research indicated that this bacterium played a specific metabolic role within the host gut microbiota, possibly by degrading carbohydrates to provide energy and nutrients to the host[34]. However, *ZOR0006* remains taxonomically unresolved, and its functional potential awaits verification via isolation, cultivation, or metagenomic approaches. *Cetobacterium*, a member of the phylum *Fusobacteria*, exhibited unique metabolic capabilities, including the biosynthesis of vitamin B12[35] and short-chain fatty acids (SCFAs)[36]. It possessed the most comprehensive set of functions in the microbial metabolic model, particularly the lactate-pyruvate interconversion module. Elevated levels of *Cetobacterium* improved gut barrier function and contributed to the maintaining of intestinal homeostasis[34]. In the present study, further correlation analysis indicated that unclassified *ZOR0006* and *Cetobacterium* were potentially relevant taxa associated with muscle quality improvement. Nevertheless, it should be emphasized that the observed improvement in muscle quality of Yellow River carp following faba bean ingestion likely reflects a combined effect of dietary components and the concomitant

shifts in the gut microbiota. Whether the microbiota alone directly drives this enhancement remains to be rigorously tested through downstream functional validation approaches such as microbiota transplantation. In summary, 6 weeks of faba-bean feeding induced significant changes in muscle texture and gut microbiota composition of Yellow River carp, which established a muscle-quality differentiation model that justified the subsequent WIMT.

Healthy microbial communities assist the host in synthesizing bioactive compounds from undigested materials, which subsequently enter systemic circulation and influence physiological activities[37]. This process is crucial for both human and animal health and holds significant potential in aquaculture. Through an in-depth investigation of gut microbiota functions, it has been confirmed that signaling pathways mediated by microbiota and their metabolites, such as the gut-muscle axis, are crucial to the host's energy metabolism and muscle functionality. The application of experimental techniques and models, such as antibiotic treatment, fecal microbiota transplantation (FMT), and germ-free (GF) mice has reinforced the central role of the gut microbiota in sustaining muscle function. Notably, FMT as a rapidly evolving technology that can significantly reshape and enhance the gut microbiota and phenotypic characteristics of recipients. Extensive application studies have been conducted in humans[38], mice[39], and livestock, particularly pigs[40, 41] and chickens[42, 43]. Skeletal muscle mass is not only associated with the movement ability and health status of humans and animals, but it also significantly affects the muscle yield and quality of livestock and aquaculture species. Therefore, adjusting host muscle metabolism through gut microbiota and its metabolites offers a new strategy to improve muscle quantity and quality. The differential microbiota and metabolites observed in various muscle models, including high-

quality meat chickens and commercial broilers[9], lean and fat pigs[40, 44] as well as atrophied and normal muscle[6], can serve as potential targets for modulating skeletal muscle metabolism and function. For this study, although faba beans enhance the muscle quality of Yellow River carp, their low sulfur-containing amino acid content, imbalanced nutrient profile, and anti-nutritional factors (ANFs) such as trypsin inhibitors, condensed tannins, and lectins[45] induce oxidative stress, impair nutrient absorption, reduce growth performance, and elevate the feed conversion ratio (FCR), thereby increasing aquaculture costs. This study raises an important question: can improved muscle quality be achieved in healthy Yellow River carp without faba bean feeding, thereby reducing aquaculture costs? To address this, we employed an established muscle quality differentiation model and microbiota transplantation to explore effective strategies for modulating muscle quality through gut microbiota and their metabolites.

In recent years, with the maturation of microbial transplantation technology, its applications have expanded into aquaculture, particularly among fish species. Before microbial transplantation, a short-term course of mixed broad-spectrum antibiotics is commonly employed to reduce the abundance of the background gut microbiota, thereby thereby improving the effectiveness of transplantation[46]. Moreover, studies showed that WIMT more effectively reshaped the entire gut microbial community than conventional FMT[26, 27]. One study conducted intestinal microbiota transplantation between two marine carnivorous fish species inhabiting distinct environments, transferring the gut microbiota from the donor atlantic salmon (*Salmo salar*) into the recipient gilthead seabream (*Sparus aurata*) after antibiotic-mediated clearance of the seabream's baseline microbiota. The results showed that cross-species microbial transplantation enables the transfer of

specific microbes and their functions[47]. In this study, a two-week antibiotic treatment was also conducted prior to WIMT, the results indicated that the species richness and evenness of the gut microbiota significantly decreased, suggesting that the background microbiota of Yellow River carp were effectively diminished. However, the serum biochemical parameters revealed that this treatment caused some hepatic injury in Yellow River carp. Notably, after 8 weeks of microbiota transplantation, the WIMT group improved blood lipid levels by reducing TG and LDL-C without hepatic injury, suggesting that WIMT reverses the adverse effects of short-term antibiotic treatment in Yellow River carp. Consistently, FMT promoted gut microbiota restoration, intestinal healing, and metabolic normalization in florfenicol-treated koi carp (*Cyprinus carpio* var. koi), indicating that FMT can ameliorate antibiotic-induced dysbiosis and maintain gut health[48]. Nevertheless, potential adverse effects associated with antibiotic pretreatment should be minimized to ensure the safety and efficacy of subsequent microbiota transplantation.

The growth performance of fish is a fundamental indicator in the field of aquaculture, as it directly impacts the economic viability and sustainability[49]. The presence of the gut microbiome, particularly through targeted manipulation of specific taxa, can effectively promote growth in aquatic animals[50]. Whether WIMT in this study negatively impacts the growth of Yellow River carp warrants primary attention. A previous study showed that transplanting gut microbiota from adult large yellow croaker (*Larimichthys crocea*) to larvae reshaped the intestinal microecology and improved growth performance[51]. Transplantation of the microbiome from high-fillet-yield adult rainbow trout donors accelerates somatic growth in microbiome-depleted larvae of the low-fillet-yield line[52]. However, these benefits depend on donor phenotype, recipient background, and

dietary context. In the present study, the PCFB group exhibited a significant decline in growth performance, which may be partially attributable to oxidative stress induced by faba bean ANFs. Previous studies have demonstrated that faba bean consumption induces systemic oxidative stress in fish, leading to cellular damage and metabolic perturbations, consequently suppressing growth performance[20-22, 53]. Notably, the WIMT group maintained normal growth levels concomitant with improved redox homeostasis (as evidenced by elevated GSH/GSSG ratio and T-SOD activity), suggesting that the transplanted microbiota may confer protective effects against oxidative stress. Such protection indicates that the gut microbiota alone does not mediate the negative growth effects associated with faba bean ingestion; rather, ANFs constitute the primary factors of growth suppression.

The intestine serves as an essential organ in fish for absorbing nutrients and regulating immune responses, and its structural integrity is a vital indicator of intestinal health. Previous studies demonstrated that prolonged feeding of faba beans altered the intestinal structure of fish, elevated the relative abundance of LPS-producing Gram-negative and flagellated bacteria[23], increased intestinal permeability, and induced inflammatory stress responses[24, 25]. Therefore, it is essential to investigate whether WIMT induces similar inflammatory stress in Yellow River carp. In both clinical settings and animal models, elevated serum LPS levels are widely employed as a hallmark of intestinal barrier dysfunction[54]. Under normal physiological conditions, the intestinal mucosal barrier remains intact, preventing LPS from entering the bloodstream. However, when this barrier function is compromised, LPS can permeate the intestinal mucosa and enter the systemic circulation, triggering inflammatory responses and tissue damage. In this study, the PCFB group

exhibited the shortest total intestinal length, sparse and shortened villi, and a thinner muscular layer. The upregulation of the key mediators of epithelial injury and immune activation (*tnf-α* and *il-1β*), together with the concurrent downregulation of barrier genes (*cldn*, *ocln*, and *zo-1*) and the abnormal elevation of both intestinal and serum LPS levels, collectively confirmed that faba bean feeding compromised intestinal barrier integrity and induced inflammatory responses. Conversely, the WIMT group displayed normal intestinal morphology and immune gene expression, up-regulated barrier genes, and showed only a minor rise in intestinal LPS, indicating that the intact barrier function effectively prevented bacterial translocation even though the transplanted microbiota potentially contained LPS-producing species. Thus, the present data indicate that the gut microbiota is not the primary cause of the adverse effects induced by faba beans; in the absence of bean-derived ANFs, the transplanted microbiota can independently exert intestinal barrier-protective effects and thereby provide a physiological basis for subsequent muscle quality improvement.

In aquatic animals, research on the direct connection between microbial transplantation and muscle quality is limited. However, evidence from related studies on microbial interventions provides compelling insights into the gut-muscle axis. For example, in *trachinotus ovatus*, a complete gut microbiota improved its composition by mediating the colonization of some probiotics represented by *Lactobacillus* in the intestine, thereby enhancing host metabolic efficiency of proteins and lipids[55]. In *Macrobrachium rosenbergii*, specific bacteria such as *Lactobacillus* and *Blautia* were positively correlated with muscle-related metabolites like alpha-ketoglutaric acid and L-arginine. These metabolites are crucial for protein synthesis and muscle

maintenance[56]. In this study, the results aligned with our expectations. Although the improvements in texture indicators in the WIMT group were less pronounced than those in the PCFB group, significant enhancements in hardness, chewiness, and shear force were still observed for both raw and cooked muscle. This finding suggests that the muscle texture of the recipient Yellow River carp was partially replicated from the donor. What phenotypic indicators' changes have affected the modification of muscle texture? Collagen, as the primary structural component of the extracellular matrix (ECM), plays a pivotal role in determining the mechanical properties of muscle texture[57]. Increased total collagen and insoluble collagen are strongly associated with enhanced hardness and toughness of muscle tissue, a phenomenon attributed to the maturation and covalent cross-linking of collagen fibers[58]. Following WIMT, there was an increase in both total and insoluble collagen in Yellow River carp muscle, accompanied by a reduction in collagen solubility. Histological sections revealed a significant presence of collagen fibers, which contributed to enhanced textural properties, including hardness and chewiness. Muscle routine composition is a critical indicator for assessing muscle quality and nutritional composition. The results show significantly lower muscle fat levels in the WIMT and PCFB groups, reinforcing the rise in muscle hardness. In summary, a series of phenotypic results directly demonstrate that gut microbiota can regulate the metabolism and function of Yellow River carp muscle, thereby improving muscle quality.

Further muscle transcriptome sequencing revealed the underlying molecular regulatory pathways and provided more precise intervention measures and theoretical support for enhancing muscle quality. Previous studies using RNA-Seq analysis identified differentially expressed genes and key

metabolic pathways in the white muscle of Yellow River carp fed faba beans, primarily related to the ECM, as well as fatty acid and amino acid metabolism[53]. The analysis of this study shows that the metabolic pathways in the PCFB group are mainly focused on cell movement and structure, carbohydrate and lipid metabolism and synthesis, organelle function and autophagy, and cell fate and signal transduction, largely aligning with prior studies. These differential metabolic pathways, including motor proteins (such as myosin and dynein) are vital for intracellular transport and muscle contraction, facilitating mechanical force generation[59]. The integration of ECM-receptor interactions and cell-cell adhesion mechanisms is crucial for the structural stability and functional integrity of muscle tissue. Integrins and cadherins, through their roles in focal adhesions and adherens junctions, coordinate the transmission of mechanical forces and biochemical signals, thereby regulating cell adhesion, migration, and ECM remodeling[60]. Additionally, studies have indicated that dietary exposure to faba beans induces oxidative stress in Yellow River carp[58]. This study shows that enrichment of the autophagy-animal pathway acts as a defense mechanism against oxidative stress triggered by faba-bean ANFs, thereby ameliorating metabolic dysfunction and muscle atrophy. Enrichment of the FoxO signaling pathway also enhances cellular antioxidant capacity and consequently increases organismal resistance to oxidative stress. Furthermore, the adipocytokine signaling pathway, mediated by adipocyte-derived cytokines such as leptin and adiponectin, activates downstream molecules including AMPK, and thus helps regulate energy balance and lipid metabolism, improves nutrient-utilization efficiency, and reduces fat deposition. What metabolic pathway changes occur in muscle tissue following WIMT? The results showed that the autophagy-animal and adipocytokine signaling pathways remained significantly enriched.

Moreover, research demonstrated that microbial-derived SCFAs enhanced mitophagy by upregulating key mitophagy-related genes[61]. The enrichment of propionate metabolism and fatty acid degradation pathways further highlights the pivotal role of gut microbiota-derived propionate and acetate in regulating muscle energy metabolism and improving muscle quality. Research indicated that acetic acid inhibited lipid accumulation in skeletal muscle by boosting lipolysis and fatty acid oxidation, while simultaneously dampening fatty acid synthesis through the PPARα, AMPK, and extracellular signal-regulated kinase 1/2 (ERK1/2) signaling pathways[62]. The enrichment of the PPAR signaling pathway observed in this study further supports this finding. Additionally, as core components of mitochondrial energy metabolism, the enrichment of the TCA cycle and oxidative phosphorylation demonstrates the critical role of the transplanted microbiota and their metabolites in enhancing mitochondrial function and energy synthesis. AMPK serves as the primary sensor for energy stress; once activated, it not only directly phosphorylates FoxO3a but also triggers silent information regulator 1 (SIRT1) by increasing the oxidized/reduced nicotinamide adenine dinucleotide ratio (NAD^+/NADH). SIRT1 then deacetylates FoxO3a and PGC-1α, thereby enhancing their transcriptional activity in tandem. Deacetylated FoxO3a up-regulates antioxidant and autophagy-related genes, reinforcing cellular antioxidant defense, while deacetylated PGC-1α also synergizes with PPARα to accelerate mitochondrial biogenesis and fatty acid oxidation, ultimately improving muscle energy metabolism and oxidative homeostasis[63, 64]. Our results further validated that in both the PCFB and WIMT groups, the expression of genes associated with key autophagy, lipid catabolism, and the AMPK-PGC-1α-FoxO axis was significantly upregulated. In summary, molecular evidence collectively suggests that WIMT

potentially acts through the AMPK-PGC-1α-FoxO axis associated with mitophagy-animal and adipocytokine signaling pathways to orchestrates energy metabolism, lipid catabolism, and protein synthesis while sustaining systemic metabolic homeostasis, thereby contributing to improved muscle quality in Yellow River carp.

The role of gut microbiota in mediating these effects is further supported by observed changes in microbial composition, functional capacity, and the metabolite profile. This study indicated that the main phyla in the intestinal microbiota of Yellow River carp included *Pseudomonadota*, *Fusobacteriota*, *Bacillota*, and *Actinomycetota*. These phyla were essential in managing nutrient metabolism, modulating immune responses, and preserving gut homeostasis. *Pseudomonadota* represents a phylum characterized by immense ecological and metabolic diversity, their dual roles as both beneficial symbionts and opportunistic pathogens underscore the complexity of their interactions with aquatic hosts and environments. The *Enterobacteriaceae* within this phylum exhibit remarkable adaptability to suboptimal conditions like nutrient scarcity and oxidative stress due to their metabolic versatility, transitioning from commensal to pathogenic states, particularly in the gut where microbiota imbalances trigger their overgrowth[65]. In this study, although the PCFB group exhibited the lowest relative abundance of *Pseudomonadota*, members of the *Enterobacteriaceae* family within this phylum, specifically the potential opportunistic pathogens such as *Citrobacter* (*Citrobacter freundii*), *Kluyvera* (*Kluyvera cryocrescens*), *Serratia* (*Serratia* sp., *Serratia* sp. ES-1), *Enterobacter* (*Enterobacter cloacae*) and *Priestia* (*Priestia megaterium*) were the most enriched. Studies showed that the increased presence of Gram-negative bacteria led to the production of endotoxins, such as LPS and flagellin, which activated pro-inflammatory gene

expression through Toll-like receptor (TLR) signaling pathways[26]. Microbial functional prediction elucidates the potential mechanisms underlying the interactions between microbes and the host. Bugbase phenotypic prediction indicated that the PCFB group had more mobile elements and higher potential pathogenicity. Furthermore, the LPS biosynthesis pathway (ko00540) was significantly enriched, a finding corroborated by our LPS assay results. Integrating the aforementioned intestinal phenotypic results, the PCFB group showed marked intestinal inflammation and structural changes, largely fueled by an imbalance in gut microbiota and the triggering of pro-inflammatory pathways.

Analysis of gut microbiota composition and metabolic profiles in recipient fish enables the identification of key microbial species and functional pathways linked to improved muscle quality. In this study, *Pseudomonadota* levels in the WIMT group did not differ significantly from the CG group, and there was no notable enrichment of *Enterobacteriaceae* opportunistic pathogens. This can be explained by the role of WIMT, which involves the transplantation of the complete intestinal microbiota, in sustaining a balanced and healthy microbial community while preventing the excessive proliferation of certain groups, such as potential pathogens. Additionally, the inclusion of mucus-associated microbiota in WIMT (generally missing in FMT) might contribute to the stability of the microbial ecosystem by creating protective barriers that prevent pathogen adherence and invasion. *Fusobacteriota*, especially the genus *Cetobacterium*, predominate in the gut microbiomes of numerous freshwater fish species. Studies showed that in Nile tilapia fed diets containing different proportions of faba beans, *Cetobacterium* dominated all experimental groups. However, its relative abundance decreased as the proportion of dietary faba beans increased[66].

Notably, our results diverged from previous findings. The investigation showed *Cetobacterium* as the predominant genus in the gut microbiota for both the PCFB and WIMT groups. Subsequent random forest analysis identified *C. somerae* as a candidate biomarker, which closely aligns with our previous 6-week feeding study involving faba beans. Research demonstrated that *C. somerae* increased host defense against pathogens by altering gut microbiota composition and strengthening gut barrier integrity[36]. A recent study also demonstrated that *C. somerae* promoted L-carnitine biosynthesis by supplying the metabolic precursor TMAB (4-trimethylammoniobutanoate), thereby enhancing mitochondrial fatty acid β-oxidation and reducing fat deposition in fish[67]. SCFAs modulate immune function, support gut barrier integrity, and are important signaling molecules connecting microbial activity to the health of the host[68]. For example, the acetic acid produced by *C. somerae* enhanced immunity by increasing antimicrobial peptide and interleukin-22 (il-22) levels[69]. Supplementation of grass carp diets with *C. somerae* elevated intestinal acetic acid levels, enhancing antioxidant capacity, improving intestinal digestion and absorption, and promoting growth and development[70]. In this study, the analysis of SCFAs in the intestinal contents of the PCFB and WIMT groups revealed that acetic acid was the most abundant, with levels significantly higher than those in the CG group. Further testing of the fermentation broth of *C. somerae* also confirmed that acetic acid was produced by *C. somerae*. As a SCFA, acetic acid lowers intestinal pH, suppresses harmful bacteria, and maintains microbial homeostasis. Studies showed that *C. somerae* enhanced glucose homeostasis and insulin expression in zebrafish, mediated through acetate production and parasympathetic activation, this improved host milieu favored *C. somerae* colonization[35]. Although the PCFB group exhibited the highest diversity and

abundance of potential pathogens, the increase in the abundance of *C. somerae* may indicate a potential self-protective mechanism within the intestine of Yellow River carp, thereby mitigating the detrimental effects of pathogenic bacteria on the host. Studies found that during acute ammonia intoxication (AI), *C. somerae* proliferated in the gut and produced argininosuccinic acid (ARA), which helped bolster the host's resistance to AI[71]. Nevertheless, additional research is necessary to confirm the possible protective mechanisms implicated in this study. After WIMT, *C. somerae* from the donor microbiota is introduced into the recipient's gut. It successfully establishes and maintains a high abundance due to its strong colonization ability and metabolic advantages, thereby helping to restore and maintain gut microbiota balance. This effect is corroborated by the improved histological and barrier metrics observed in the WIMT group. Notably, WIMT also led to increased abundance of certain potentially opportunistic genera (*Shewanella*, *Kluyvera*, and *Streptococcus*), which may partially account for the marginally elevated intestinal LPS levels in this group. Nevertheless, these taxa remained at relatively low abundances and did not induce significant inflammatory responses, indicating that the overall balance of the microbial community, rather than the presence of specific taxa, determines host health status.

The common enriched metabolic pathways identified by Metacyc and KEGG predictions for the gut microbiota in the PCFB and WIMT groups offer key clues about how the gut microbial community governs muscle growth and quality in fish. Among the identified common metabolic pathways, the amino acid synthesis pathway is the most enriched. Branched-chain amino acids (BCAAs; pathways: PWY-5104, PWY-5103, and BRANCHED-CHAIN-AA-SYN-PWY) and other amino acids (PWY-2942, ko00471, ko00473) are essential for muscle protein synthesis and

energy regulation. Studies found that in common carp, BCAAs enhanced the expression of myogenic regulatory factors, facilitating muscle protein synthesis and subsequently improving muscle growth and protein deposition[72, 73]. Additionally, BCAAs reduced fat deposition in fish and improved muscle quality through various mechanisms, including the inhibition of fat synthesis, promotion of fat oxidation, enhancement of liver health, and regulation of energy metabolism[74]. Notably, gut microbiota produces SCFAs through carbohydrate metabolic pathways (CALVIN-PWY, ko00030, ko00660), which modulate energy and lipid metabolism, enhance nutrient absorption, and ultimately improve muscle development and overall quality in fish. Research demonstrates acetic acid activates AMPK and serves as a key signaling molecule linking microbial metabolites to host energy sensing[75, 76]. Cellular investigations revealed that acetic acid boosted AMPKα phosphorylation, while simultaneously upregulating both the expression and transcriptional activity of PPARα. This cascade ultimately led to increased expression of lipid oxidation-related genes, thereby enhancing the lipid oxidation capacity[77]. Based on the co-enrichment pathways predicted from gut microbiota functions and those derived from the muscle transcriptome, our findings indicate that WIMT establishes gut muscle communication through various related converging metabolic axes, such as amino acid synthesis and SCFAs production. Additionally, the gut microbiota and their metabolites are pivotal in steering the host's energy metabolism, boosting mitochondrial performance, and maintaining cellular redox balance through multiple metabolic routes. These effects are supported by the enrichment of pathways linked to muscle mitochondrial autophagy, oxidative phosphorylation, citric acid cycle, and pyruvate metabolism. However, owing to the inherent limitations of functional prediction methods, these

enriched pathways represent putative biological hypotheses rather than definitive metabolic functions. Future studies integrating metagenomic sequencing, metatranscriptomics, and other complementary approaches are therefore warranted to validate these predictions. Among these metabolic axes, the SCFAs metabolomic data obtained in this study, together with prior evidence demonstrating that *C. somerae* exerts biological functions through acetic acid production[35, 69, 70], collectively suggest acetic acid as the putative primary effector. We therefore hypothesise that a principal mechanism involves *C. somerae*, a key bacterial strain in WIMT, which generates substantial SCFAs, particularly acetic acid, through carbohydrate metabolism. This acetic acid then traverses the gut-muscle axis to influence distant muscle tissues, activating the AMPK-PGC-1α-FoxO signaling cascade, enhances adipocytokine signaling and up-regulates PPARα expression, thereby enhancing lipid catabolism, reducing intramuscular lipid deposition, and ultimately improving muscle quality. Therefore, optimizing gut microbiota composition and function enhances fish health and muscle quality.

While SCFAs metabolomic and functional prediction data implicate acetic acid as the putative primary effector, other potential metabolites may also participate in gut-muscle crosstalk. Further non-targeted metabolomics analyses of gut contents provide additional evidence for the role of gut microbiota in regulating the muscle quality of Yellow River carp. WIMT induces significant alterations in the gut microbiota's metabolic profile, which may subsequently influence essential physiological processes in muscle, including energy metabolism, protein synthesis, and inflammatory responses. The substances with the most significant increases in relative abundance are amino acids and their derivatives. KEGG functional enrichment analysis further confirmed that

the synthetic metabolic pathways related to amino acids are the most enriched. Specifically, glutamate-related metabolism (including L-Pyroglutamic acid and 4-Aminobutyric acid, GABA), glutamine metabolism (comprising D-(-)-Glutamine and DL-Glutamine), branched-chain amino acid metabolism (such as 2-Methylglutaric acid and 2-Isopropylmalic acid), and glutathione metabolism, which is closely related to antioxidant function ((including L-Glutathione oxidized and Glutathione (reduced)), align with the predicted metabolic pathways of gut microbiota functions. The antioxidant and immune-modulating effects resulting from the metabolism of Flavonoid metabolites in the gut, such as kaempferol, trifolin, kaempferitrin, enhance antioxidant defense and boost immunity in fish. These findings elucidate the complex link between gut microbiota and host muscle health, while also identifying new avenues and potential targets for future nutritional interventions and quality improvement. Nevertheless, the relative contributions of these metabolites to piscine muscle quality warrant further investigation through targeted functional studies.

The LPS-induced intestinal inflammation model is extensively employed to study oxidative stress and immune responses in fish[78]. Given that faba bean feeding elevated intestinal and serum LPS levels and induced intestinal inflammation in Yellow River carp, this *in vivo* validation experiment was conducted to: (1) verify the effects of *C. somerae* and acetic acid on muscle quality under normal physiological conditions via feeding trials, and (2) specifically validate the efficacy of *C. somerae* under LPS-induced inflammatory conditions. Muscle fat and collagen content are critical determinants of muscle texture properties. Under normal physiological conditions, the results were consistent with our expectations. Exogenous supplementation of *C. somerae* and sodium acetate

improved muscle texture properties in the CS and SA groups by reducing crude fat content while increasing crude protein and collagen levels. Research demonstrated that LPS induced inflammatory responses and oxidative stress through the Toll-like receptor 4 (TLR4) and NF-κB signaling pathways. This activation of the ubiquitin-proteasome system subsequently accelerated the degradation of skeletal muscle proteins[79]. In the blunt snout bream (*Megalobrama amblycephala*), LPS-induced TNFα upregulated the expression of adipose triglyceride lipase (ATGL) in both liver and muscle, leading to a reduction in fat accumulation[80]. This study found that LPS stimulation resulted in a decrease in crude fat and crude protein in the muscle of Yellow River carp, while simultaneously increasing the dry matter content. These results corroborate previous findings regarding LPS-induced changes in muscle composition and recapitulate the muscle phenotype of faba bean-fed Yellow River carp. Exogenous supplementation of *C. somerae* (CS-LPS) reduced muscle protein degradation and increased collagen content, and thereby improved the muscle texture properties of Yellow River carp. Furthermore, *C. somerae* upregulated the expression of genes associated with the AMPK-PGC-1α-FoxO pathway and involved in muscle autophagy and lipid catabolism under both normal and LPS-induced inflammatory conditions, and these effects were largely replicated by its metabolic product, acetic acid, thus confirming our hypothesis. Collectively, the *in vivo* feeding experiment further substantiated that *C. somerae* and acetic acid enhance the muscle quality in Yellow River carp. The findings of this study hold promising translational potential for aquaculture applications. Acetic acid or acetic acid-producing strains (e.g., *C. somerae*) may be administered via feed additives or probiotics to modulate host metabolism and enhance muscle quality. Furthermore,

sodium acetate represents a cost-effective and safe potential feed additive amenable to large-scale application. Nevertheless, the long-term stability, optimal supplementation dosage, and large-scale application efficacy across diverse aquaculture systems remain to be systematically assessed through pilot-scale trials.

Despite these promising findings, several limitations should be acknowledged. First, antibiotic pretreatment for microbiota depletion may induce transient physiological stress, necessitating the optimization of depletion methods or exploration of alternative strategies such as germ-free models in future studies. Second, mechanistic conclusions were primarily based on transcriptional-level findings and await validation through proteomic or functional enzymatic analyses coupled with myocyte experiments. Third, functional validation was confined to acetic acid as the primary SCFA metabolite, whereas the contributions of other metabolite classes, including amino acids and flavonoids, remain to be elucidated through cell-based high-throughput screening and subsequent *in vivo* functional validation. Finally, given the species-specific nature of gut microbiota, the donor-recipient model employed herein reflects specific developmental stages and dietary contexts; consequently, the generalizability of WIMT effects across distinct species, developmental stages, or environmental conditions requires further investigation.

In conclusion, based on the differences in gut microbiota between conventionally fed and faba bean-fed Yellow River carp, this study utilizes whole intestinal microbiota transplantation (WIMT) to demonstrate that gut microbiota regulates muscle quality. Further screening identified the beneficial strain *C. somerae* and its key metabolite acetic acid. Subsequent feeding experiments demonstrated that both *C. somerae* and acetic acid significantly improved muscle texture. This

study establishes a foundation for elucidating the bidirectional information exchange mechanism of the fish gut-muscle axis, provides a theoretical basis for microbiota-targeted enhancement of muscle quality. Furthermore, it offers a practical solution for developing commercial feed additives based on the identified key associated factors, opening a new route for quality upgrading and economic efficiency gains in Yellow River carp aquaculture.

Methods

Ethics statement

The study adhered to ethical guidelines for the treatment of animals, and was approved by the Institutional Animal Care and Use Committee of Henan Normal University (Document number: HNSD-2025BS-0307).

Animals and experiments design

The fish used in the experiment underwent a two-week acclimation period at the Zhongkang breeding cooperative in Luohe City (Henan, China). Throughout this time, they were maintained on a standard commercial diet (35% protein, Tongwei Co., Ltd., China), with feedings occurring three times per day, and health was closely monitored. The study was organized into three independent yet sequentially connected feeding experiments following the pipeline: (1) differential model establishment, (2) microbiota transplantation for target screening, and (3) targeted functional validation.

Experiment 1 aimed to establish a divergent muscle-quality model and compare the intestinal

microbiota structure of Yellow River carp exhibiting contrasting muscle phenotypes. Two experimental groups were established: a control group (CF) and a faba bean group (FB), as shown in **Fig. 1A**. Before the experiment began, 90 healthy Yellow River carp with similar specifications (average weight, 479.19 ± 21.80 g) were randomly placed in pond cages (3 × 3 × 1.5 m). Three cages were assigned to each group, with 30 fish in each cage. The CF group received commercial feed, while the FB group was fed soaked faba beans (12-hour soak). Both groups were acclimated to their respective diets for 1 week before starting the 6 weeks feeding experiment.

Experiment 2 employed WIMT to verify the direct effects of gut microbes on muscle quality and to identify beneficial microorganisms and metabolites potentially responsible for the observed muscle-quality improvement. A total of 270 healthy, uniform-sized Yellow River carp (initial weight: 510.70 ± 25.89 g) were randomly allocated to 9 pond cages (3 × 3 × 1.5 m), with three cages per treatment and 30 fish per cage. The experiment's detailed design is depicted in **Fig. 3A**. Three experimental groups were established: control group (CG), positive control faba bean group (PCFB), and whole-intestinal microbiota transplantation group (WIMT). The CG group received the basal diet, the PCFB group was fed 12 h-soaked faba beans, and the WIMT group received microbiota transplanted from donor fish that had been fed faba beans for 6 weeks. To ensure an identical experimental duration across all groups, the WIMT feed was administered according to the three-phase protocol below. During phase 1 (1−4 weeks), the fish were provided with a basal diet. In phase 2 (4−6 weeks), their diet was supplemented with mixed broad-spectrum antibiotics to deplete background microbiota, thereby minimizing potential interference with subsequent microbiota transplantation. In phase 3 (6−14 weeks), microbiota transplantation was performed by

feeding the fish a basal diet coated with a whole-intestinal bacterial suspension from donor fish. After a 1-week acclimation period, a 14-week feeding experiment was initiated.

Experiment 3 was designed to functionally validate the associated microorganisms and metabolites identified in experiment 2 and to evaluate their specific effects on muscle quality improvement in Yellow River carp. In this experiment, 540 healthy, uniformly sized Yellow River carp (initial weight: 127.26 ± 2.53 g) were randomly assigned to 18 pond cages (2 × 2 × 1.5 m) at 30 fish per cage, giving three cages per treatment. The experimental procedure is illustrated in **Fig. 10A**. Under normal physiological conditions, three experimental groups were established: control group (CG), probiotic group (4×10^8 CFU/g *C. somerae* CFH_001, CS), and acetate-replenished group (1.5% sodium acetate, SA; inclusion level with reference to previous study[81]) to confirm the roles of the associated microorganism and its metabolites in modulating muscle quality. In addition, to mimic the stress response induced by faba bean feeding in Yellow River carp, LPS-induced inflammation was used to assess the associated microorganism's effects on muscle quality. The experimental setup included three distinct groups: a control group (CG-PBS), an LPS-induced group (LPS), and a probiotic-protected group (CS-LPS). The CG-PBS group received injections of phosphate-buffered saline (PBS), whereas LPS (derived from *E. coli* O55:B5) was administered to both the LPS and CS-LPS groups at a dosage of 1 mg/kg body weight, with all injections performed on a biweekly basis. Prior to the 8-week feeding trial, all test fish underwent a 1-week acclimation period to adapt to the study conditions.

All the experimental fish were fed three times a day, receiving 2% to 4% of their body weight in food, with the amount adjusted according to their feeding status and weather conditions.

Experimental net cages were installed in a 10-acre outdoor pond fitted with three high-power aerators and a recirculating water system. During the rearing period, pond water temperature was maintained at 22−31 °C, dissolved oxygen at 7−10 mg/L, and pH at 7.0−8.5.

Preparation of *Cetobacterium somerae* CFH_001

The strain *C. somerae* CFH_001 was isolated and screened by our research group, and its almost-complete 16S rRNA gene sequence has been deposited in GenBank under accession number PX700593. Procedures were adapted from published methods with appropriate modifications for the present study[82]. For the preparation of the seed culture, 100 μL of glycerol-preserved bacterial suspension was inoculated into 10 mL of Gifu Anaerobic Medium (GAM) and incubated at 37 ℃ for 12 hours to reach the logarithmic growth phase. Afterward, 1.5 mL of the seed culture was introduced into 300 mL of GAM and allowed to incubate at 37 ℃ for a full 24-hour period. The culture was left undisturbed until it reached the stationary phase, at which point the bacterial concentration stabilized at 4×10^8 CFU/mL. After cultivation, the bacterial fermentation broth was frozen at −80 ℃ and lyophilized for subsequent feeding experiments. The culture supernatant of *C. somerae* CFH_001 (CS-CS) was obtained by centrifugation of the fermentation broth at 5000 g for 10 minutes at 4 ℃ and was subsequently used for SCFAs analysis.

Preparation of whole-intestinal microbiota suspension and experimental feeds

Yellow River carp that had been fed faba beans for 6 weeks were selected as donors for whole-intestinal microbiota transplantation. The workflow is illustrated in **Fig. 3B**. The bacterial suspension was prepared by integrating previously reported methods with minor adjustments[47, 48].

In brief, after a 12-hour fast, the donor fish was dissected, and the intact intestinal tissue was immediately placed on ice. Adipose tissue and other substances adhering to the outer wall of the intestine were then carefully removed, and the outer surface was thoroughly rinsed with 0.9% sterile saline several times. Subsequently, the entire intestinal contents were carefully squeezed out using tweezers and transferred into an EP tube. After 6 g of intestinal contents were mixed with 40 mL of 0.9% sterile saline and vortexed to homogenize, the mixture was filtered through a sterile 10 μm filter to prepare the whole-intestinal bacterial suspension. The freshly prepared whole-intestinal bacterial suspension (300 mL/kg) was sprayed onto the basal feed daily and air-dried in a shaded area for use the following day. The basal diet contained fish meal, soybean meal, and rapeseed meal as protein sources, rice bran and wheat flour for carbohydrates, and soybean oil for fat. The feed formulation and proximate composition for each group in the WIMT experiment are detailed in **Supplementary Table S8**. For the preparation of the antibiotic-supplemented feed, the mixed broad-spectrum antibiotics were added to sterile saline at concentrations of neomycin (200 mg/kg), ampicillin (200 mg/kg), metronidazole (200 mg/kg), gentamicin (200 mg/kg), and vancomycin (10 mg/kg) per kilogram of feed. This mixture was sprayed onto the basic feed weekly, air-dried, and frozen at −20 °C for future use. To prepare the *C. somerae*-supplemented feed, the freeze-dried bacterial powder was dissolved in sterile physiological saline and uniformly sprayed onto the basal feed, resulting in a feed containing 4×10^8 CFU/g of *C. somerae*. The feed was also air-dried, stored at −20 °C, and prepared weekly to maintain bacterial viability.

Samples collection

For the WIMT group, intestinal microbial samples were collected both before and after antibiotic treatment. Following the feeding period at 4 and 6 weeks, the experimental fish were starved for 12 hours followed by anesthesia with MS-222 (55 mg/L). After dissection, intestinal contents were harvested and promptly flash-frozen in liquid nitrogen, and stored at −80 °C for 16S rRNA gene amplicon sequencing.

Upon completion of the entire feeding experiment, the fish were starved for 12 hours and anesthetized using an anesthetic agent. Each cage of experimental fish was weighed and measured, and the number, final weight, and body length were recorded. The experimental fish were dissected to isolate the hepatopancreas and mesenteric fat from the viscera mass, which were subsequently weighed to calculate indicators related to growth performance. To calculate the carcass ratio (CR), the fish were weighed after the visceral mass were removed and the head and fins were detached. Feed conversion rate (FCR) = feed consumed / (final weight - initial weight). Equations for other growth performance indices are given in the footnotes to **Supplementary Table S1**. Additionally, the intact intestine was removed, and its length was measured. Approximately 1 mL of blood was drawn from the tail vein using a sterile syringe. The samples were left at ambient temperature for 6 hours, then centrifuged at 4 °C and 3500 rpm for 10 min to separate the serum. The serum was subsequently frozen −80 °C for later biochemical analysis. A suitable amount of white muscle tissue was collected from below the dorsal fin and stored in a sterile 1.5 mL enzyme-free centrifuge tube. The sample was promptly frozen in liquid nitrogen and then kept at −80 °C for enzyme activity detection, RNA extraction, transcriptome sequencing, and collagen content determination. The remaining white muscle tissue was utilized to evaluate muscle texture characteristics and

conventional nutritional components. Intestinal contents were collected for a comprehensive microbiome analysis, which included LPS content determination, 16S rRNA gene amplicon sequencing, metabolomics and SCFAs profiling. A small quantity of of midgut tissue was collected and transferred to a sterile, enzyme-free 1.5 mL centrifuge tube, then rapidly frozen in liquid nitrogen and stored at −80 °C for subsequent RNA extraction. Portions of white muscle tissue below the dorsal fin and midgut tissue were collected and fixed in a 4% paraformaldehyde solution for histomorphological analysis. The muscle tissue was subjected to Masson's trichrome and hematoxylin-eosin (HE) staining, while the midgut tissue was stained with HE.

Detection of serum biochemical indicators

The concentrations of albumin (Alb), triglyceride (TG), total cholesterol (T-CHO), high-density lipoprotein cholesterol (HDL-C), low-density lipoprotein cholesterol (LDL-C), and the activities of aspartate aminotransferase (AST/GOT) and alanine aminotransferase (ALT/GPT) in serum were quantified using commercial assay kits from Nanjing Jiancheng Bioengineering Institute (NJBI), Nanjing, China, strictly adhering to the provided guidelines.

Measurement of antioxidant capacity in serum and muscle

Antioxidant activity markers, including glutathione (GSH), glutathione disulfide (GSSG), glutathione peroxidase (GSH-Px), total superoxide dismutase (T-SOD), total antioxidant capacity (T-AOC), hydrogen peroxide (H_2O_2), and malondialdehyde (MDA), were quantified using standardized assay kits from NJBI according to the manufacturer's instructions.

Determination of LPS content

Serum and intestinal content LPS levels were quantified using the Pierce™ Chromogenic Endotoxin Quantitation Kit (A39552; Thermo Fisher Scientific, China) according to the manufacturer's instructions.

Assessment of muscle texture characteristics

Texture analysis of muscle samples was conducted with the texture analyzer (AMETEK Brookfield CTX, USA), adhering to the protocol outlined by Mi et al.[83]. Specifically, fresh samples were tested for raw meat texture, while cooked samples were steamed for 5 minutes, cooled, and then analyzed. The texture properties of muscle tissue, including hardness, chewiness, springiness, cohesiveness, resilience, gumminess and adhesiveness were evaluated using an 8 mm flat-ended cylindrical probe (TA-AACC36). The test conditions were: 5 mm/s pre-test speed, 2 mm/s test speed, 5 g trigger force, and 60% compression. Furthermore, the shearing force of muscle was measured using a 1 mm shearing device (TA-SBA-WB-1) to vertically shear the muscle.

Analysis of nutritional components in feeds and muscle

The moisture content in both feeds and muscle was measured using the direct drying method at 105 °C, following the Chinese National Standard GB5009.3-2016. Ash content was measured by incinerating samples at 550 °C following GB5009.4-2016. Crude protein content was determined by the kjeldahl method, following GB/T 6432-2018 for feeds and GB5009.5-2016 for muscle. Crude fat content was measured via soxhlet extraction, adhering to GB/T 6433-2006 for feeds and

GB5009.6-2016 for muscle.

Measurement of muscle collagen content

Total collagen was determined by multiplying measured hydroxyproline (Hyp) by 7.25[84]. The Hyp content was quantified using commercial assay kits (NJBI, A030-3-1), with minor modifications to the protocol as specified in the instruction manual. To determine the soluble collagen content in muscle, the samples were initially preprocessed. Approximately 0.4 g of muscle tissue was weighed, placed it in a 2 mL tube, and 1.6 mL of 25% Ringer's solution was added for homogenization. The mixture was heated at 77 ℃ for 70 min, then centrifuged at 4 ℃ at 1000 rpm for 30 min, and the extraction process was repeated twice before the supernatants were combined. 500 μL of supernatant was combined with 500 μL of concentrated hydrochloric acid (6 mol/L final concentration) and hydrolyzed at 100 ℃ for 24 h. The subsequent detection was performed using the previously mentioned assay kit and procedure. Insoluble collagen content was calculated by deducting soluble collagen from total collagen.

Tissue morphological analysis

The muscle and midgut tissues were stained using the HE high-definition constant staining kit (G1076) from Servicebio (Wuhan, China), following the manufacturer's instructions. To bring the collagen fibers into sharp relief, the muscle tissue was treated with the masson stain kit (G1006) from the same supplier, according to the protocol. Subsequently, perform microscope inspection (NIKON ECLIPSE E100), image acquisition (NIKON DS-U3) and analysis using Image J software.

Transcriptome sequencing of muscle

Nucleic acids were extracted from the muscle tissue using TRIzol reagent, and high-quality samples underwent library preparation after quality assessment. The library construction process mainly included the purification and fragmentation of mRNA, synthesis of the first and second cDNA strands, adapter ligation (adapter primer sequences: adapter 3 = "AGATCGGAAGAGCACACGTCTGAACTCCAGTCAC"; adapter 5 = "AGATCGGAAGAGCGTCGTGTAGGGAAAGAGTGT"), purification and size selection of the ligation products, PCR amplification, purification of the PCR products, and library quality control (Qsep-400). The prepared libraries underwent sequencing using the Illumina NovaSeq 6000.

Quantitative real-time PCR

RNA was extracted from muscle and intestine samples using RNAiso Plus (TaKaRa, Dalian, China). The extracted RNA was reversed transcribed to cDNA using the PrimeScript RT reagent Kit with gDNA Eraser. All primers in this study were designed using Primer-BLAST, with efficiency validated via standard curve analysis (90−110%). The sequences of the primers utilized for real-time PCR were located in **Supplementary Table S9**, *18S rRNA* was the referenced gene. The real-time PCR reaction setup and protocol followed Cheng et al.'s methodology[85]. Relative expression levels of the target genes were determined using the $2^{-\Delta\Delta Ct}$ method[86].

16S rRNA gene amplicon sequencing

DNA was isolated from the samples using the OMEGA Soil DNA Kit (M5635-02, Omega Bio-

Tek, USA). Next-generation sequencing (NGS) of 16S rRNA amplicons was utilized to investigate the gut microbiota of fish fed faba beans for 6 weeks and those treated with antibiotics. Bacterial-specific primers and sequencing were conducted according to the procedures outlined in our previous study[85]. Third-generation sequencing (TGS) of complete 16S rRNA amplicons was employed to study gut microbiota after WIMT. Full-length 16S rRNA of bacteria was amplified using V1−V9 region-tailored primers, 27F (5'-barcode+AGAGTTTGATCMTGGCTCAG-3') and 1492R (5'-ACCTTGTTACGACTT-3'). Sequencing libraries were prepared utilizing the SMRTbell® Prep Kit 3.0 from Pacific Biosciences. The qualified libraries were sequenced on the PacBio Sequel II system employing Circular Consensus Sequencing (CCS). The bioinformatics analysis also followed the protocol described in the previous study[85]. Microbial metabolic functions were predicted using PICRUSt2, based on KEGG and MetaCyc databases.

Determination of SCFAs

The analysis of SCFAs in both intestinal contents and CS-CS was performed using the GC-MS/MS platform (Agilent, 8890-7000D) in multiple reaction monitoring (MRM) mode with a triple quadrupole mass spectrometer, and a self-constructed database was employed to achieve the absolute quantification of SCFAs related compounds.

Metabolomic sequencing of intestinal contents

Metabolites from intestinal contents sample were extracted, followed by the preparation of quality control (QC) and blank samples. Detection was performed using LC-MS (QExactive^{TM}HF-X, ThermoFisher, Germany) with a HypersilGold (C18) column, scanning m/z 100−1500. Raw data

were preprocessed to predict molecular formulas based on molecular ion peaks and fragment ions, followed by comparison with the mzCloud, mzVault, and Masslist databases. Blank samples removed background ions, and the raw quantitative data were normalized. Compounds in QC samples that exhibited a Coefficient of Variation (CV) > 30% were removed, leading to the eventual identification and relative quantification outcomes of the metabolites. The identified metabolites were annotated with the KEGG, HMDB, and LIPID MAPS database.

Statistical analysis

The Shapiro-Wilk and Levene's tests evaluated normality and variance homogeneity in all datasets. An unpaired two-tailed Student's t-test was performed using SPSS 23.0 (IBM Corp., USA) software to compare the means of the two groups. For multi-group experimental data, ANOVA and Duncan's post hoc test were used. Growth performance was analyzed at the cage level, while all other parameters were analyzed at the individual level, with sample sizes detailed in the corresponding figure legends. Experimental data were expressed as mean ± standard error of the mean (SEM) or presented as box plots. $P < 0.05$ was considered statistically significant. Statistical analyses of data related to muscle fiber and intestinal morphology were conducted using Fiji ImageJ (version 1.54 m) software. GraphPad Prism (version 8.0, USA) and Adobe Illustrator 2022 (version 26.4.1) were used for figure generation and data image layout design.

Availability of data and materials

The "Gut microbiome sequencing data (fed with faba beans for 6 weeks)" are available in the NCBI SRA repository with the accession ID

https://www.ncbi.nlm.nih.gov/search/all/?term=PRJNA1311008, reference number PRJNA1311008.

The "Gut microbiome sequencing data (antibiotic treatment)" can be accessed in the NCBI SRA repository with the accession ID https://www.ncbi.nlm.nih.gov/search/all/?term=PRJNA1310288, reference number PRJNA1310288.

The "Gut microbiome sequencing data (WIMT)" are deposited in the NCBI SRA repository and can be found using the accession ID https://www.ncbi.nlm.nih.gov/search/all/?term=PRJNA1310847, reference number PRJNA1310847.

The "Muscle tissue transcriptome sequencing data" are stored in the NCBI SRA repository and are accessible via the accession ID https://www.ncbi.nlm.nih.gov/sra/PRJNA1344608, reference number PRJNA1344608.

The "SCFAs data from intestinal contents" are available in the NGDC OMIX repository with the accession ID https://ngdc.cncb.ac.cn/omix/release/OMIX012256, reference number OMIX012256.

The "SCFAs data from CS-CS" can be accessed in the NGDC OMIX repository using the accession ID https://ngdc.cncb.ac.cn/omix/release/OMIX012255, reference number OMIX012255.

The "Non-targeted metabolomics data of intestinal contents" are deposited in the MetaboLights repository and can be found using the accession ID https://www.ebi.ac.uk/metabolights/MTBLS13128, reference number MTBLS13128.

Acknowledgments

This work was supported by the National Natural Science Foundation of China (grant numbers U22A20532, 32473180); and the Special Fund for Henan Agriculture Research System (grant numbers HARS-22-16-S). The authors acknowledge the participants' contributions to this research, and we are grateful to Professor Xiaolin Meng, Doctor Qingyang Su, and Master Yuan Liu (College of Fisheries, Henan Normal University, Xinxiang, China) for isolating and culturing the *Cetobacterium somerae* CFH_001 strain.

Authors' contributions

All authors, LJC, YJL, YJZ, CBQ, LPY, XY and GXN contributed to the conceptualizations, methodology and experimentations of the manuscript. LJC, YJL and YJZ: investigation, animal husbandry, sample collection, measurement of experimental parameters, analysis, and interpretation of data. LJC: visualization and writing the original draft. LJC, YJL, and YJZ: writing, reviewing and editing. LJC, YJL, CBQ, LPY and XY: validation, analysis, and interpretation of data, reviewing and editing the manuscript. GXN: supervision, project administration and funding acquisition. All the authors reviewed and approved the final manuscript.

Competing interests

All the authors declare that they have no conflict of interest.

References

1. Wang, A. R., Ran, C., Ringø, E. & Zhou, Z. G. Progress in fish gastrointestinal microbiota research. *Reviews in Aquaculture* **10**, 626-640 (2018).
2. Feng, L. T., Chen, Z. N. & Bian, H. J. Skeletal muscle: molecular structure, myogenesis, biological functions, and diseases. *Medicine Communications* **5**, e649 (2024).
3. Hawley, J. A. Microbiota and muscle highway-two way traffic. *Nature Reviews Endocrinology* **16**, 71-72 (2020).
4. Chew, W. X. *et al*. Gut-muscle crosstalk. A perspective on influence of microbes on muscle function. *Frontiers in Medicine* (*Lausanne*) **9**, 1065365 (2023).
5. He, Y. W. *et al*. Gut microbes-muscle axis in muscle function and meat quality. *Science China-Life Sciences* Published online April 8 (2025).
6. Lahiri, S. *et al*. The gut microbiota influences skeletal muscle mass and function in mice. *Science Translational Medicine* **11**, eaan5662 (2019).
7. Liu, C. R. *et al*. Understanding the gut microbiota and sarcopenia: a systematic review. *Journal of Cachexia, Sarcopenia and Muscle* **12**, 1393-1407 (2021).
8. Frampton, J., Murphy, K. G., Frost, G. & Chambers, E. S. Short-chain fatty acids as potential regulators of skeletal muscle metabolism and function. *Nature Metabolism* **2**, 840-848 (2020).
9. Lei, J. Q. *et al*. Intestinal Microbiota Regulate Certain Meat Quality Parameters in Chicken. *Frontiers in Nutrition* **25**, 747705 (2022).
10. Luo, Z. B. *et al*. Fecal transplant from myostatin deletion pigs positively impacts the gut-muscle axis. *Elife* **12**, e81858 (2023).
11. Chapagain, P., Walker, D., Leeds, T., Cleveland, B. M. & Salem, M. Distinct microbial assemblages associated with genetic selection for high- and low- muscle yield in rainbow trout. *BMC genomics* **21**, 820 (2020).
12. Su, W. F. *et al*. Recirculating aquaculture-fasting strategy (RASF) to modulate gut microbiota and enhance the fish meat quality of bighead carp (*Aristichthys nobilis*). *Food Chemistry* **481**, 143946 (2025).
13. Wang, E. L. *et al*. Rice flowering improves the muscle nutrient, intestinal microbiota diversity, and liver metabolism profiles of tilapia (*Oreochromis niloticus*) in rice-fish symbiosis. *Microbiome* **10**, 231 (2022).
14. He, Y. L. *et al*. Decoding the gut-microbiota-muscle nexus: Multi-omics integration reveals mTOR

driven flesh modulation in rice-fish co-cultured common carp (*Cyprinus carpio*). *Aquaculture* **612**, 743090 (2026).

15. Wu, H. X. *et al*. Oligosaccharides improve the flesh quality and nutrition value of Nile tilapia fed with high carbohydrate diet. *Food Chemistry: Molecular Sciences* **3**, 100040 (2021).
16. Wu, H. X. *et al*. Microbiota derived butyrate affected the muscle texture of Nile tilapia (*Oreochromis niloticus*) fed with different protein sources. *Food Chemistry* **393**, 133392 (2022).
17. Zhang, Y., Liang, X., Zhan, W., Chen, L. & Lou, B. Short-chain fatty acids affect skeletal muscle composition, fiber recruitment, and metabolism of the small yellow croaker (*Larimichthys polyactis*). *Aquaculture Reports* **45**, 103169 (2025).
18. Li, L. K. *et al*. Valerate enhances flesh hardness by inhibiting muscle proliferation and differentiation in Nile tilapia (*Oreochromis niloticus*): An in vivo and in vitro study. *Aquaculture* **600**, 742222 (2025).
19. Khalili, T. S. & Sampels, S. Nutritional Value of Fish: Lipids, Proteins, Vitamins, and Minerals. *Reviews in Fisheries Science & Aquaculture* **26**, 243-253 (2018).
20. Song, D. Y. *et al*. Effects of faba bean on growth performance and fillet texture of Yellow River carp, *Cyprinus carpio haematopterus*. *Aquaculture Reports* **17**, 100379 (2020).
21. Yu, E. M. *et al*. Proteomic and metabolomic basis for improved textural quality in crisp grass carp (*Ctenopharyngodon idellus* C.et V) fed with a natural dietary prooxidant. *Food Chemistry* **325**, 126906 (2020).
22. Chen, L. J. *et al*. Reactive oxygen species (ROS)-mediated regulation of muscle texture in grass carp fed with dietary oxidants. *Aquaculture* **8**, 737150 (2021).
23. Li, Z. F. *et al*. Diet influences the accumulation of short-chain fatty acids associated with the gut microbiota in the grass carp (*Ctenopharyngodon idellus*) hindgut. *Applied Ecology and Environmental Research* **17**,13435-13453 (2019).
24. Zhou, L. *et al*. Intestinal Microbiota of Grass Carp Fed Faba Beans: A Comparative Study. *Microorganisms* **7**, 465 (2019).
25. Yu, K. *et al*. Exploring the muscle-hardening mechanisms via the muscle-gut axis in tilapia (*Oreochromis niloticus*) fed with faba bean (*Vicia faba* L.) supplementary diets. *Aquaculture Reports* **37**, 102268 (2024).
26. Li, N. *et al*. Spatial heterogeneity of bacterial colonization across different gut segments following inter-species microbiota transplantation. *Microbiome* **8**, 161 (2020).
27. Yang, Y. P. *et al*. Whole intestinal microbiota transplantation is more effective than fecal microbiota transplantation in reducing the susceptibility of DSS-induced germ-free mice colitis. *Frontiers in*

Immunology **14**, 1143526 (2023).

28. Listrat, A. *et al*. How Muscle Structure and Composition Influence Meat and Flesh Quality. *The Scientific World Journal* **2016**, 3182746 (2016).
29. Wang, Z., *et al*. The flesh texture of teleost fish: Characteristics and interventional strategies. *Reviews in Aquaculture* **16**, 508-535 (2024).
30. Dong, M. *et al*. Dietary protein levels changed the hardness of muscle by acting on muscle fiber growth and the metabolism of collagen in sub-adult grass carp (*Ctenopharyngodon idella*). *Journal of Animal Science and Biotechnology* **13**, 109 (2022).
31. Shi, Y. *et al*. Dietary sanguinarine supplementation recovers the decrease in muscle quality and nutrient composition induced by high-fat diets of grass carp (*Ctenopharyngodon idella*). *Animal Nutrition* **17**, 208-219 (2024).
32. Zhang, X. Y. *et al*. Mechanisms of hepatic dysfunction in Nile tilapia (*Oreochromis niloticus*) fed a high-fava bean (*Vicia faba* L.) diet. *Animal Nutrition* **22**, 61-71 (2025).
33. Xu, G. L. *et al*. Impact of Faba Bean (*Vicia faba* L.) Diet and Subsequent Withdrawal on GIFT Tilapia (*Oreochromis niloticus*) Muscle Quality. *Fishes* **10**, 170 (2025).
34. Gallet, A. *et al*. Disruption of fish gut microbiota composition and holobiont's metabolome during a simulated Microcystis aeruginosa (*Cyanobacteria*) bloom. *Microbiome* **11**, 108 (2023).
35. Qi, X. Z. *et al*. Vitamin B12 produced by *Cetobacterium somerae* improves host resistance against pathogen infection through strengthening the interactions within gut microbiota. *Microbiome* **11**, 135 (2023).
36. Wang, A. R. *et al*. Intestinal *Cetobacterium* and acetate modify glucose homeostasis via parasympathetic activation in zebrafish. *Gut Microbes* **13**, 1-15 (2021).
37. Fan, Y. & Pedersen, O. Gut microbiota in human metabolic health and disease. *Nature Reviews Microbiology* **19**, 55-71 (2021).
38. Novelle, M. G., Naranjo-Martínez, B., López-Cάnovas, J. L. & Díaz-Ruiz A. Fecal microbiota transplantation, a tool to transfer healthy longevity. *Ageing Research Reviews* **103**, 102585. (2025).
39. Mo, X. X. *et al*. Faecal microbiota transplantation from young rats attenuates age-related sarcopenia revealed by multiomics analysis. *Journal of Cachexia, Sarcopenia and Muscle* **14**, 2168-2183 (2023).
40. Yin, J., *et al*. Obese Ningxiang pig-derived microbiota rewires carnitine metabolism to promote muscle fatty acid deposition in lean DLY pigs. *Innovation (Camb)* **4**, 100486 (2023).
41. Zhou, H. *et al*. Gut microbiota absence and transplantation affect growth and intestinal functions: An investigation in a germ-free pig model. *Animal Nutrition* **7**, 295-304 (2021).

42. Wu, D. Y. *et al*. Effects of fecal microbiota transplantation and fecal virome transplantation on LPS-induced intestinal injury in broilers. *Poultry Science* **103**, 103316 (2024).
43. Liu, Q. Y. *et al*. Early fecal microbiota transplantation continuously improves chicken growth performance by inhibiting age-related *Lactobacillus* decline in jejunum. *Microbiome* **13**, 49. (2025).
44. Han, Q., Huang, X. G., Yan, F. Y., Yin, J. & Xiao, Y. P. The Role of Gut Microbiota in the Skeletal Muscle Development and Fat Deposition in Pigs. *Antibiotics* (*Basel*) **11**, 793 (2022).
45. Meng, Z. et al. Nutritive value of faba bean (*Vicia faba* L.) as a feedstuff resource in livestock nutrition: A review. Food Science & Nutrition 9, 5244-5262 (2021).
46. Hintze, K. J. *et al*. Broad scope method for creating humanized animal models for animal health and disease research through antibiotic treatment and human fecal transfer. *Gut Microbes* **5**, 183-91 (2014).
47. Ruiz, A., Gisbert, E. & Andree, K. B. Impact of the diet in the gut microbiota after an inter-species microbial transplantation in fish. *Scientific Reports* **14**, 4007 (2024).
48. Han, Z. R. *et al*. Fecal microbiota transplantation accelerates restoration of florfenicol-disturbed intestinal microbiota in a fish model. *Communications Biology* 7, 1006 (2024).
49. Garlock, T. M. *et al*. Environmental, economic, and social sustainability in aquaculture: the aquaculture performance indicators. *Nature Communications* **15**, 5274 (2024).
50. Zhang, Z. M. *et al*. Potential Functions of the Gut Microbiome and Modulation Strategies for Improving Aquatic Animal Growth. *Reviews in Aquaculture* **17**, e12959 (2025).
51. Zhang, J. M. *et al*. Effects of fecal bacteria on growth, digestive capacity, antioxidant capacity, intestinal health of large yellow croaker (*Larimichthys crocea*) larvae. *Aquaculture* **562**, 738796 (2023).
52. Raymo, G., Ali, A., Ahmed, R. O. & Salem, M. Early-Life Fecal Transplantation from High Muscle Yield Rainbow Trout to Low Muscle Yield Recipients Accelerates Somatic Growth through Respiratory and Mitochondrial Efficiency Modulation. *Microorganisms* **12**, 261 (2024).
53. Song, D. Y. *et al*. Effects of faba bean (*Vicia faba L*.) on fillet quality of Yellow River carp (*Cyprinus carpio*) via the oxidative stress response. *Food Chemistry* **388**, 132953 (2022).
54. Ghosh, S. S., Wang, J., Yannie, P. J. & Ghosh, S. Intestinal Barrier Dysfunction, LPS Translocation, and Disease Development. *Journal of the Endocrine Society* **4**, bvz039 (2020).
55. Kong, M. *et al*. A Well-Established Gut Microbiota Enhances the Efficiency of Nutrient Metabolism and Improves the Growth Performance of *Trachinotus ovatus*. *International Journal of Molecular Sciences* **25**, 5525 (2024).
56. Lan, X. *et al*. Alterations of the Gut Microbiota and Metabolomics Associated with the Different Growth Performances of *Macrobrachium rosenbergii* Families. *Animals* (*Basel*) **13**, 1539 (2023).

57. Chapman, M. A., Mukund, K., Subramaniam, S., Brenner, D. & Lieber, R. L. Three distinct cell populations express extracellular matrix proteins and increase in number during skeletal muscle fibrosis. *American Journal of Physiology-Cell Physiology* **312**, C131-C143 (2017).
58. Chen, W. J., Lin, I. H., Lee, C. W. & Chen, Y. F. Aged Skeletal Muscle Retains the Ability to Remodel Extracellular Matrix for Degradation of Collagen Deposition after Muscle Injury. *International Journal of Molecular Sciences* **22**, 2123 (2021).
59. Hellerschmied, D. *et al*. Molecular features of the UNC-45 chaperone critical for binding and folding muscle myosin. *Nature Communications* **10**, 4781 (2019).
60. Hadjisavva, R., Anastasiou, O., Ioannou, P. S., Zheltkova. M. & Skourides P. A. Adherens junctions stimulate and spatially guide integrin activation and extracellular matrix deposition. *Scientific Reports* **40**, 111091 (2022).
61. Li, Y. B. *et al*. Microbial metabolite sodium butyrate enhances the anti-tumor efficacy of 5-fluorouracil against colorectal cancer by modulating PINK1/Parkin signaling and intestinal flora. *Scientific Reports* **14**, 13063 (2024).
62. Liu, L., Fu, C.Y. & Li, F. C. Acetate Affects the Process of Lipid Metabolism in Rabbit Liver, Skeletal Muscle and Adipose Tissue. *Animals* (*Basel*) **9**, 799 (2019).
63. Qian, L. *et al*. Peroxisome proliferator-activated receptor gamma coactivator-1 (PGC-1) family in physiological and pathophysiological process and diseases. *Signal transduction and targeted therapy* **9**, 50 (2024).
64. Fasano, C., Disciglio, V., Bertora, S., Signorile, M. L. & Simone, C. FOXO3a from the Nucleus to the Mitochondria: A Round Trip in Cellular Stress Response. *Cells* **8**, 1110 (2019).
65. Stecher, B. The Roles of Inflammation, Nutrient Availability and the Commensal Microbiota in Enteric Pathogen Infection. Microbiology Spectrum **3** (2015).
66. He, X. G. *et al*. Effects of Broad Bean Diet on the Growth Performance, Muscle Characteristics, Antioxidant Capacity, and Intestinal Health of Nile Tilapia (*Oreochromis niloticus*). *Animals* (*Basel*) **13**, 3705 (2023).
67. Li, L. K. *et al*. Intestinal microbiota contributes to the heterogeneity of fat deposition by promoting mitochondrial fatty acid β-oxidation. *Gut Microbes* **17**, 2593076 (2025).
68. Mann, E.R., Lam, Y. K & Uhlig, H. H. Short-chain fatty acids: linking diet, the microbiome and immunity. *Nature Reviews Immunology* **24**, 577-595 (2024).
69. Liao, X. M. et al. Vitamin D influences gut microbiota and acetate production in zebrafish (*Danio rerio*) to promote intestinal immunity against invading pathogens. *Gut microbes* **15**, 2187575 (2023).

70. Chen, Y. X. *et al*. Probiotic efficacy of *Cetobacterium somerae* (CGMCC No. 28843): promoting intestinal digestion, absorption, and structural integrity in juvenile grass carp (*Ctenopharyngodon idella*). *Journal of Animal Science and Biotechnology* **16**, 103 (2025).
71. Wang, S. D., Li, X., Zhang, M. Z. & Li, M. *Cetobacterium somerae*-derived argininosuccinic acid promotes intestinal and liver ureagenesis to alleviate ammonia intoxication. *Microbiome* **13**, 163 (2025).
72. Cao, X. L. *et al*. Determining the Potential Roles of Branched-Chain Amino Acids in the Regulation of Muscle Growth in Common Carp (*Cyprinus carpio*) Based on Transcriptome and MicroRNA Sequencing. *Aquaculture Nutrition*. **2023**, 7965735 (2023).
73. Cao, X. L. *et al*. Branched-Chain Amino Acids Target miR-203a/fosb Axis to Promote Skeletal Muscle Growth in Common Carp (*Cyprinus carpio*). *Aquaculture Nutrition* **2025**, 9406490 (2025).
74. Chen, Q. *et al*. An integrated analysis of transcriptome and metabolome reveals three BCAAs relieve lipid accumulation by inhibiting lipid synthesis and promoting lipid oxidation in the liver of largemouth bass (*Micropterus salmoides*). *Aquaculture* **581**, 19 (2024).
75. Maruta, H., Abe, R. & Yamashita, H. Effect of Long-Term Supplementation with Acetic Acid on the Skeletal Muscle of Aging Sprague Dawley Rats. *International journal of molecular sciences* **23**, 4691 (2022).
76. Iwao, M. *et al*. Supplementation of branched-chain amino acids decreases fat accumulation in the liver through intestinal microbiota-mediated production of acetic acid. *Scientific reports* **10**, 18768 (2020).
77. Li, L. *et al*. Acetic Acid Influences BRL-3A Cell Lipid Metabolism via the AMPK Signalling Pathway. *Cellular Physiology and Biochemistry* **45**, 2021-2030 (2018).
78. Liu, Y. *et al*. Vitamin D3 mitigates lipopolysaccharide-induced oxidative stress, tight junction damage and intestinal inflammatory response in yellow catfish, *Pelteobagrus fulvidraco*. *Comp Biochem Physiol C Toxicol Pharmacol* **243**, 108982 (2021).
79. Doyle, A., Zhang G. H., Abdel Fattah, E. A., Eissa, N. T. & Li, Y. P. Toll-like receptor 4 mediates lipopolysaccharide-induced muscle catabolism via coordinate activation of ubiquitin-proteasome and autophagy-lysosome pathways. *FASEB Journal* **25**, 99-110 (2011).
80. Dai, Y. J. *et al*. Molecular cloning of adipose triglyceride lipase (ATGL) gene from blunt snout bream and its expression after LPS-induced TNF-α factor. *Fish Physiology and Biochemistry* **44**, 1143-57 (2018).
81. Feng, J. C., *et al*. Dietary sodium acetate (SA) improves the growth performance, intestinal health, and carbohydrate metabolism of juvenile common carp (*Cyprinus carpio*). *Aquaculture Reports* **27**, 101350 (2022).

82. Xie, M. X., *et al*. Effects of *Cetobacterium somerae* fermentation product on gut and liver health of common carp (*Cyprinus carpio*) fed diet supplemented with ultra-micro ground mixed plant proteins. *Aquaculture* **543**, 736943 (2021).
83. Mi, J. L. *et al*. Dietary (−)-Epicatechin supplementation regulates myofiber development, fillet quality, and antioxidant status of Yellow River carp (*Cyprinus carpio*). *Aquaculture* **572**, 739542 (2023).
84. Campos, V. J. *et al*. Characterization of fillets and skins from two varieties of genetically improved farmed Nile tilapia (*Oreochromis niloticus*). *PLoS ONE* **20**, e0314928 (2025).
85. Cheng, L. J. *et al*. *Lactiplantibacillus plantarum* Ameliorated Growth Performance and Intestinal Inflammation by Modulating Gut Microbial Structure and Function of Yellow River Carp (*Cyprinus carpio*). *Probiotics Antimicrob Proteins* Published online May 30 (2025).
86. Livak, K. J. & Schmittgen, T. D. Analysis of relative gene expression data using real-time quantitative PCR and the 2(-Delta Delta C(T)) Method. *Methods* **25**, 402-408 (2001).

Figure legends

Fig. 1 Effects of faba bean diet on Yellow River carp growth and muscle quality. A Experimental groups and timeline. **B** Representative images of fish from the two experimental groups. **C** Comparison of growth performance and FCR in CF and FB groups (n=3). **D** Muscle texture properties of raw and cooked samples in the CF and FB groups (n=18). **E** White muscle tissue below the dorsal fin, hematoxylin-eosin (HE) stained, 100 × magnification (scale bar, 200 μm). **F** Muscle fiber diameter distribution, average minimum Feret diameter (MFD), density, and the percentage of total area occupied by muscle fibers were evaluated in both CF and FB groups (n=12). **G** Total hydroxyproline (Hyp) and collagen content in CF and FB groups (n=12). **H** Muscle composition (wet weight, WW) in different experimental groups (n=12). The data in panels C, D and F (muscle fiber diameter distribution) were presented as mean ± SEM. Other data were presented as box plots, with the boxes indicating the median and interquartile range. Experimental data were analyzed by an unpaired, 2-tailed Student's *t* test. $P < 0.05$ was considered statistically significant, ns ($P > 0.05$); * ($P \leq 0.05$); ** ($P \leq 0.01$); *** ($P \leq 0.001$).

Fig. 2 Effects of faba bean diet on intestinal microbiota composition of Yellow River carp. A Alpha diversity indices in CF and FB groups (n=3). **B** Non-metric Multidimensional Scaling (NMDS) analysis. **C** The heatmap analysis of species composition indicates that deeper shades of red signify higher abundance, whereas deeper shades of green represent lower abundance (Top 20 species at the genus level). **D** Heatmap of Spearman's correlations between differential microbiota

and muscle quality. Red color, positive correlation; green color, negative correlation; * ($P \leq 0.05$), ** ($P \leq 0.01$).

Fig. 3 Effects of WIMT on growth performance, antioxidant capacity and muscle texture of Yellow River carp. A Experimental groups and corresponding timeline. **B** The key procedural steps in WIMT. **C** Representative fish images in different experimental groups. **D** Growth performance in different experimental groups (n=3). **E** Serum antioxidant capacity in different experimental groups (n=12). **F** Muscle antioxidant capacity in different experimental groups (n=12). **G** The mRNA expression levels of antioxidant-related genes (n=12). **H** Muscle texture properties of raw and cooked samples in different experimental groups (n=18). The two experimental groups were compared exclusively with the CG group, experimental data were analyzed by an unpaired, 2-tailed Student's *t* test. The data in panels D and H were presented as mean ± SEM; the data in panels E, F and G were presented as box plots, with the boxes indicating the median and interquartile range. $P < 0.05$ was considered statistically significant, ns ($P > 0.05$); * ($P \leq 0.05$); ** ($P \leq 0.01$); *** ($P \leq 0.001$).

Fig. 4 Effects of WIMT on muscle quality-related indicators and transcriptome in Yellow River carp. A Masson staining of the white muscle tissue below the dorsal fin at 100 × magnification (scale bars, 200 μm) showed collagen fibers in blue and muscle fibers in red. **B** Muscle fiber diameter distribution, average MFD, density, and the percentage of total area occupied by muscle fibers were evaluated in different experimental groups (n=12). **C** Collagen

content and solubility in different experimental groups (n=12). **D** Muscle composition in different experimental groups (n=12). **E** Volcano plot of differentially expressed genes (DEGs) in PCFB vs CG group (n=3). **F** Volcano plot of DEGs in WIMT vs CG group (n=3). **G** KEGG pathway enrichment analysis of DEGs in PCFB vs CG group. **H** KEGG pathway enrichment analysis of DEGs in WIMT vs CG group. **I** Relative expression of muscle genes related to autophagy and lipid metabolism in the different experimental groups (n=12). **J** Relative expression of muscle genes related to the AMPK-PGC-1α-FoxO pathway in the different experimental groups (n=12). Data analysis followed the same procedures as shown in Fig. 3. The data in panels B (muscle fiber diameter distribution) and C (collagen content) were presented as mean ± SEM. Other data were presented as box plots, with the boxes indicating the median and interquartile range.

Fig. 5 Effects of WIMT on intestinal structure and barrier function of Yellow River carp. A Representative intact intestine from all experimental groups. **B** Intestinal tissue sections were evaluated by HE staining at 20 × magnification (scale bar, 1000 μm) and 100 × magnification (scale bar, 200 μm) (n=12). **C** Entire intestinal lengths (n=18). **D** Intestinal villus height and muscularis thickness (n=12) across experimental groups. **E** Intestinal and serum LPS levels in different groups (n=9). **F** Gene expression of intestinal immunity and barrier function in different experimental groups (n=12). Data analysis followed the same procedures as shown in Fig. 3; data were presented as box plots, with boxes indicating the median and interquartile range.

Fig. 6 Effects of short-term antibiotic treatment on gut microbiota and serum biochemical in

Yellow River carp. A Alpha-diversity index (n=4). **B** Hierarchical clustering analysis at the phylum level using the Bray-Curtis distance algorithm. **C** Significance analysis of differences in key phyla (n=4). **D** Serum biochemical parameters in BA and AA groups (n=12). BA, before antibiotic treatment; AA, after antibiotic treatment. Data analysis followed the procedures shown in Fig. 1; data were presented as box plots, with boxes indicating the median and interquartile range.

Fig. 7 Effects of WIMT on gut microbiota structure in Yellow River carp. A Analysis of alpha-diversity index in different experimental groups (n=3). **B** Microbial structure NMDS analysis of different experimental groups (with Stress < 0.05). **C** Taxonomic composition analysis at the phylum level (Top 20). **D** Taxonomic composition analysis at the genus level (Top 20). **E** Significance analysis of species-level clustering heatmap in different experimental groups (Top 20, red triangles indicate significant differences). **F** Random forest analysis at the species level in different experimental groups.

Fig. 8 Effects of WIMT on the function of intestinal microbiota in Yellow River carp. A PCA analysis of microbial function in different experimental groups. **B** Bugbase functional prediction analysis across different experimental groups. **C** Analysis of differential metabolic pathways based on the MetaCyc database (Top 20). **D** Analysis of differential metabolic pathways based on the KEGG database (Top 20).

Fig. 9 Effects of WIMT on gut microbiota metabolites in Yellow River carp. A Comparative analysis of SCFAs in gut contents of different experimental groups (n=4). **B** SCFAs content in CS-CS (n=3). **C** The classification and proportion of metabolites in the CG and WIMT groups were analyzed in positive ion modes (n=4). **D** The classification and proportion of metabolites in the CG and WIMT groups were analyzed in negative ion modes (n=4). **E** Volcano plot of differential metabolites in the WIMT vs CG comparison (positive ion mode). Significant metabolites were selected based on VIP > 1.0, |FC| > 2, and $P < 0.05$. **F** Volcano plot of differential metabolites in the WIMT vs CG comparison (negative ion mode). **G** PCA analysis of CG and WIMT groups under positive ion modes. **H** PCA analysis of CG and WIMT groups under negative ion modes. **I** Heatmap analysis of the top 10 significantly upregulated different metabolites in the CG and WIMT groups under positive ion modes. **J** Heatmap analysis of the top 10 significantly upregulated different metabolites in the CG and WIMT groups under negative ion modes. **K** KEGG functional enrichment analysis of differential metabolites in the WIMT vs CG comparison (positive ion mode). **L** KEGG functional enrichment analysis of differential metabolites in the WIMT vs CG comparison (negative ion mode). The data in panel A analysis followed the same procedures as shown in Fig. 3, and was presented as box plots, with the boxes indicating the median and interquartile range. Data in panel B was presented as mean ± SEM.

Fig. 10 Effects of *C. somerae* and sodium acetate on muscle quality of Yellow River carp. A Experimental design and timeline for the feeding experiment. **B** Muscle composition (dry matter,

crude fat, and crude protein) and collagen content in different experimental groups (n=12). **C** Textural characteristics of muscle in different experimental groups (n=18). **D** Relative expression of autophagy and lipid metabolism-related genes in muscle across experimental groups (n=12). **E** Relative expression of AMPK-PGC-1α-FoxO pathway-related genes in muscle across experimental groups (n=12). Experimental data were analyzed using ANOVA and Duncan's test. Data in panel B was presented as mean ± SEM, other data were presented as box plots, with the boxes indicating the median and interquartile range. Different letters indicated significant differences ($P < 0.05$). Lowercase letters were used for comparisons under normal physiological conditions (CG, CS and SA groups), while uppercase letters indicated comparisons under intestinal inflammation (CG-PBS, LPS and CS-LPS groups).

Fig. 11 Exploring the effects of faba bean-induced microbiota changes on muscle quality in Yellow River carp. Identification of *C. somerae* and acetic acid as a microbial correlate to muscle quality improvement through WIMT.

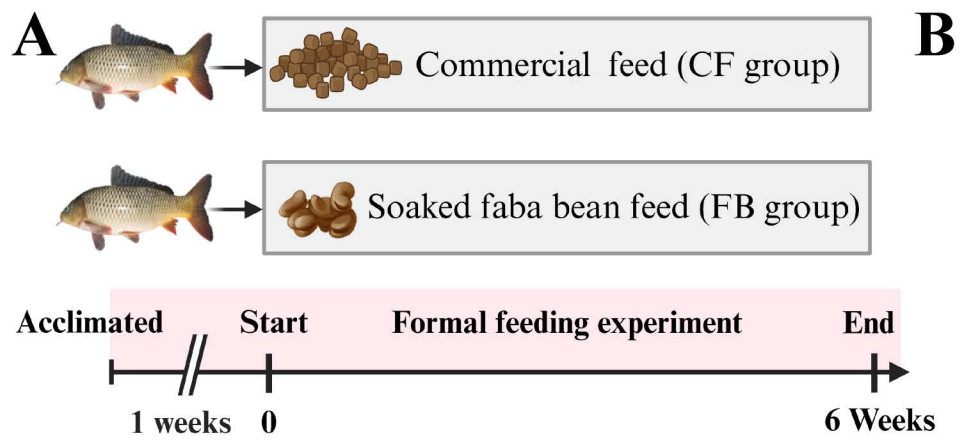
A
Commercial feed (CF group)
Soaked faba bean feed (FB group)
Acclimated
Start
Formal feeding experiment
End
1 weeks
0
6 Weeks


B
CF
FB

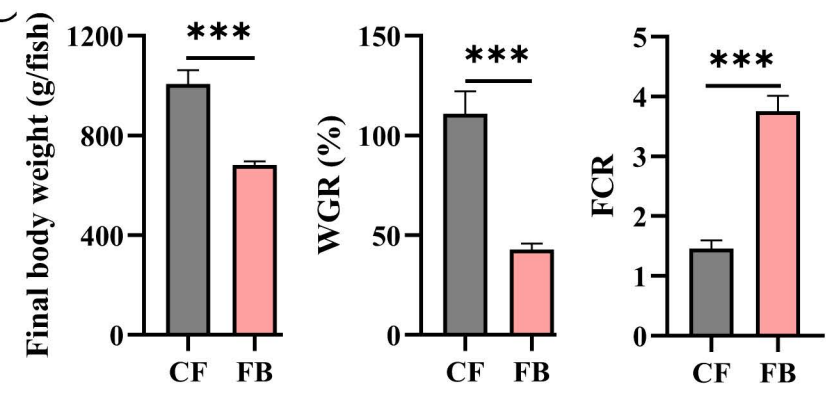
C
Final body weight (g/fish)
WGR (%)
FCR
CF
FB

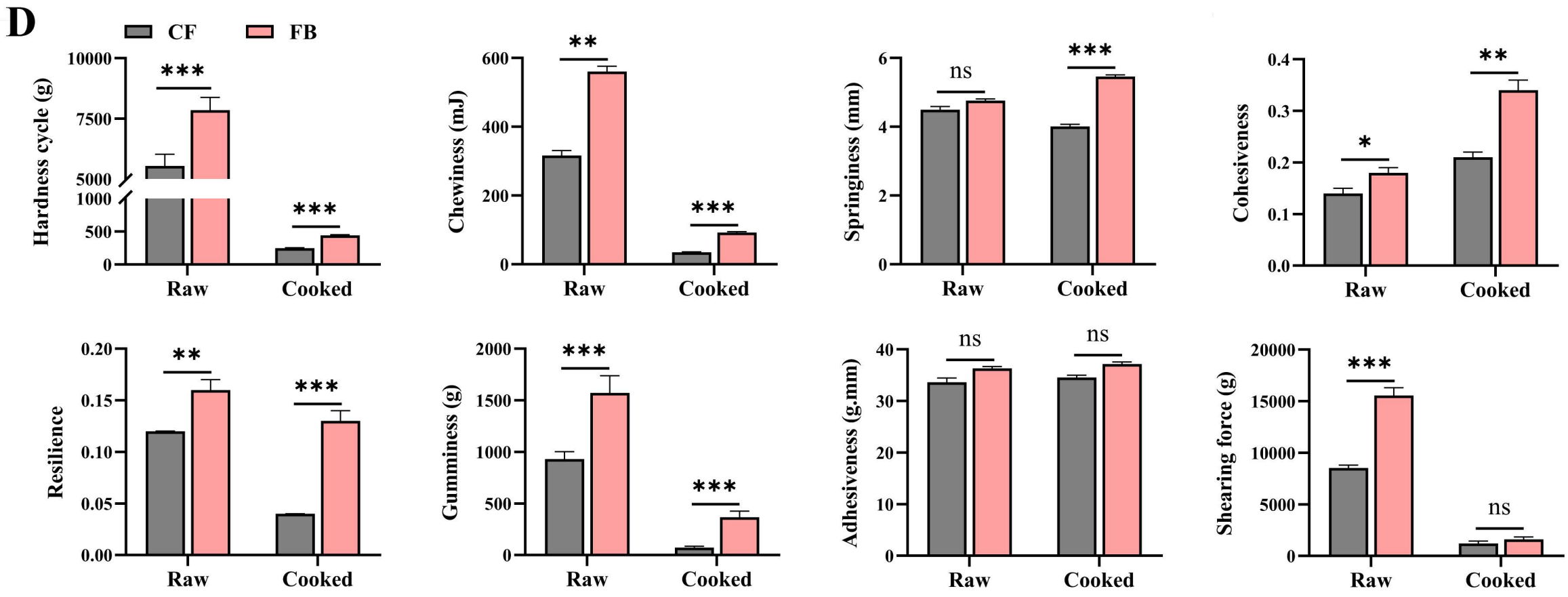
D
CF
FB
Hardness cycle (g)
Chewiness (mJ)
Springiness (mm)
Cohesiveness
Resilience
Gumminess (g)
Adhesiveness (g.mm)
Shearing force (g)
Raw
Cooked

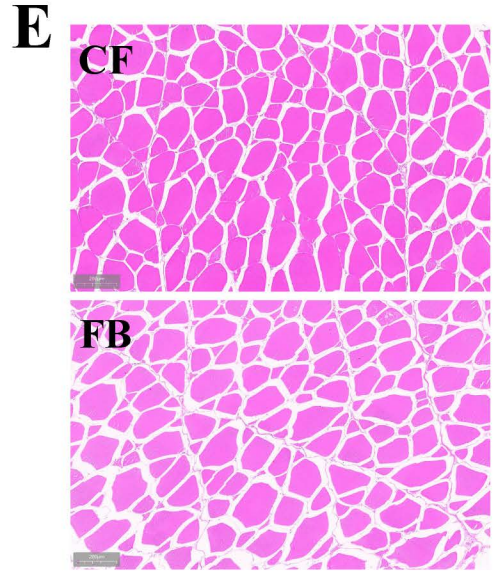
E
CF
FB

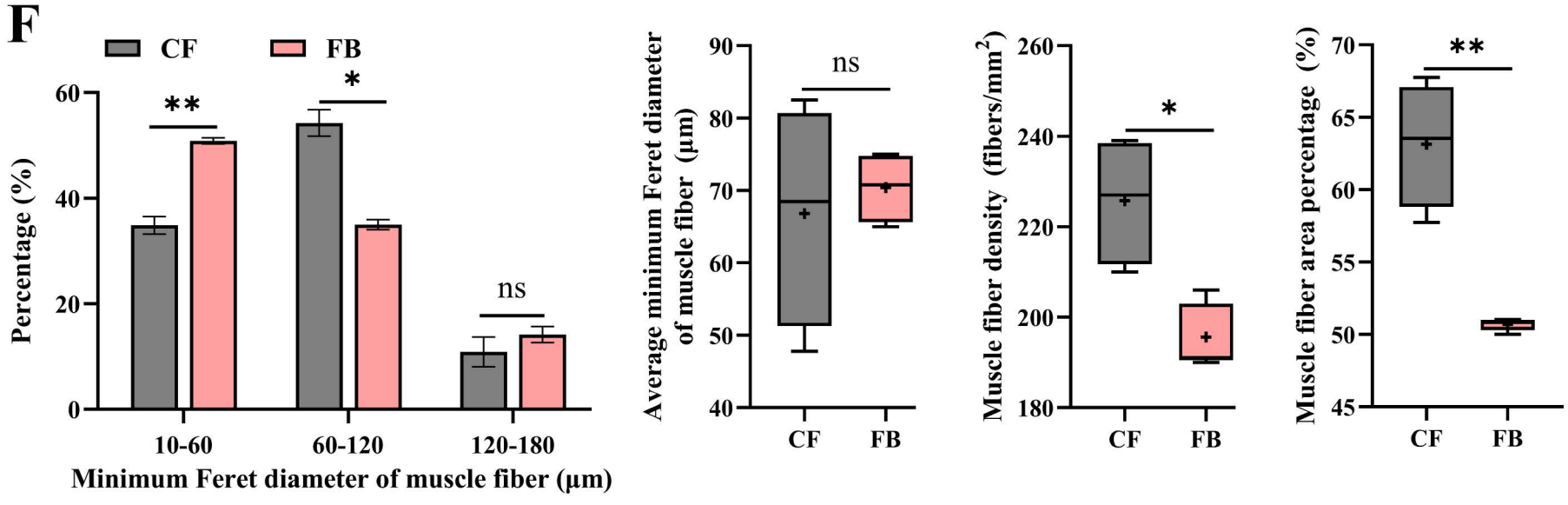
F
CF
FB
Percentage (%)
10-60
60-120
120-180
Minimum Feret diameter of muscle fiber (μm)
Average minimum Feret diameter of muscle fiber (μm)
Muscle fiber density (fibers/mm2)
Muscle fiber area percentage (%)

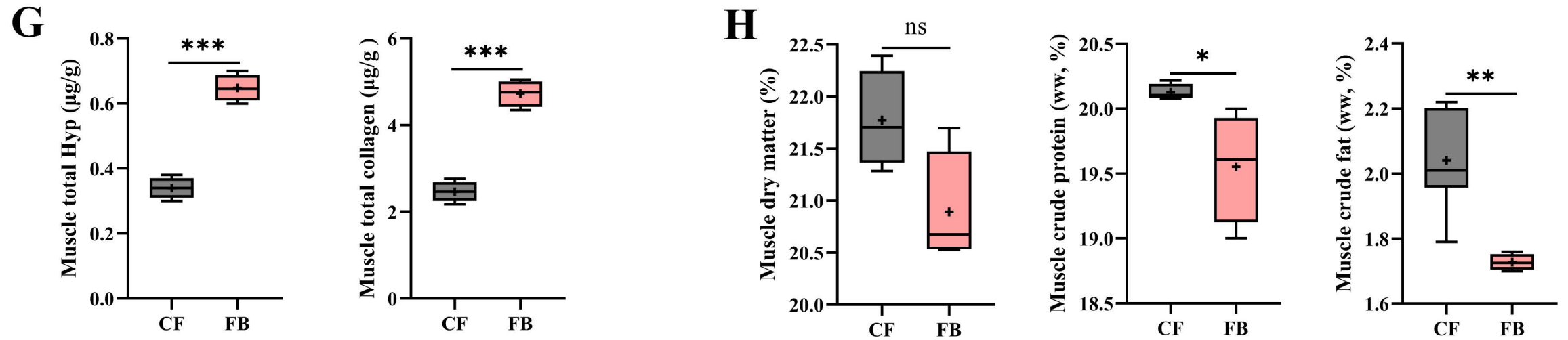
G
Muscle total Hyp (μg/g)
Muscle total collagen (μg/g)
H
Muscle dry matter (%)
Muscle crude protein (ww, %)
Muscle crude fat (ww, %)
CF
FB

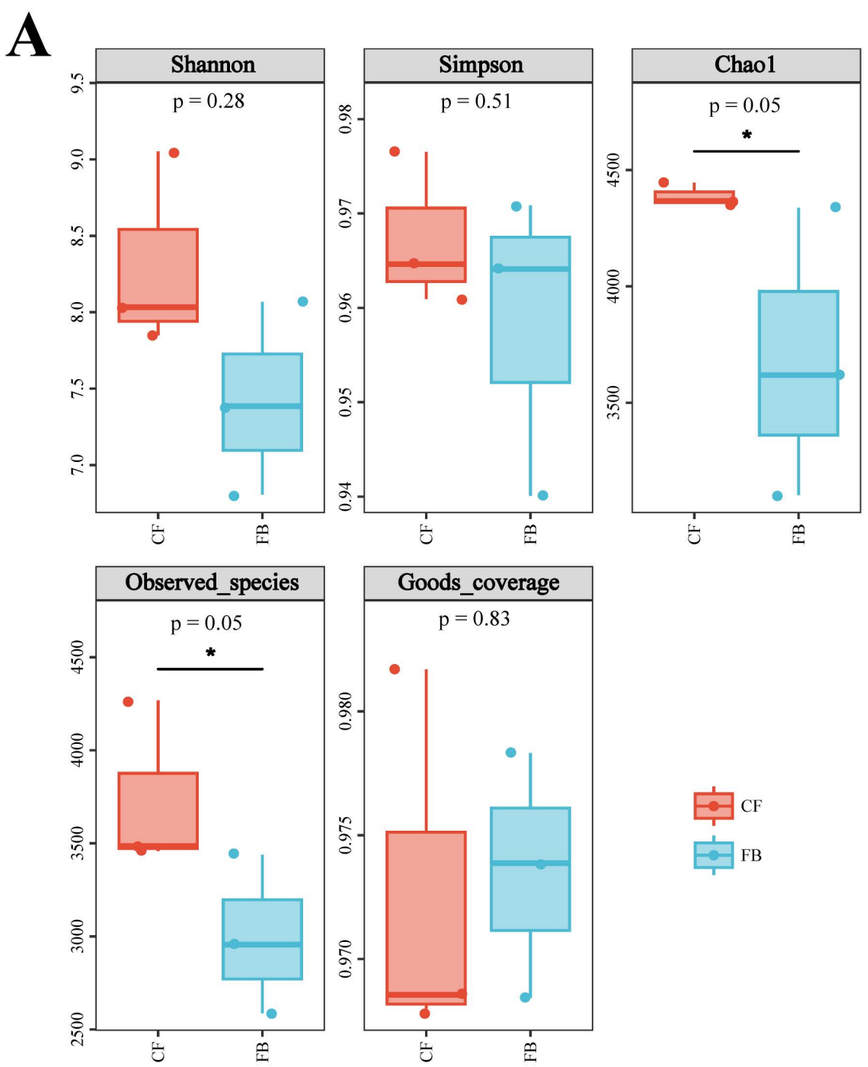
A
Shannon
p = 0.28
Simpson
p = 0.51
Chao1
p = 0.05
*
Observed_species
p = 0.05
*
Goods_coverage
p = 0.83
CF
FB

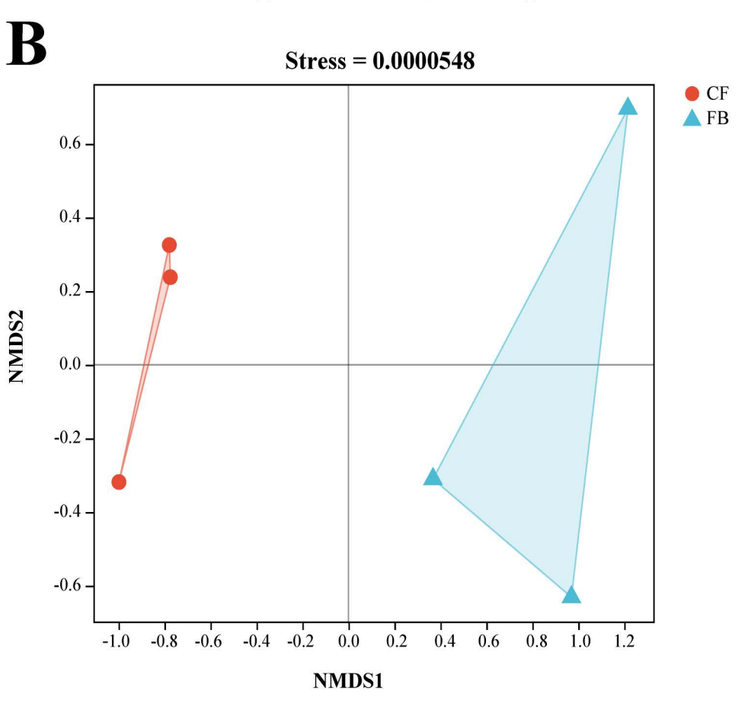
B
Stress = 0.0000548
CF
FB
NMDS1
NMDS2

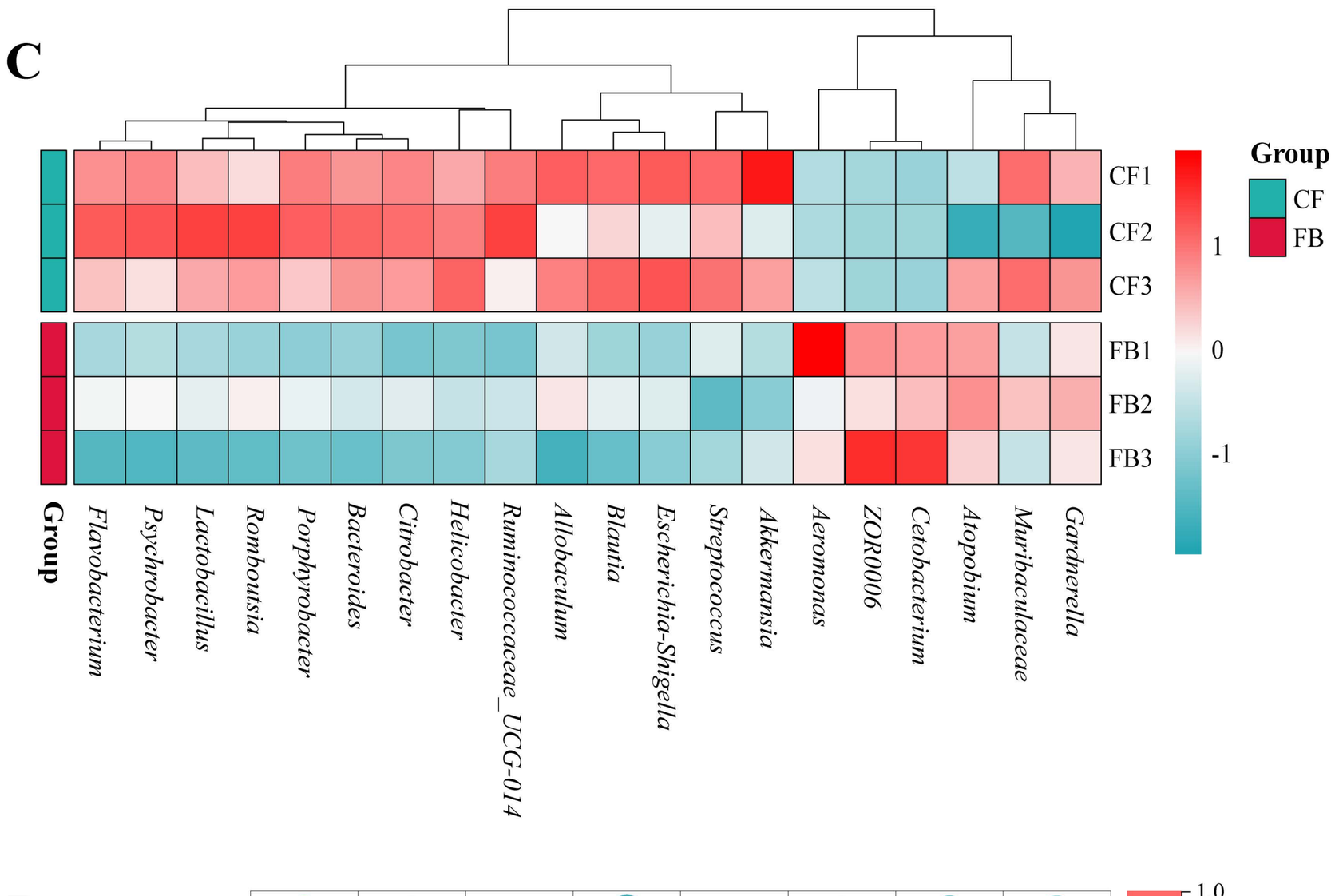
C
Group
CF
FB
CF1
CF2
CF3
FB1
FB2
FB3
1
0
-1
Flavobacterium
Psychrobacter
Lactobacillus
Romboutsia
Porphyrobacter
Bacteroides
Citrobacter
Helicobacter
Ruminococcaceae_UCG-014
Allobaculum
Blautia
Escherichia-Shigella
Streptococcus
Akkermansia
Aeromonas
ZOR0006
Cetobacterium
Atopobium
Muribaculaceae
Gardnerella

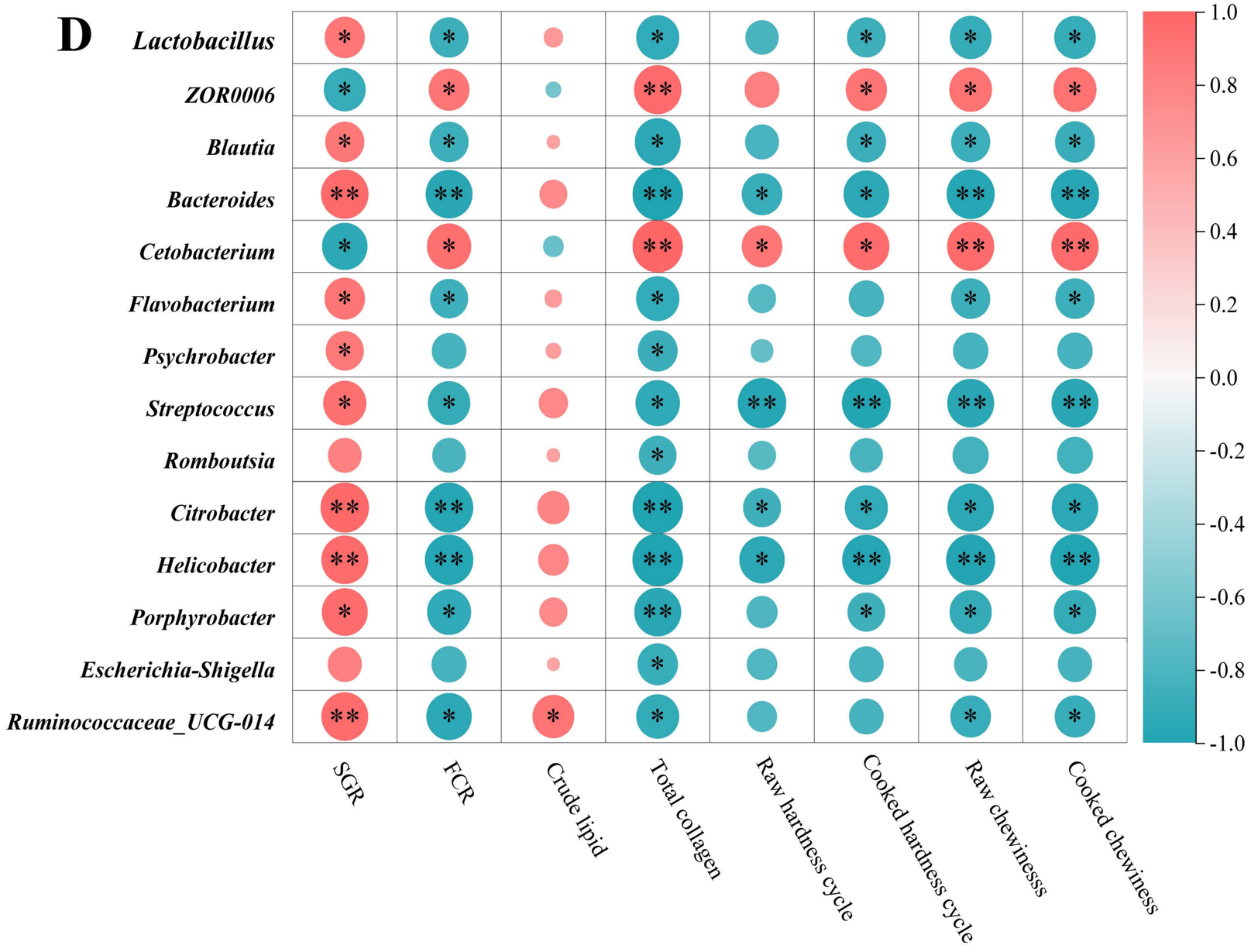
D
Lactobacillus
ZOR0006
Blautia
Bacteroides
Cetobacterium
Flavobacterium
Psychrobacter
Streptococcus
Romboutsia
Citrobacter
Helicobacter
Porphyrobacter
Escherichia-Shigella
Ruminococcaceae_UCG-014
SGR
FCR
Crude lipid
Total collagen
Raw hardness cycle
Cooked hardness cycle
Raw chewiness
Cooked chewiness
1.0
0.8
0.6
0.4
0.2
0.0
-0.2
-0.4
-0.6
-0.8
-1.0

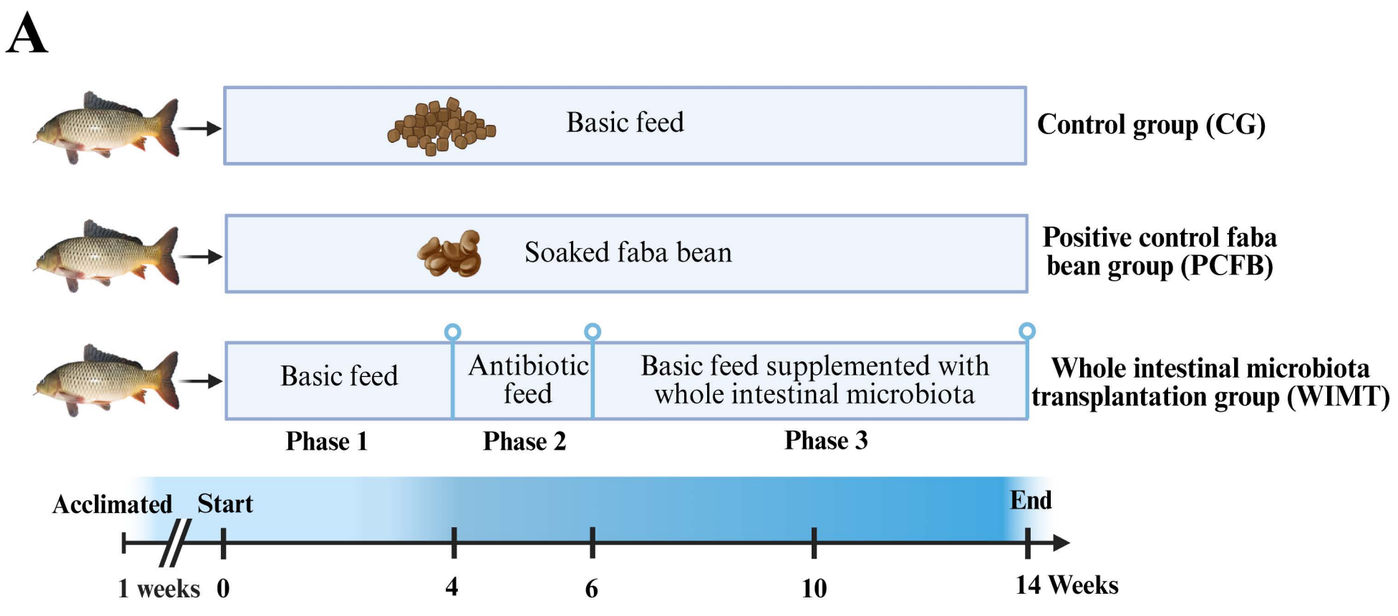
A
Basic feed
Control group (CG)
Soaked faba bean
Positive control faba bean group (PCFB)
Basic feed
Antibiotic feed
Basic feed supplemented with whole intestinal microbiota
Whole intestinal microbiota transplantation group (WIMT)
Phase 1
Phase 2
Phase 3
Acclimated
Start
End
1 weeks
0
4
6
10
14 Weeks

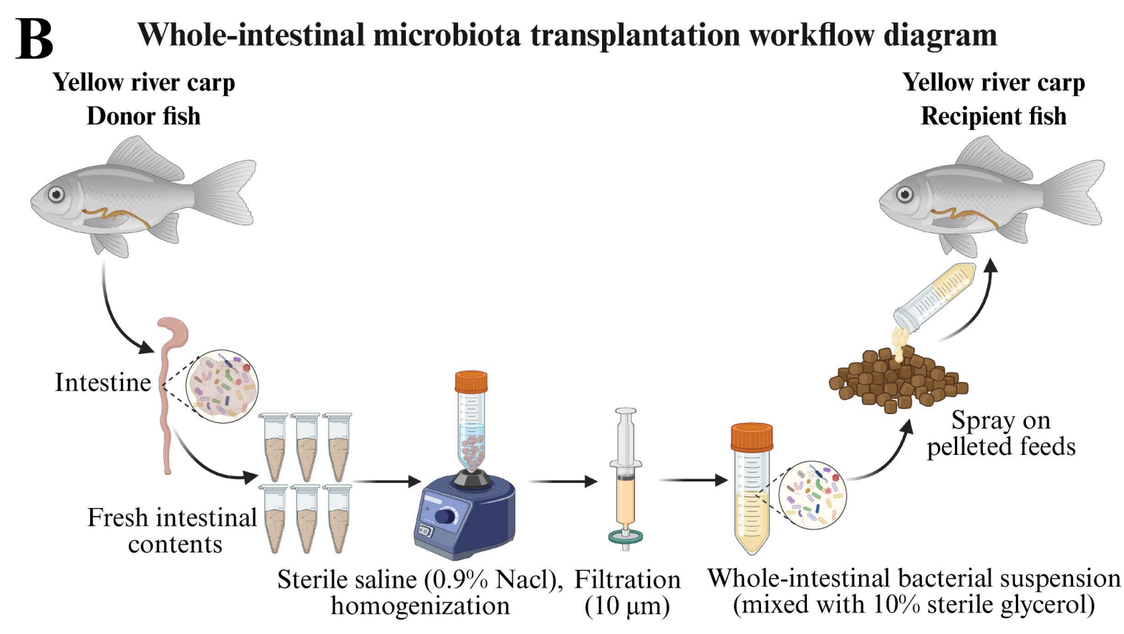
B
Whole-intestinal microbiota transplantation workflow diagram
Yellow river carp
Donor fish
Yellow river carp
Recipient fish
Intestine
Fresh intestinal contents
Sterile saline (0.9% Nacl), homogenization
Filtration (10 μm)
Whole-intestinal bacterial suspension (mixed with 10% sterile glycerol)
Spray on pelleted feeds


C
CG
PCFB
WIMT

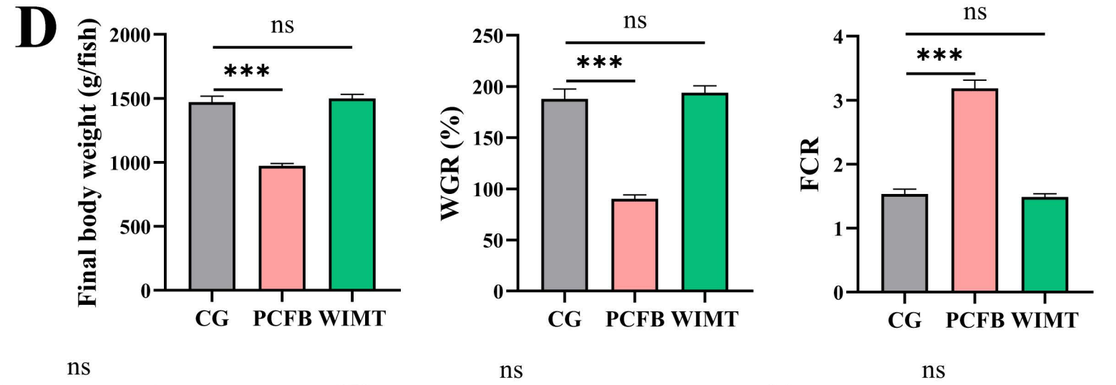
D
Final body weight (g/fish)
WGR (%)
FCR
ns
***
CG
PCFB
WIMT

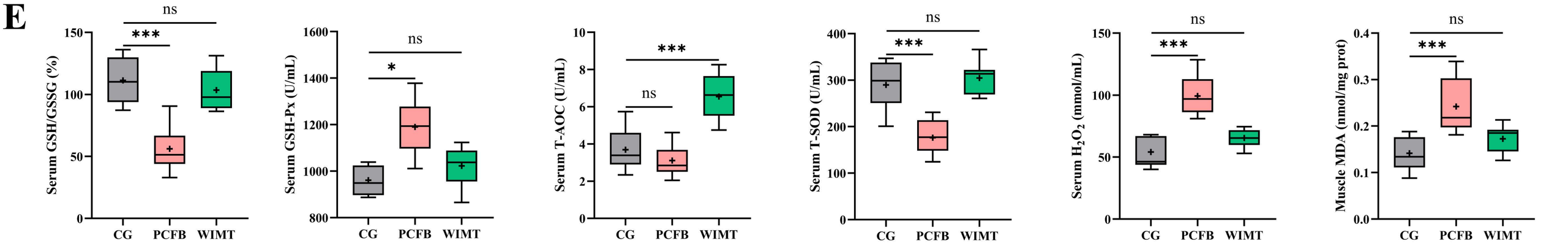
E
Serum GSH/GSSG (%)
Serum GSH-Px (U/mL)
Serum T-AOC (U/mL)
Serum T-SOD (U/mL)
Serum H2O2 (mmol/mL)
Muscle MDA (nmol/mg prot)
ns
*
***
CG
PCFB
WIMT

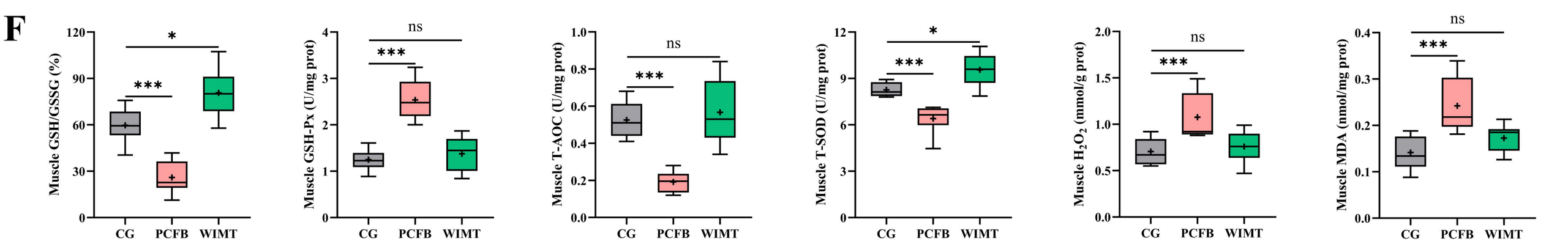
F
Muscle GSH/GSSG (%)
Muscle GSH-Px (U/mg prot)
Muscle T-AOC (U/mg prot)
Muscle T-SOD (U/mg prot)
Muscle H2O2 (mmol/g prot)
Muscle MDA (nmol/mg prot)
ns
*
***
CG
PCFB
WIMT

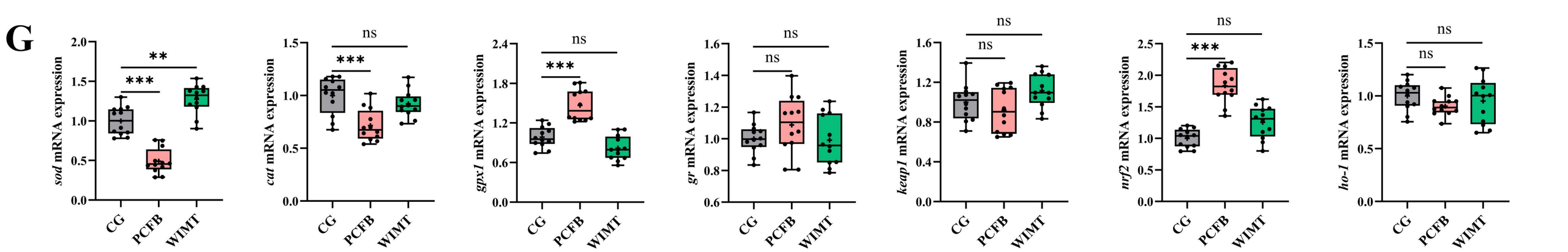
G
sod mRNA expression
cat mRNA expression
gpx1 mRNA expression
gr mRNA expression
keap1 mRNA expression
nrf2 mRNA expression
ho-1 mRNA expression
ns
**
***
CG
PCFB
WIMT

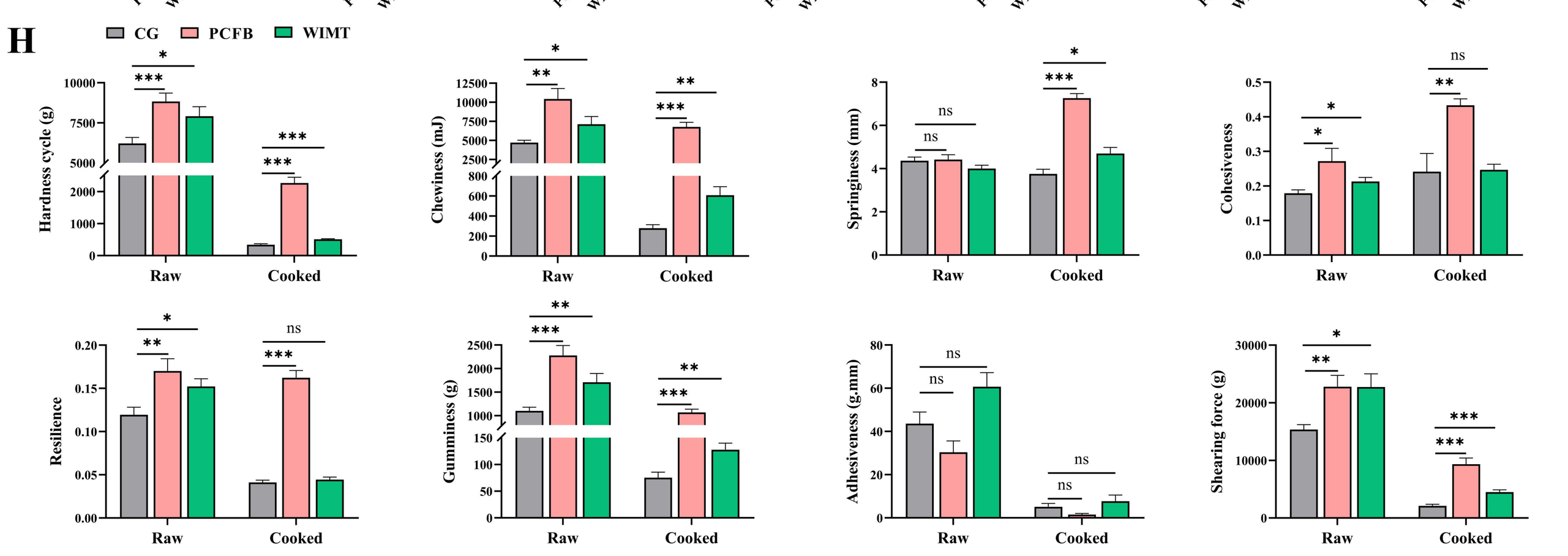
H
CG
PCFB
WIMT
Hardness cycle (g)
Chewiness (mJ)
Springiness (mm)
Cohesiveness
Resilience
Gumminess (g)
Adhesiveness (g.mm)
Shearing force (g)
Raw
Cooked
ns
*
**
***

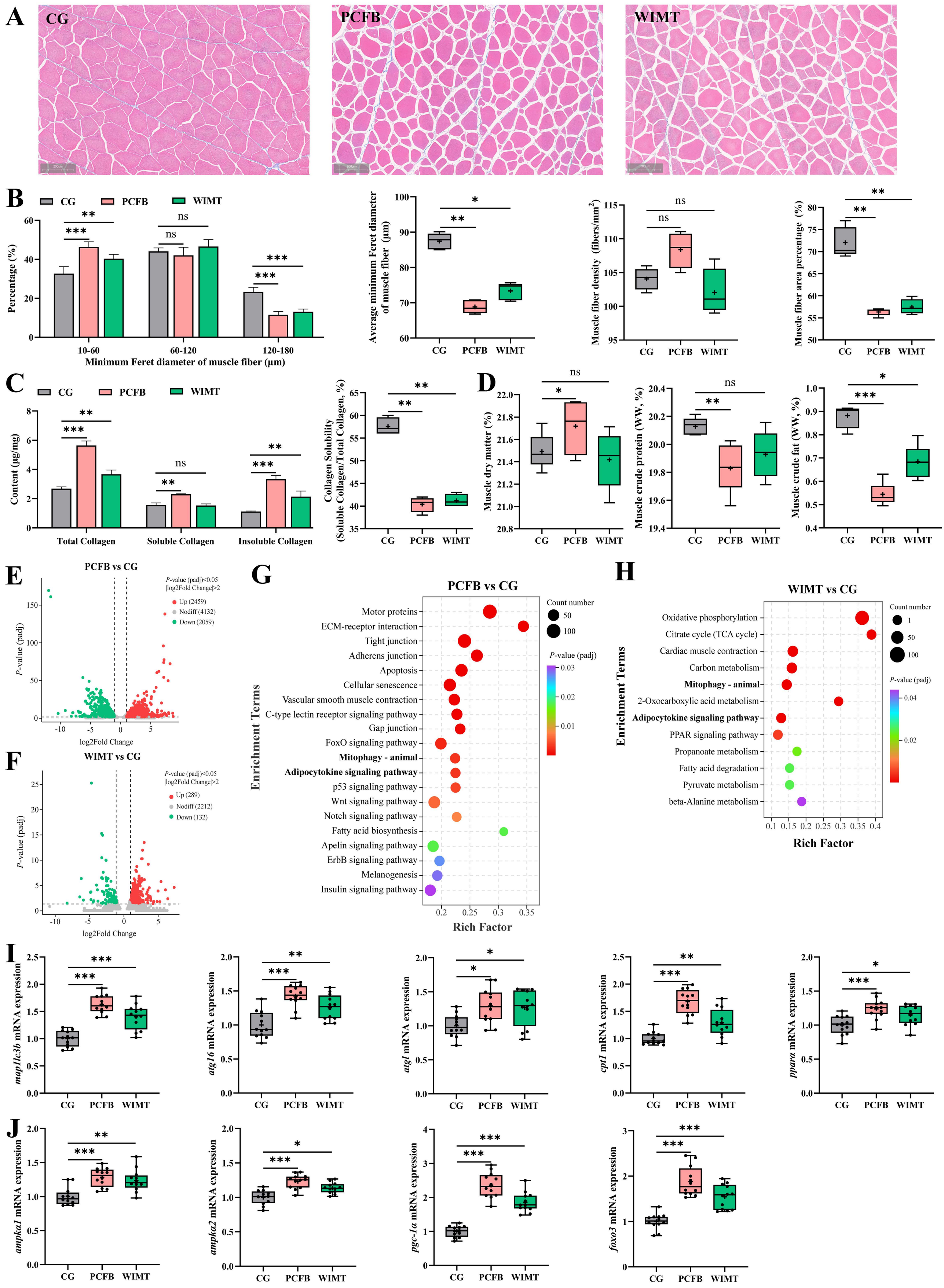
A
CG
PCFB
WIMT
B
CG
PCFB
WIMT
Percentage (%)
10-60
60-120
120-180
Minimum Feret diameter of muscle fiber (μm)
Average minimum Feret diameter of muscle fiber (μm)
Muscle fiber density (fibers/mm²)
Muscle fiber area percentage (%)
C
Content (μg/mg)
Total Collagen
Soluble Collagen
Insoluble Collagen
Collagen Solubility (Soluble Collagen/Total Collagen, %)
D
Muscle dry matter (%)
Muscle crude protein (WW, %)
Muscle crude fat (WW, %)
E
PCFB vs CG
P-value (padj)<0.05
|log2Fold Change|>2
Up (2459)
Nodiff (4132)
Down (2059)
P-value (padj)
log2Fold Change
F
WIMT vs CG
P-value (padj)<0.05
|log2Fold Change|>2
Up (289)
Nodiff (2212)
Down (132)
G
PCFB vs CG
Count number
P-value (padj)
Enrichment Terms
Motor proteins
ECM-receptor interaction
Tight junction
Adherens junction
Apoptosis
Cellular senescence
Vascular smooth muscle contraction
C-type lectin receptor signaling pathway
Gap junction
FoxO signaling pathway
Mitophagy - animal
Adipocytokine signaling pathway
p53 signaling pathway
Wnt signaling pathway
Notch signaling pathway
Fatty acid biosynthesis
Apelin signaling pathway
ErbB signaling pathway
Melanogenesis
Insulin signaling pathway
Rich Factor
H
WIMT vs CG
Count number
P-value (padj)
Enrichment Terms
Oxidative phosphorylation
Citrate cycle (TCA cycle)
Cardiac muscle contraction
Carbon metabolism
Mitophagy - animal
2-Oxocarboxylic acid metabolism
Adipocytokine signaling pathway
PPAR signaling pathway
Propanoate metabolism
Fatty acid degradation
Pyruvate metabolism
beta-Alanine metabolism
Rich Factor
I
map1lc3b mRNA expression
atg16 mRNA expression
atgl mRNA expression
cpt1 mRNA expression
pparα mRNA expression
J
ampkα1 mRNA expression
ampkα2 mRNA expression
pgc-1α mRNA expression
foxo3 mRNA expression

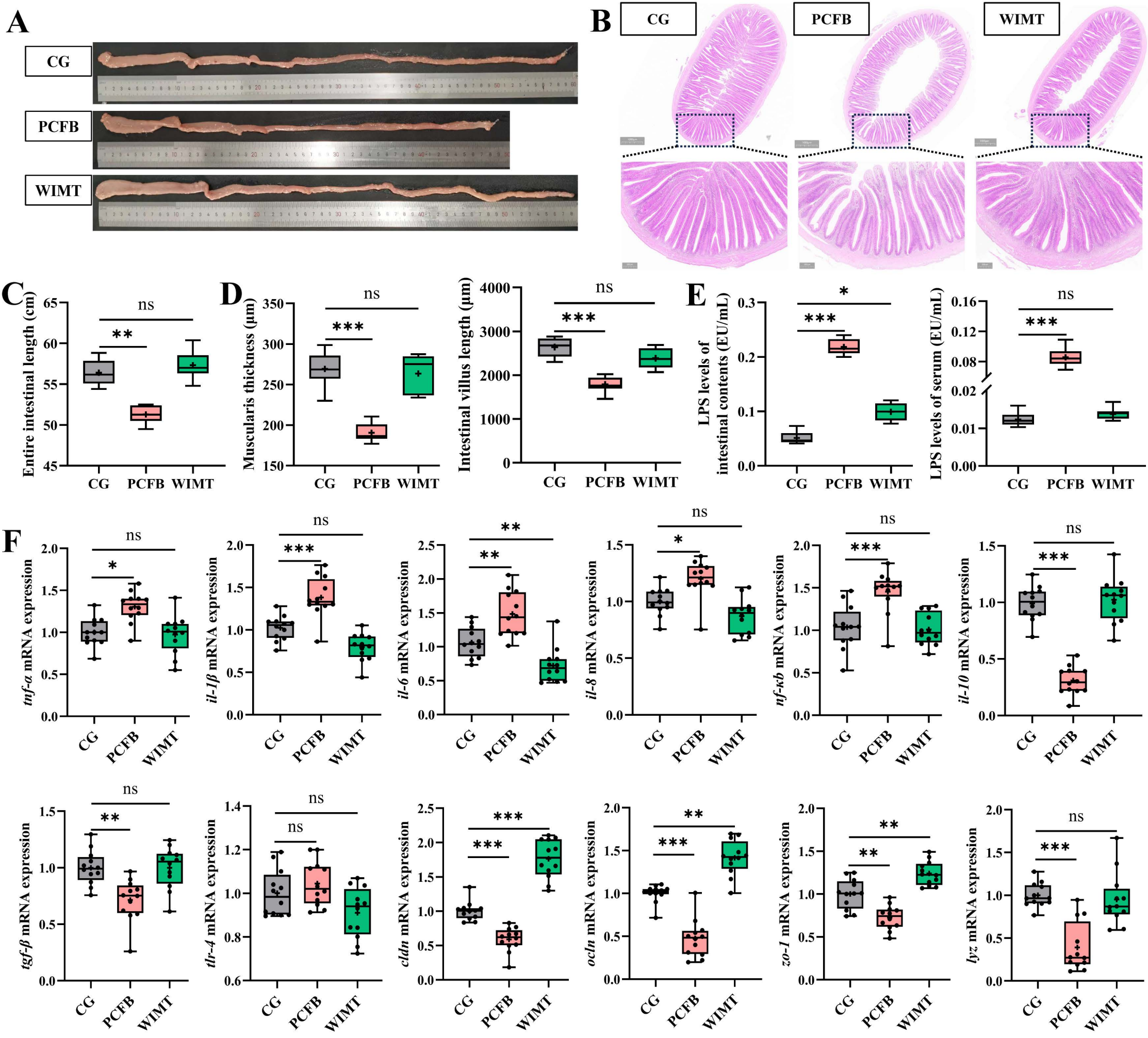
A
CG
PCFB
WIMT
B
CG
PCFB
WIMT
C
Entire intestinal length (cm)
D
Muscularis thickness (μm)
Intestinal villus length (μm)
E
LPS levels of intestinal contents (EU/mL)
LPS levels of serum (EU/mL)
F
tnf-α mRNA expression
il-1β mRNA expression
il-6 mRNA expression
il-8 mRNA expression
nf-κb mRNA expression
il-10 mRNA expression
tgf-β mRNA expression
tlr-4 mRNA expression
cldn mRNA expression
ocln mRNA expression
zo-1 mRNA expression
lyz mRNA expression
ns
*
**
***

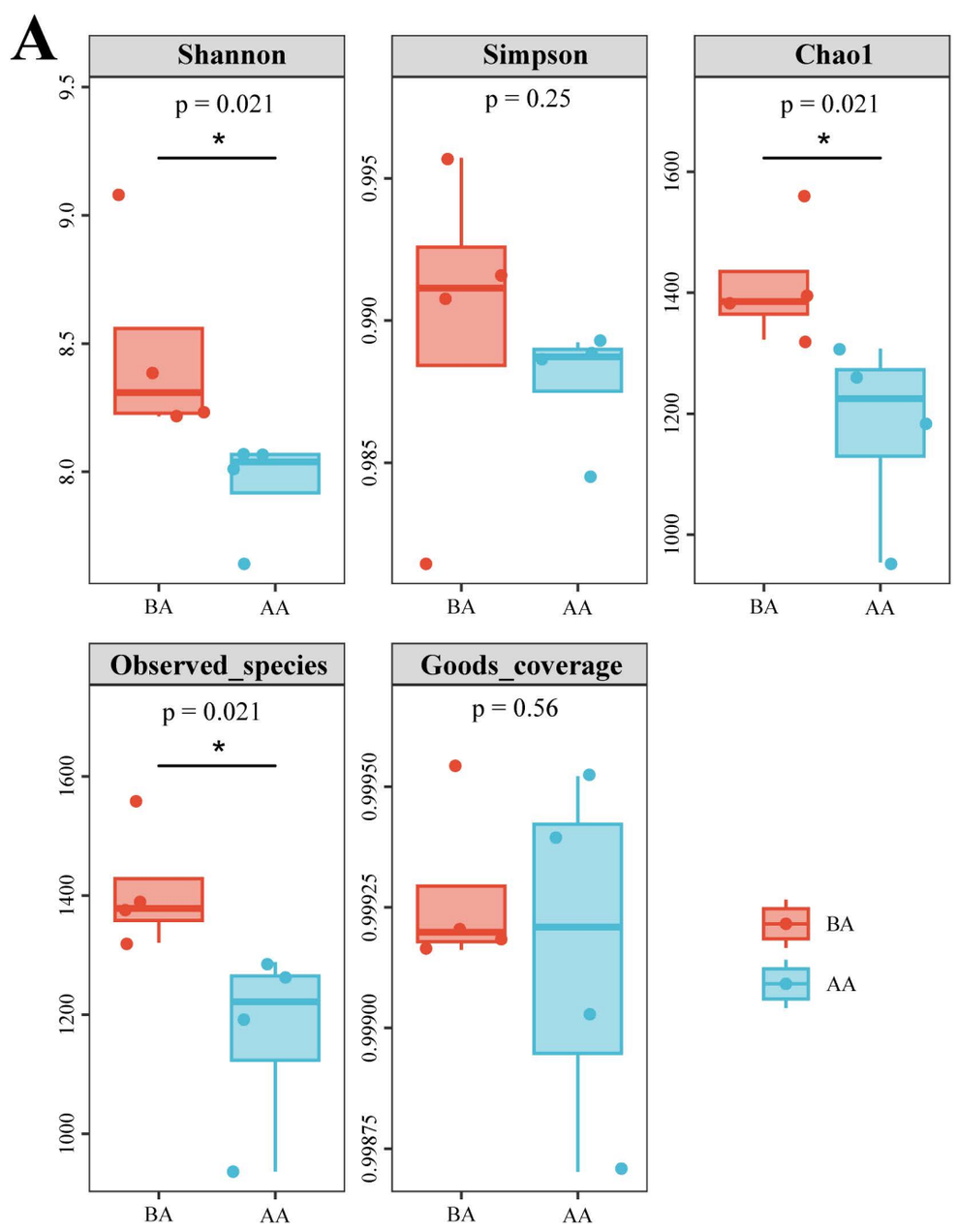
A
Shannon
p = 0.021
*
Simpson
p = 0.25
Chao1
p = 0.021
*
Observed_species
p = 0.021
*
Goods_coverage
p = 0.56
BA
AA

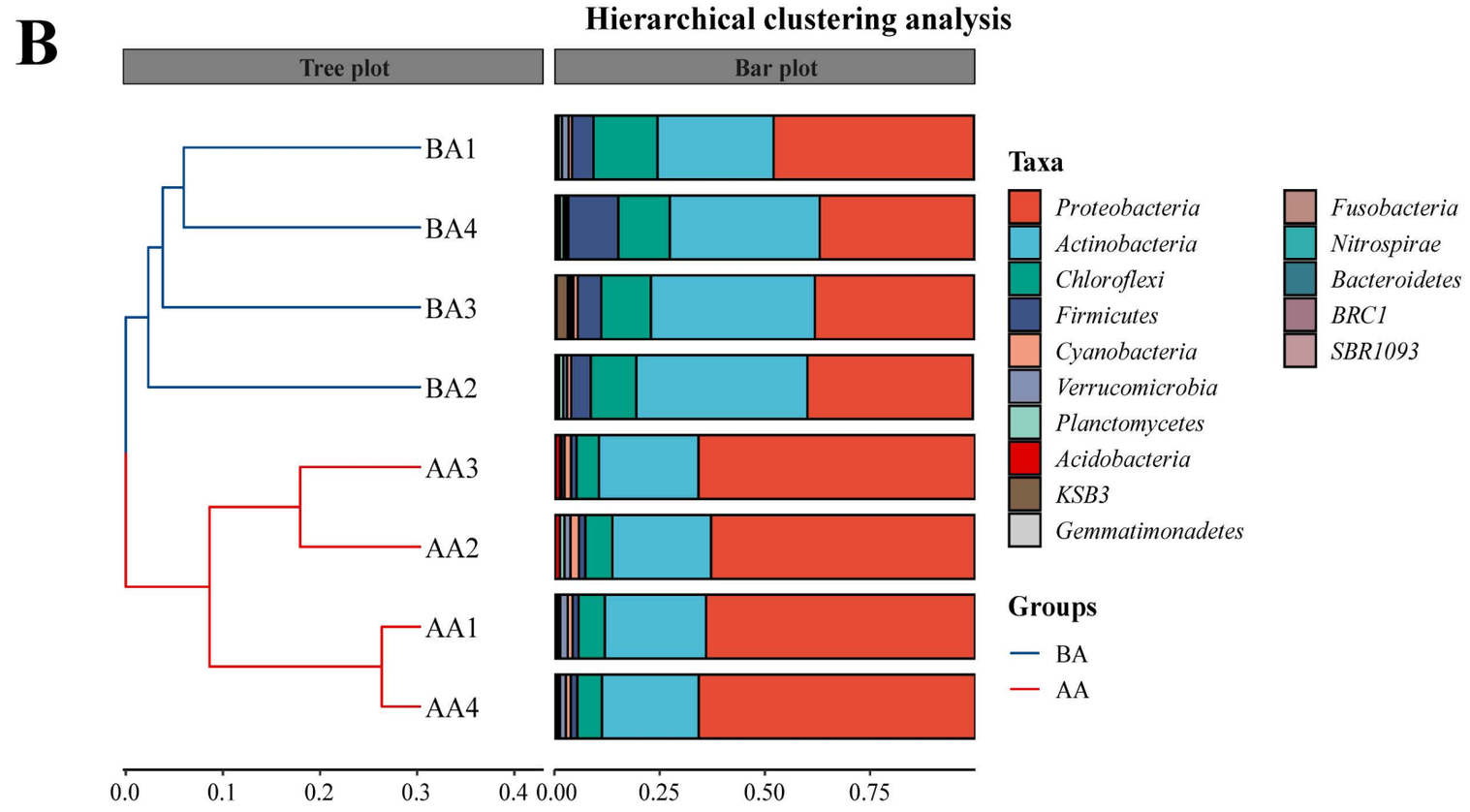
B
Hierarchical clustering analysis
Tree plot
Bar plot
BA1
BA4
BA3
BA2
AA3
AA2
AA1
AA4
Taxa
Proteobacteria
Actinobacteria
Chloroflexi
Firmicutes
Cyanobacteria
Verrucomicrobia
Planctomycetes
Acidobacteria
KSB3
Gemmatimonadetes
Fusobacteria
Nitrospirae
Bacteroidetes
BRC1
SBR1093
Groups
BA
AA

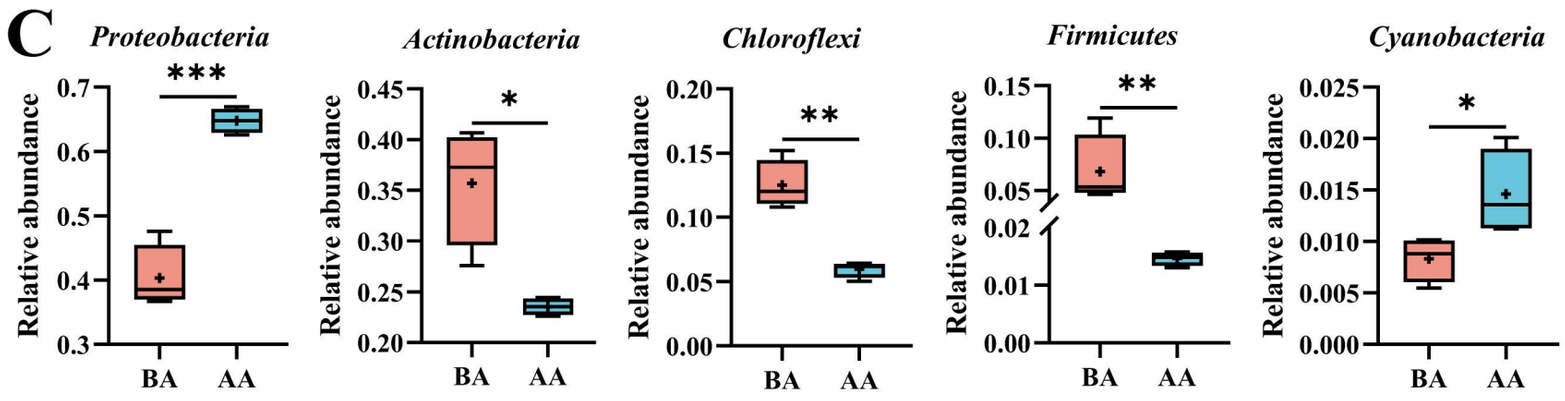
C
Proteobacteria
***
Actinobacteria
*
Chloroflexi
**
Firmicutes
**
Cyanobacteria
*
Relative abundance
BA
AA

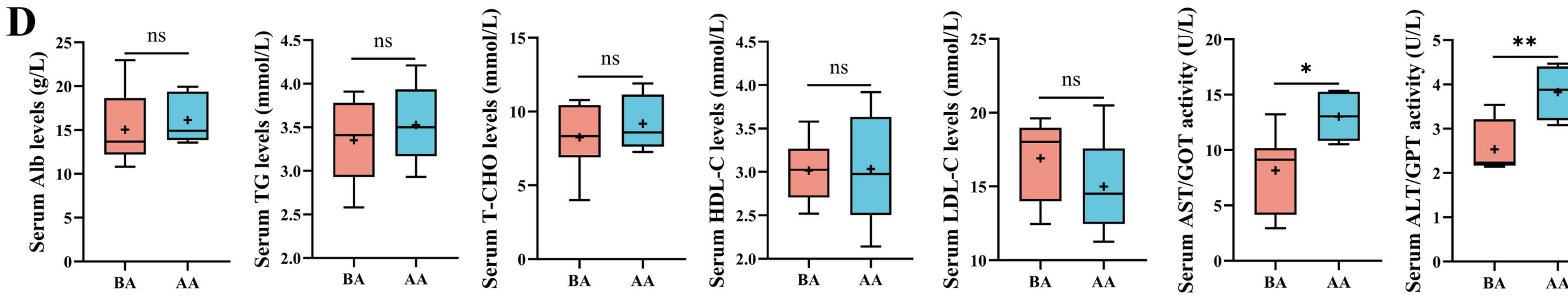
D
Serum Alb levels (g/L)
ns
Serum TG levels (mmol/L)
ns
Serum T-CHO levels (mmol/L)
ns
Serum HDL-C levels (mmol/L)
ns
Serum LDL-C levels (mmol/L)
ns
Serum AST/GOT activity (U/L)
*
Serum ALT/GPT activity (U/L)
**
BA
AA

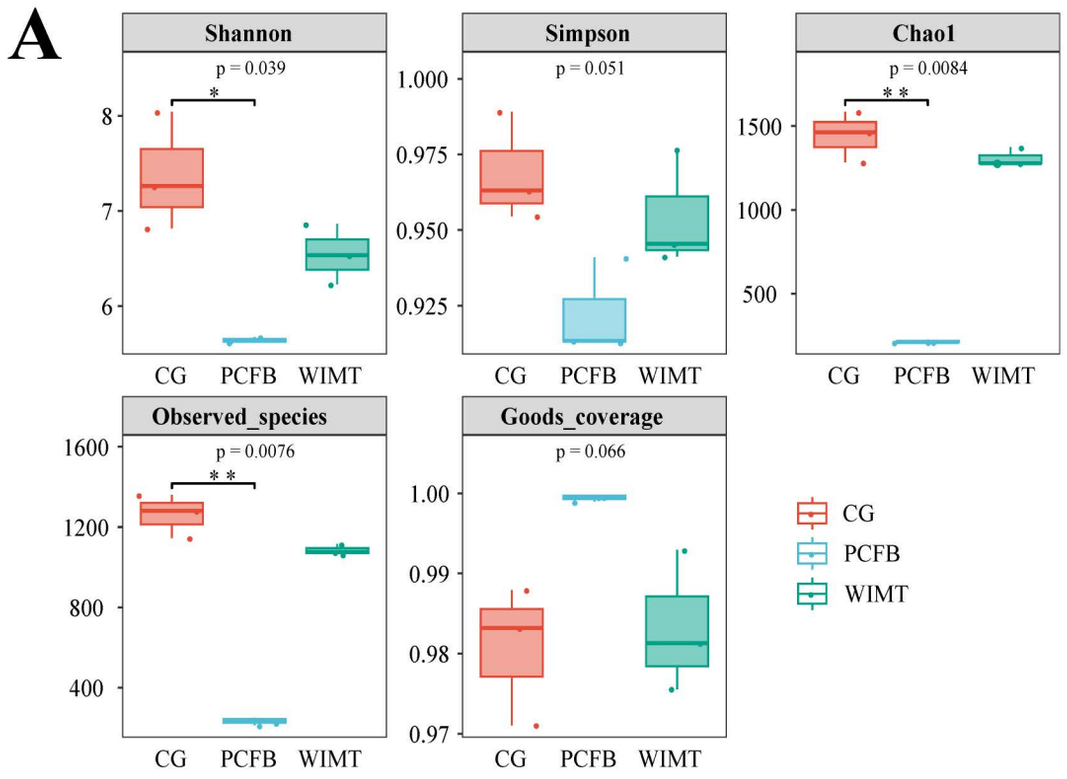
A
Shannon
p = 0.039
*
Simpson
p = 0.051
Chao1
p = 0.0084
**
Observed_species
p = 0.0076
**
Goods_coverage
p = 0.066
CG
PCFB
WIMT

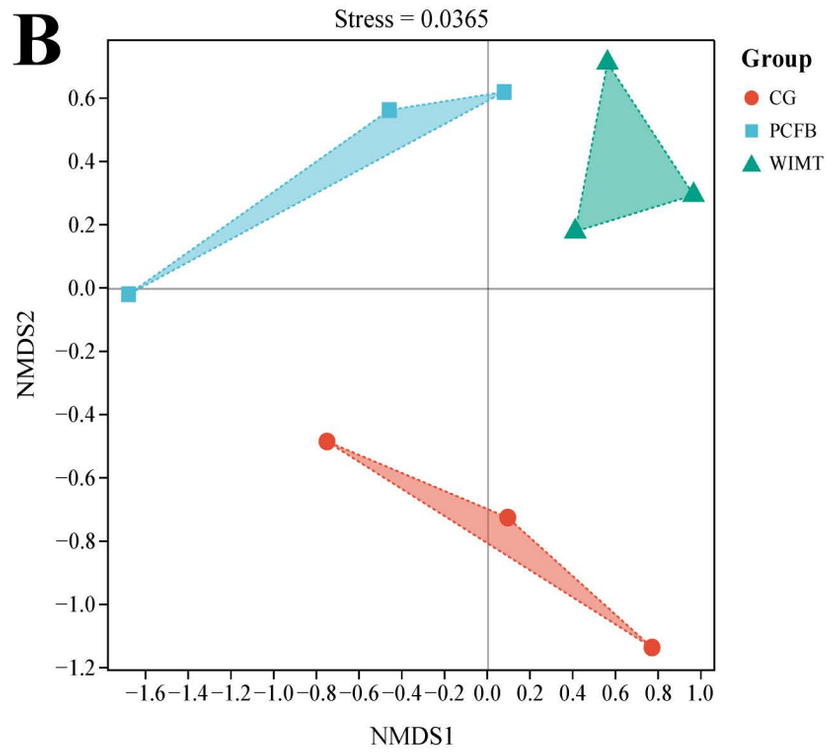
B
Stress = 0.0365
Group
CG
PCFB
WIMT
NMDS1
NMDS2

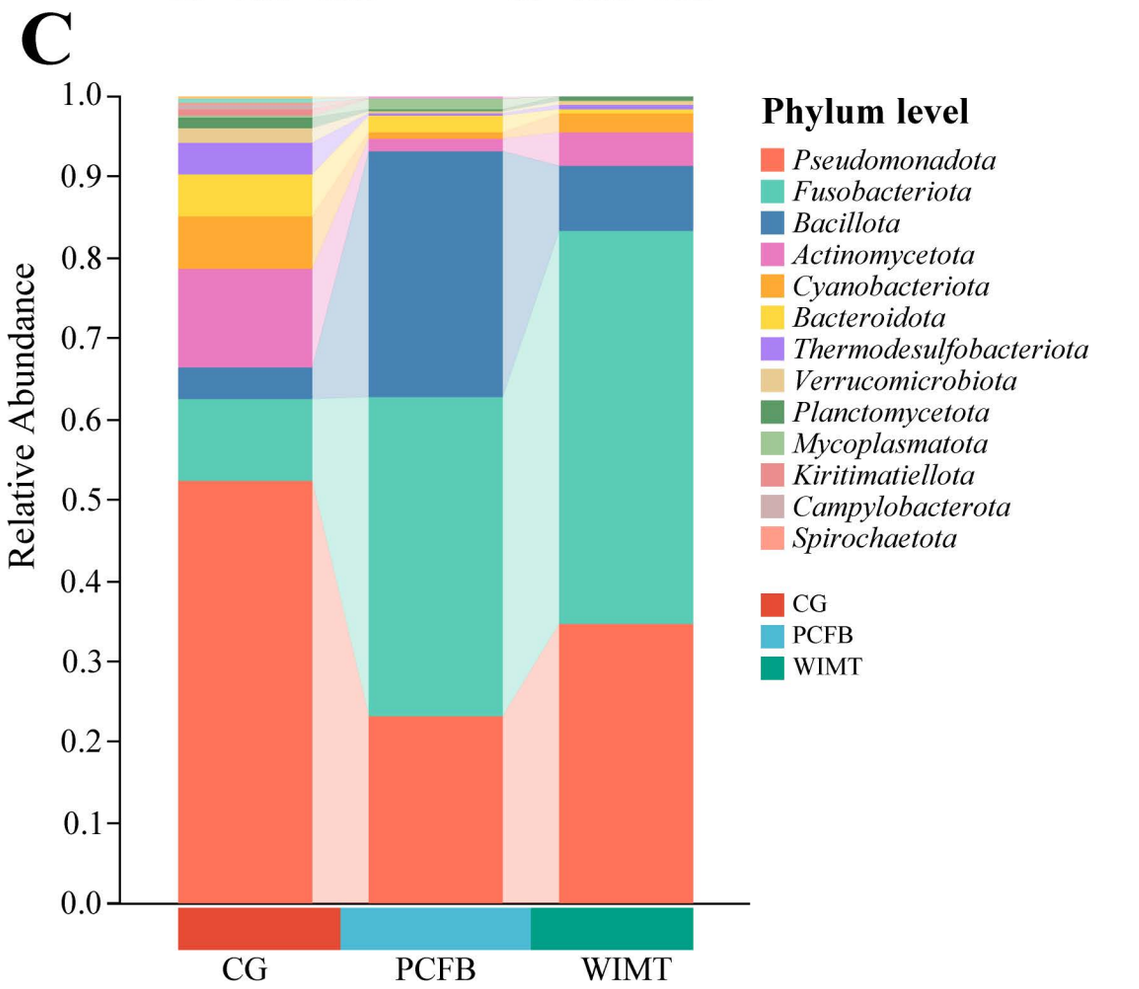
C
Relative Abundance
Phylum level
Pseudomonadota
Fusobacteriota
Bacillota
Actinomycetota
Cyanobacteriota
Bacteroidota
Thermodesulfobacteriota
Verrucomicrobiota
Planctomycetota
Mycoplasmatota
Kiritimatiellota
Campylobacterota
Spirochaetota
Acidobacteriota
Myxococcota
Chloroflexota
Nitrospirota
Armatimonadota
Elusimicrobiota
Chlamydiota
Others
CG
PCFB
WIMT

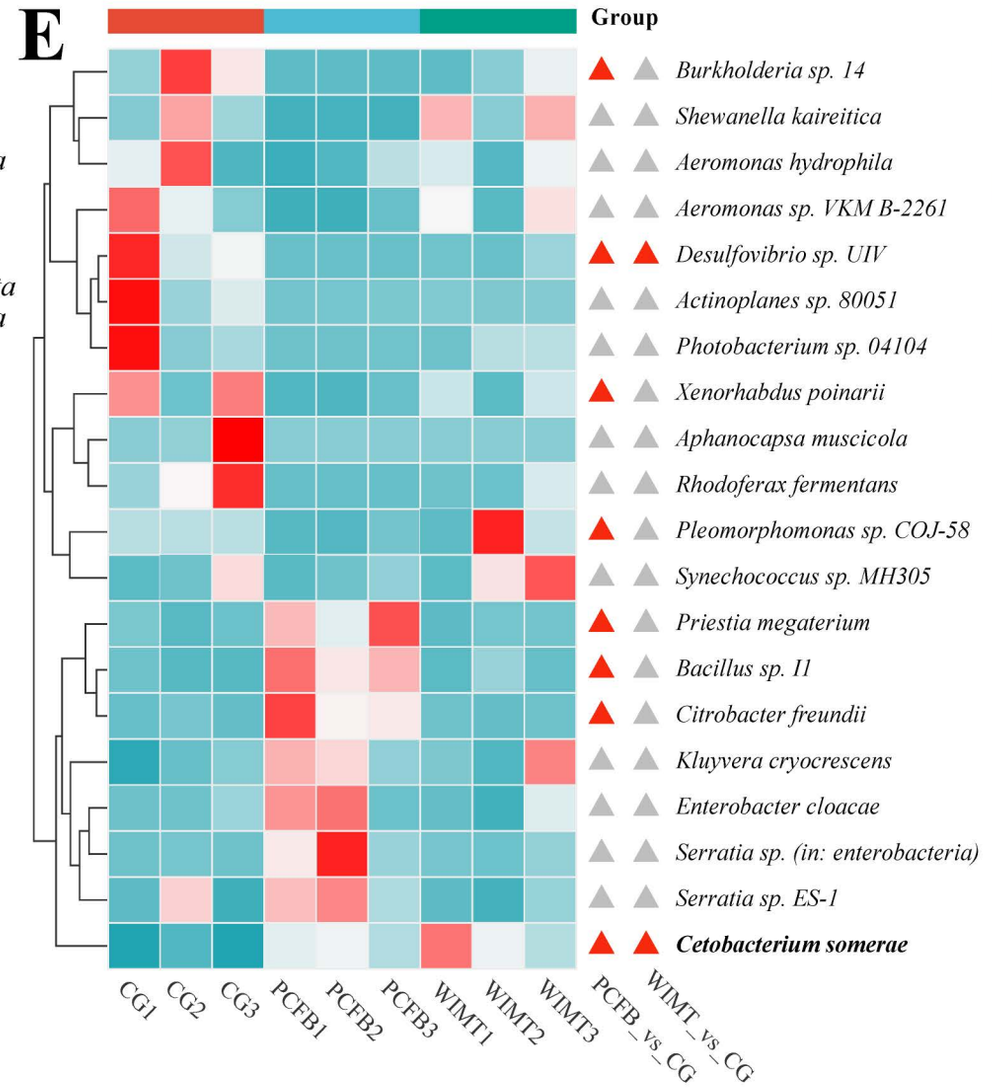
E
Group
Burkholderia sp. 14
Shewanella kaireitica
Aeromonas hydrophila
Aeromonas sp. VKM B-2261
Desulfovibrio sp. UIV
Actinoplanes sp. 80051
Photobacterium sp. 04104
Xenorhabdus poinarii
Aphanocapsa muscicola
Rhodoferax fermentans
Pleomorphomonas sp. COJ-58
Synechococcus sp. MH305
Priestia megaterium
Bacillus sp. 11
Citrobacter freundii
Kluyvera cryocrescens
Enterobacter cloacae
Serratia sp. (in: enterobacteria)
Serratia sp. ES-1
Cetobacterium somerae
CG1
CG2
CG3
PCFB1
PCFB2
PCFB3
WIMT1
WIMT2
WIMT3
PCFB_vs_CG
WIMT_vs_CG
Group
CG
PCFB
WIMT
Significance
p-value < 0.05
p-value >= 0.05

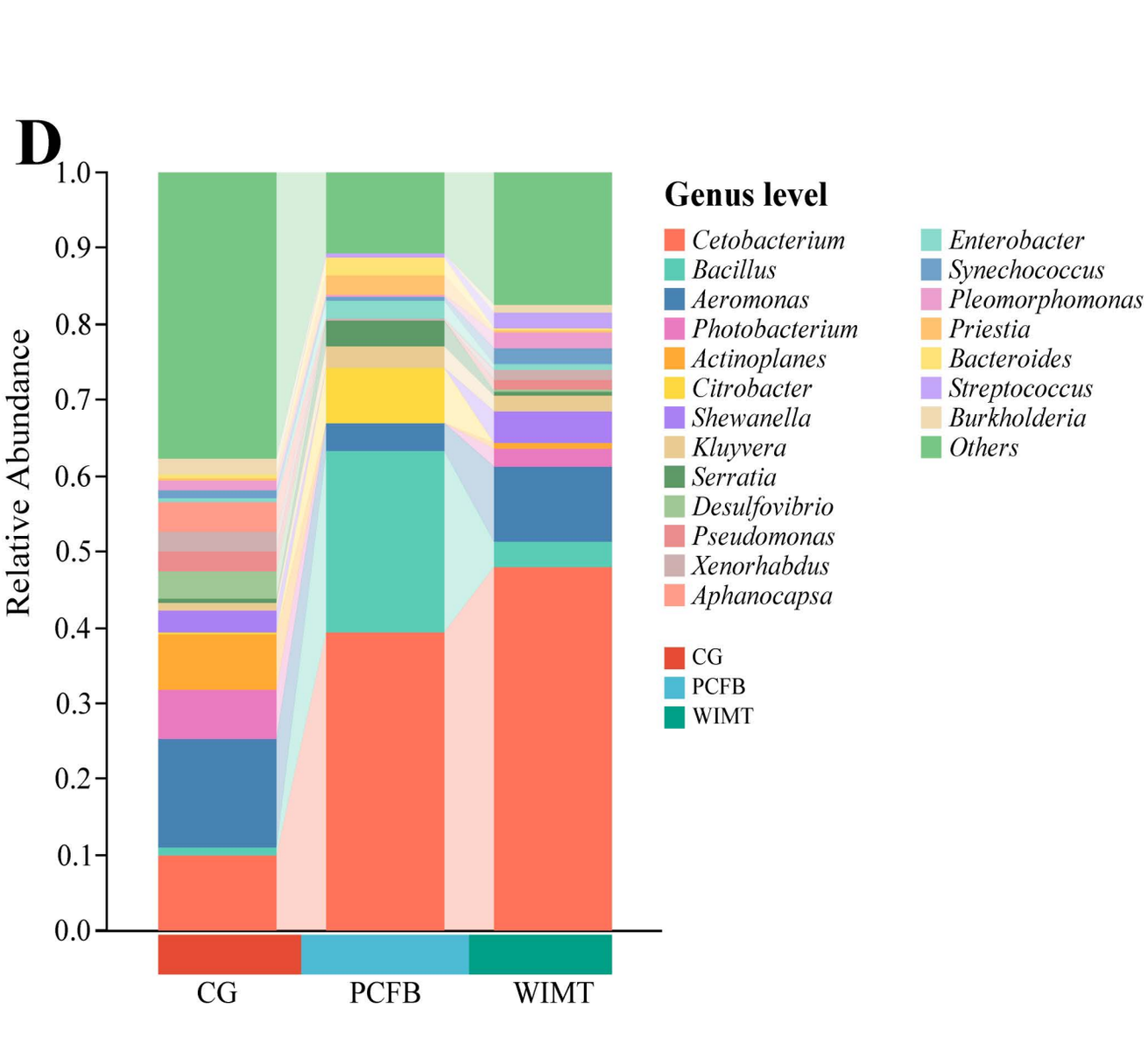
D
Relative Abundance
Genus level
Cetobacterium
Bacillus
Aeromonas
Photobacterium
Actinoplanes
Citrobacter
Shewanella
Kluyvera
Serratia
Desulfovibrio
Pseudomonas
Xenorhabdus
Aphanocapsa
Enterobacter
Synechococcus
Pleomorphomonas
Priestia
Bacteroides
Streptococcus
Burkholderia
Others
CG
PCFB
WIMT

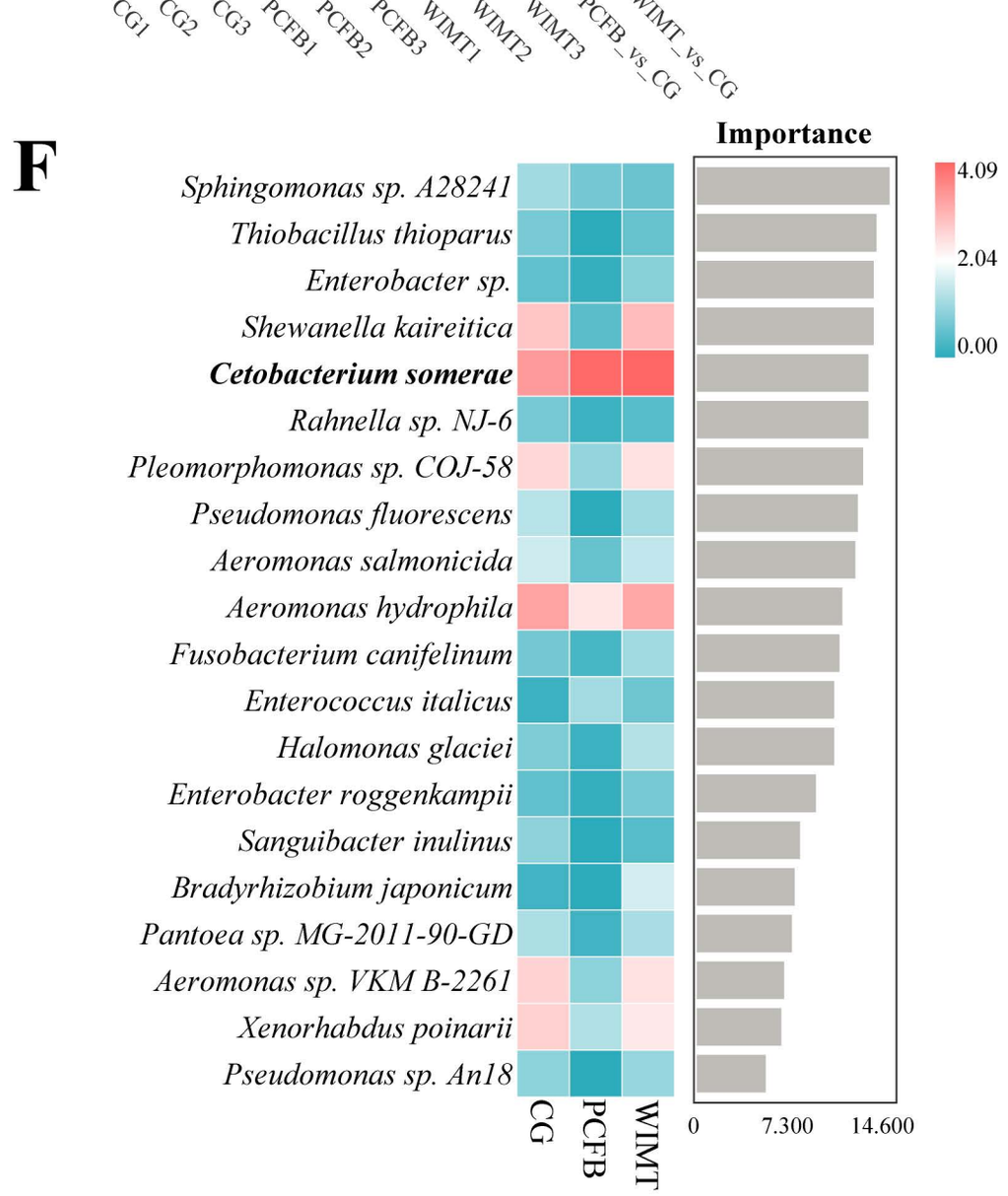
F
Importance
Sphingomonas sp. A28241
Thiobacillus thioparus
Enterobacter sp.
Shewanella kaireitica
Cetobacterium somerae
Rahnella sp. NJ-6
Pleomorphomonas sp. COJ-58
Pseudomonas fluorescens
Aeromonas salmonicida
Aeromonas hydrophila
Fusobacterium canifelinum
Enterococcus italicus
Halomonas glaciei
Enterobacter roggenkampii
Sanguibacter inulinus
Bradyrhizobium japonicum
Pantoea sp. MG-2011-90-GD
Aeromonas sp. VKM B-2261
Xenorhabdus poinarii
Pseudomonas sp. An18
CG
PCFB
WIMT

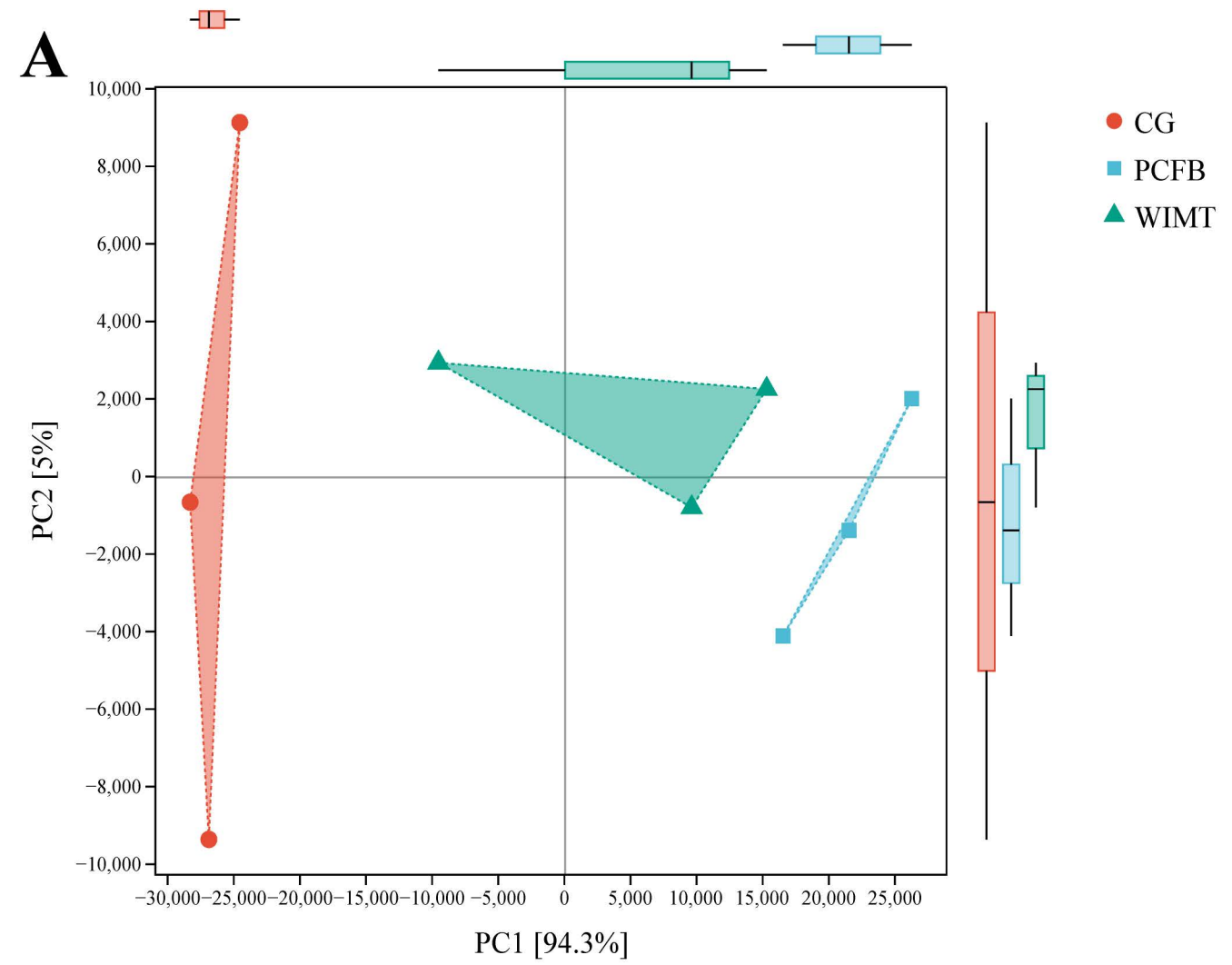
A
PC2 [5%]
PC1 [94.3%]
CG
PCFB
WIMT

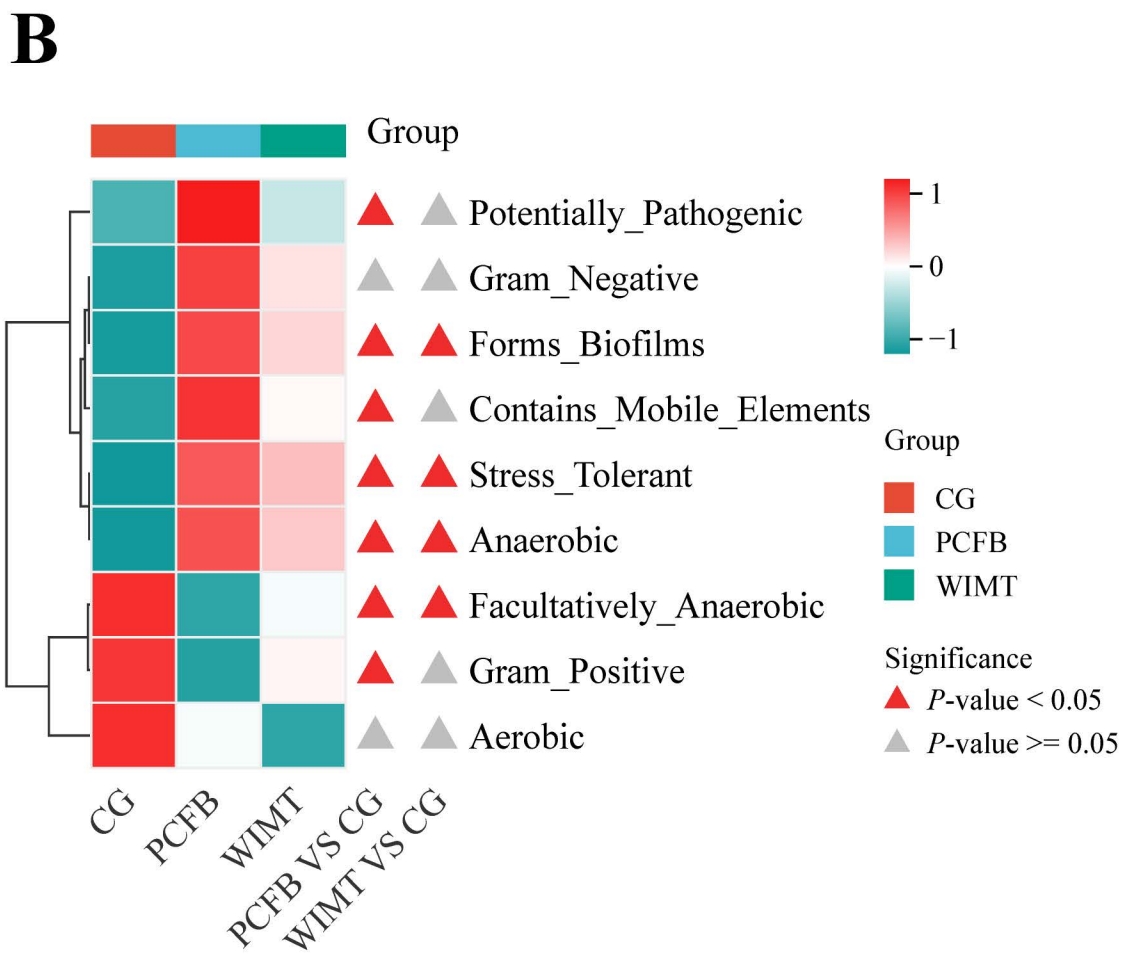
B
Group
Potentially_Pathogenic
Gram_Negative
Forms_Biofilms
Contains_Mobile_Elements
Stress_Tolerant
Anaerobic
Facultatively_Anaerobic
Gram_Positive
Aerobic
Group
CG
PCFB
WIMT
Significance
P-value < 0.05
P-value >= 0.05
CG
PCFB
WIMT
PCFB VS CG
WIMT VS CG

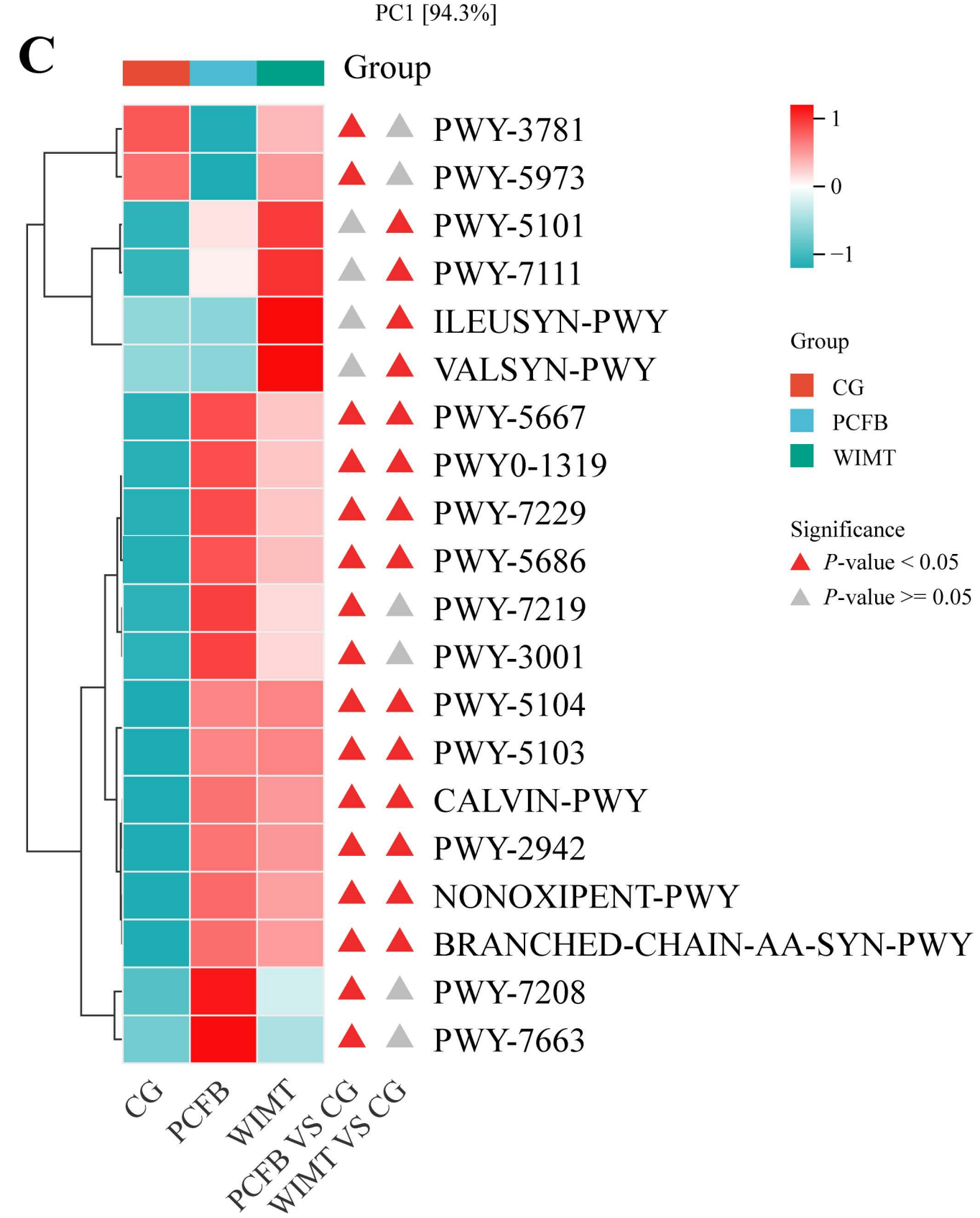
C
Group
PWY-3781
PWY-5973
PWY-5101
PWY-7111
ILEUSYN-PWY
VALSYN-PWY
PWY-5667
PWY0-1319
PWY-7229
PWY-5686
PWY-7219
PWY-3001
PWY-5104
PWY-5103
CALVIN-PWY
PWY-2942
NONOXIPENT-PWY
BRANCHED-CHAIN-AA-SYN-PWY
PWY-7208
PWY-7663
Group
CG
PCFB
WIMT
Significance
P-value < 0.05
P-value >= 0.05
CG
PCFB
WIMT
PCFB VS CG
WIMT VS CG

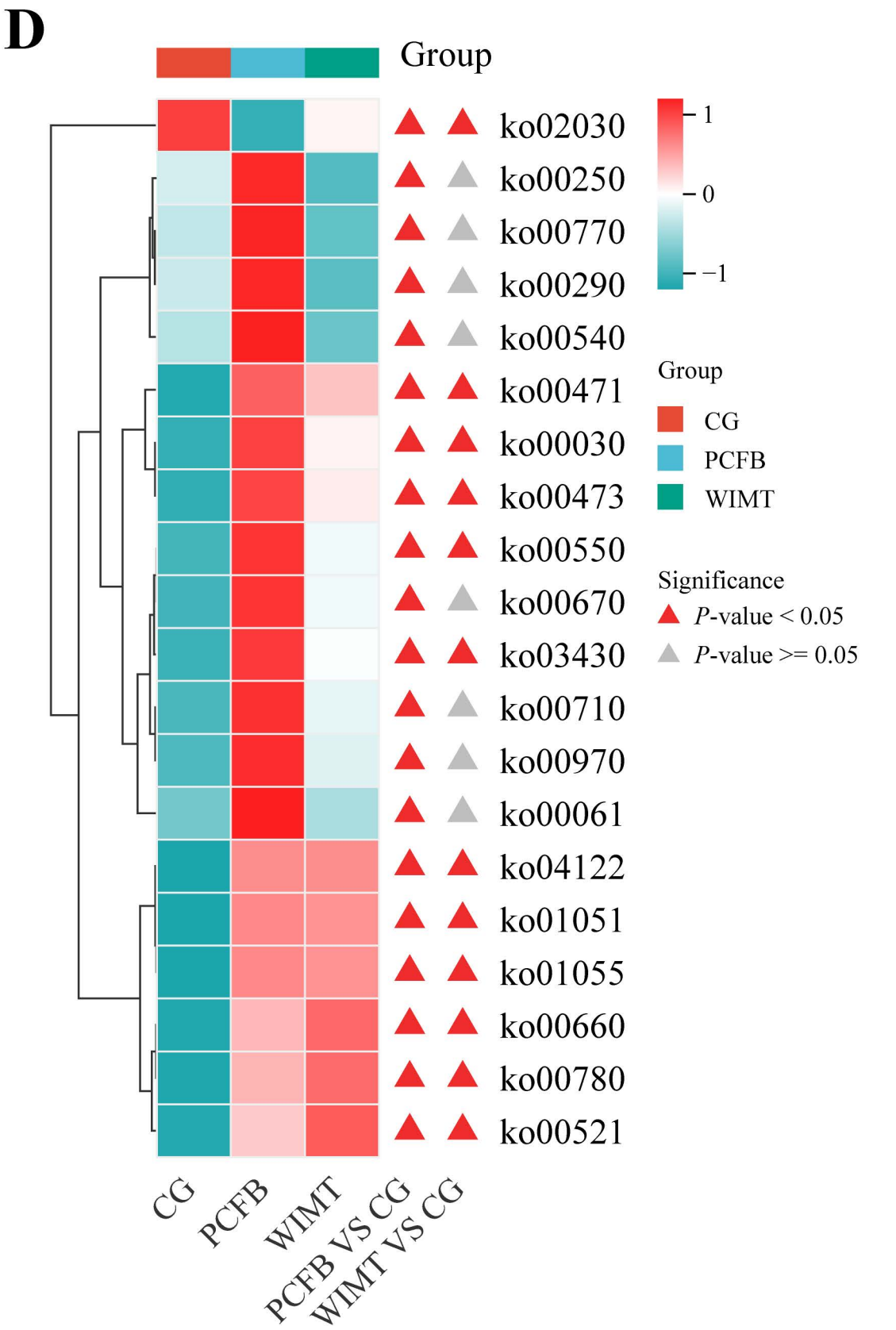
D
Group
ko02030
ko00250
ko00770
ko00290
ko00540
ko00471
ko00030
ko00473
ko00550
ko00670
ko03430
ko00710
ko00970
ko00061
ko04122
ko01051
ko01055
ko00660
ko00780
ko00521
Group
CG
PCFB
WIMT
Significance
P-value < 0.05
P-value >= 0.05
CG
PCFB
WIMT
PCFB VS CG
WIMT VS CG

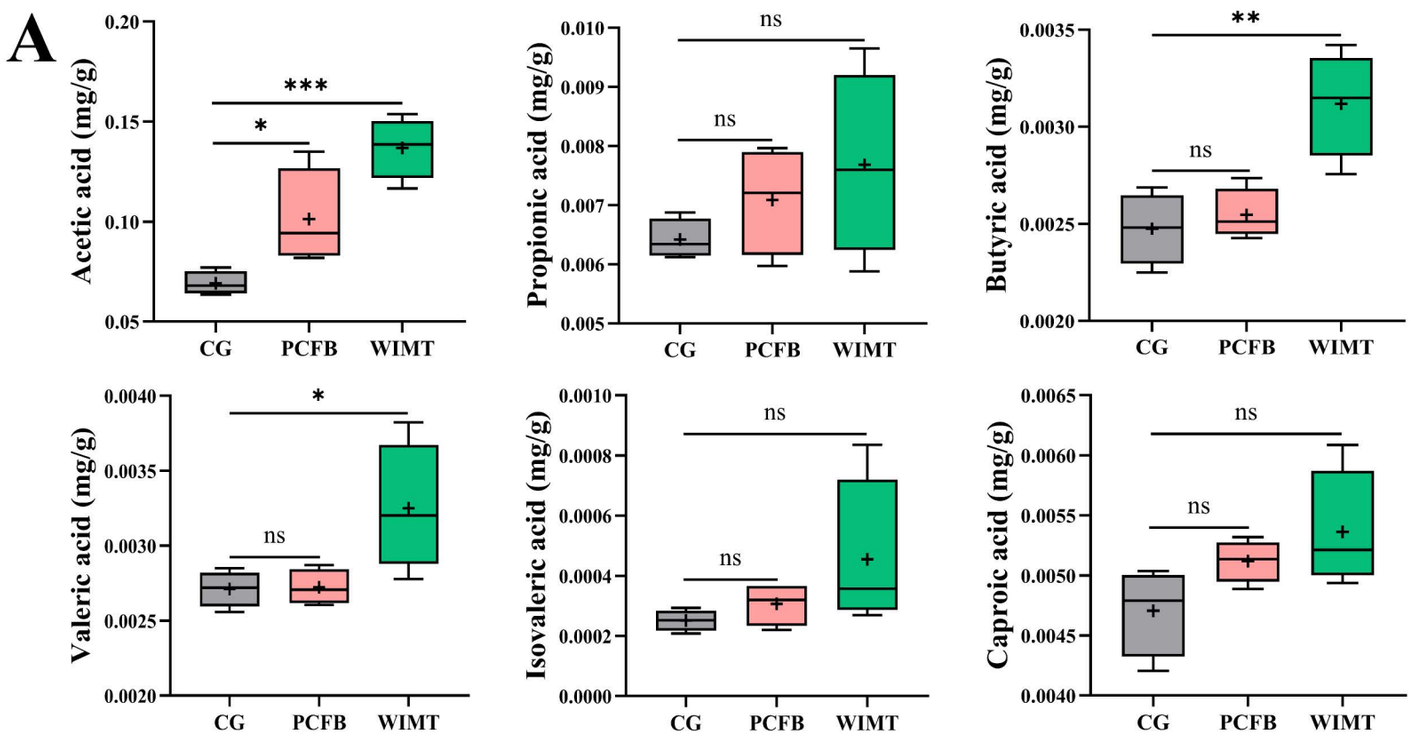
A
Acetic acid (mg/g)
Propionic acid (mg/g)
Butyric acid (mg/g)
Valeric acid (mg/g)
Isovaleric acid (mg/g)
Caproic acid (mg/g)
CG
PCFB
WIMT
ns

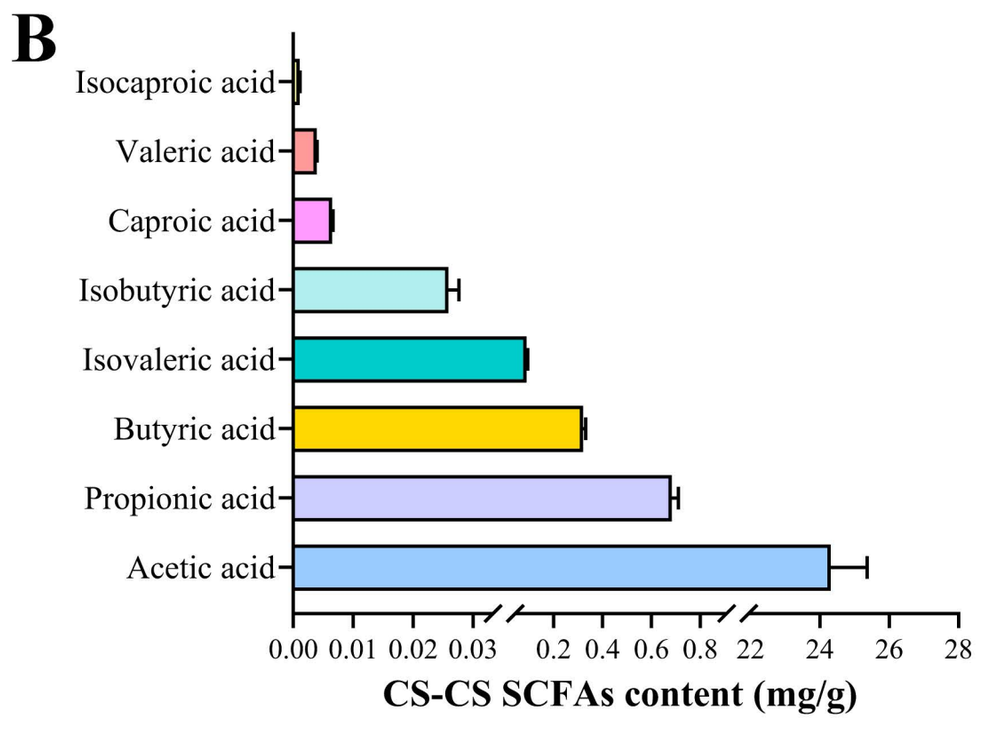
B
Isocaproic acid
Valeric acid
Caproic acid
Isobutyric acid
Isovaleric acid
Butyric acid
Propionic acid
Acetic acid
CS-CS SCFAs content (mg/g)

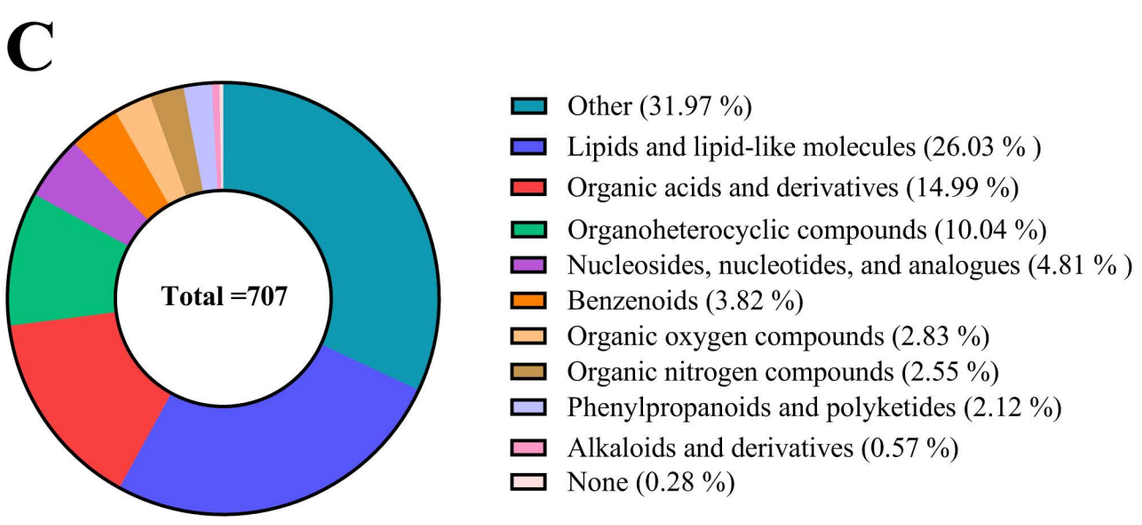
C
Total =707
Other (31.97 %)
Lipids and lipid-like molecules (26.03 %)
Organic acids and derivatives (14.99 %)
Organoheterocyclic compounds (10.04 %)
Nucleosides, nucleotides, and analogues (4.81 %)
Benzenoids (3.82 %)
Organic oxygen compounds (2.83 %)
Organic nitrogen compounds (2.55 %)
Phenylpropanoids and polyketides (2.12 %)
Alkaloids and derivatives (0.57 %)
None (0.28 %)

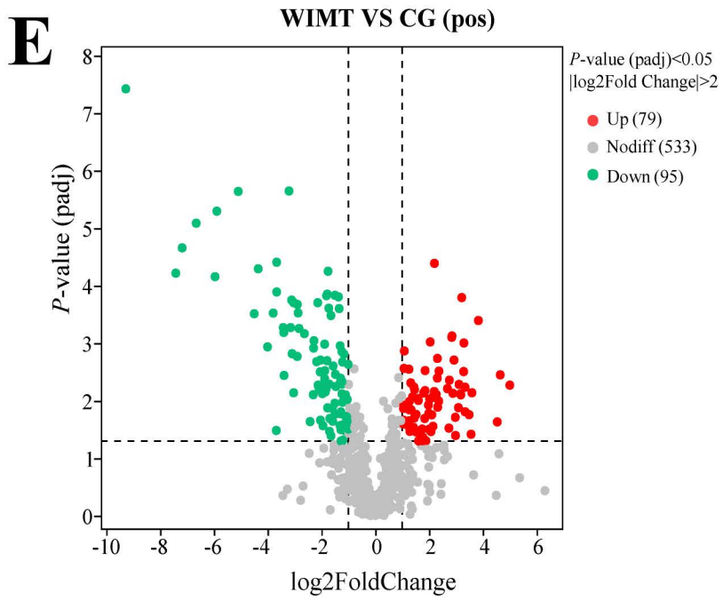
E
WIMT VS CG (pos)
P-value (padj)<0.05
|log2Fold Change|>2
Up (79)
Nodiff (533)
Down (95)
P-value (padj)
log2FoldChange

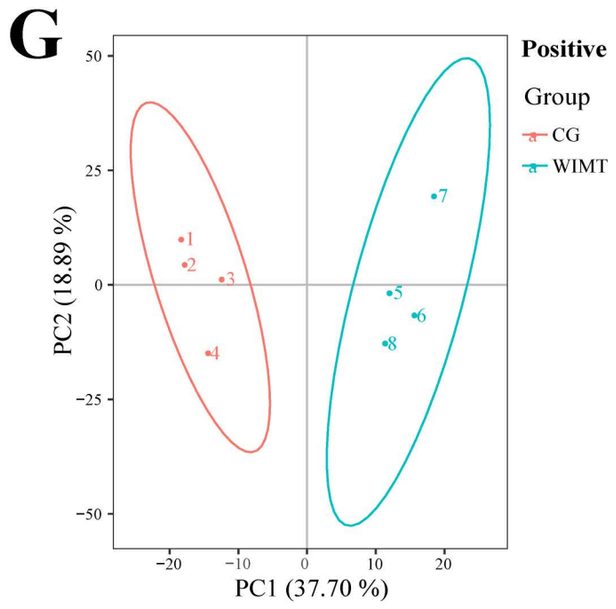
G
Positive
Group
CG
WIMT
PC2 (18.89 %)
PC1 (37.70 %)

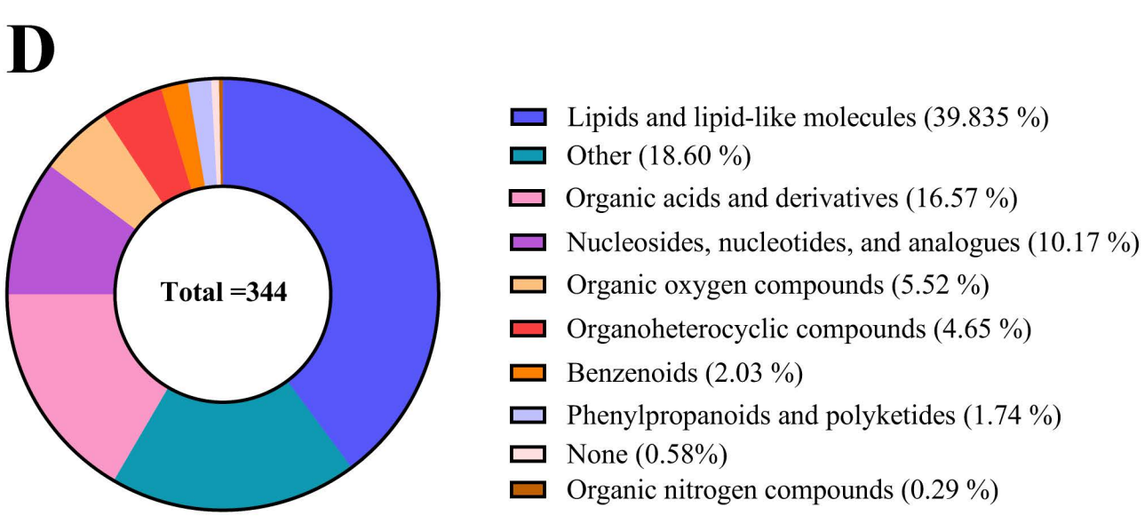
D
Total =344
Lipids and lipid-like molecules (39.835 %)
Other (18.60 %)
Organic acids and derivatives (16.57 %)
Nucleosides, nucleotides, and analogues (10.17 %)
Organic oxygen compounds (5.52 %)
Organoheterocyclic compounds (4.65 %)
Benzenoids (2.03 %)
Phenylpropanoids and polyketides (1.74 %)
None (0.58%)
Organic nitrogen compounds (0.29 %)

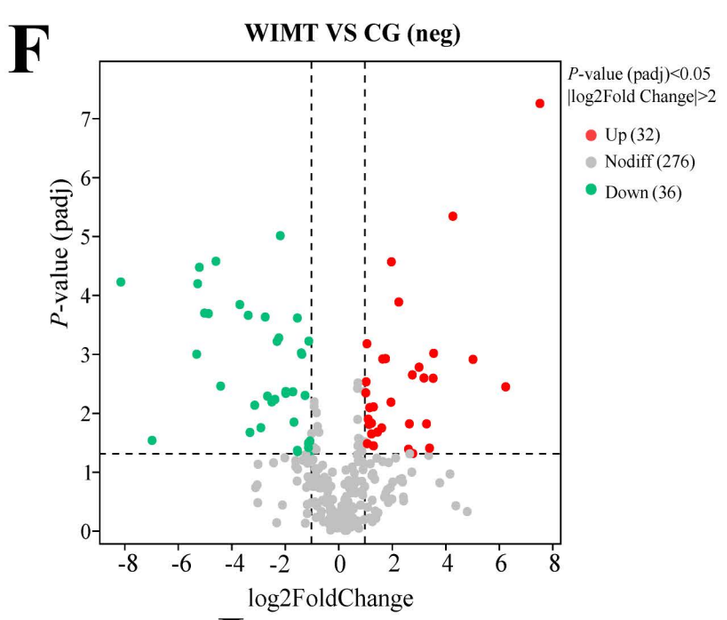
F
WIMT VS CG (neg)
P-value (padj)<0.05
|log2Fold Change|>2
Up (32)
Nodiff (276)
Down (36)
P-value (padj)
log2FoldChange

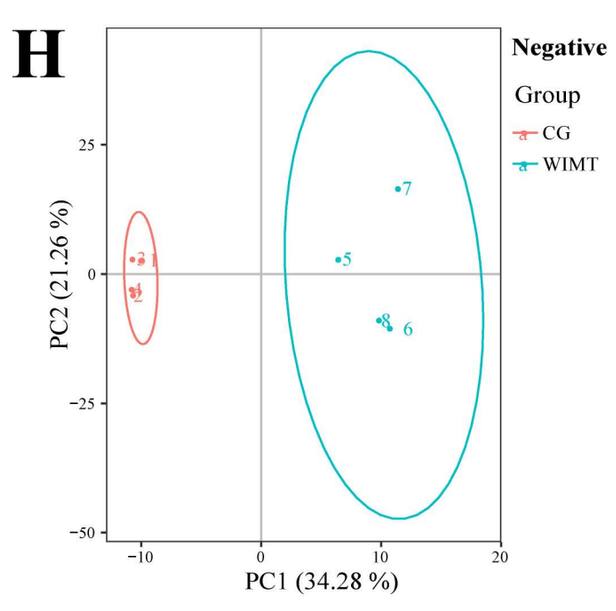
H
Negative
Group
CG
WIMT
PC2 (21.26 %)
PC1 (34.28 %)

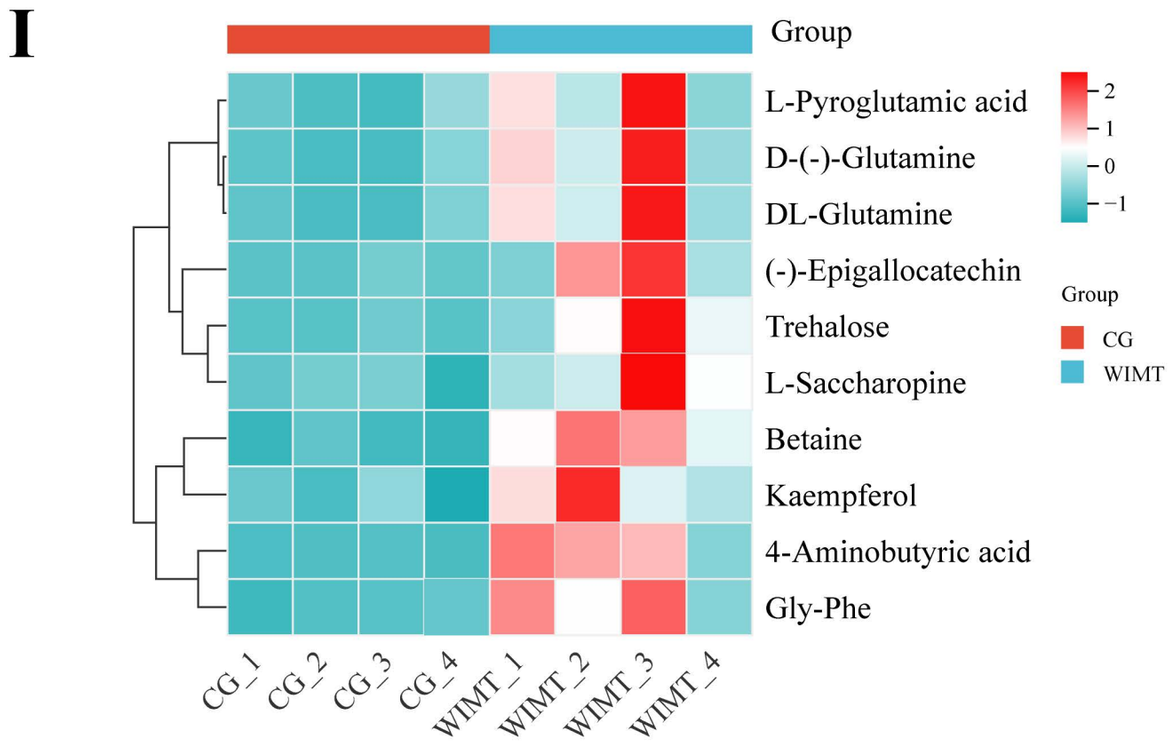
I
Group
L-Pyroglutamic acid
D-(-)-Glutamine
DL-Glutamine
(-)-Epigallocatechin
Trehalose
L-Saccharopine
Betaine
Kaempferol
4-Aminobutyric acid
Gly-Phe
CG_1
CG_2
CG_3
CG_4
WIMT_1
WIMT_2
WIMT_3
WIMT_4

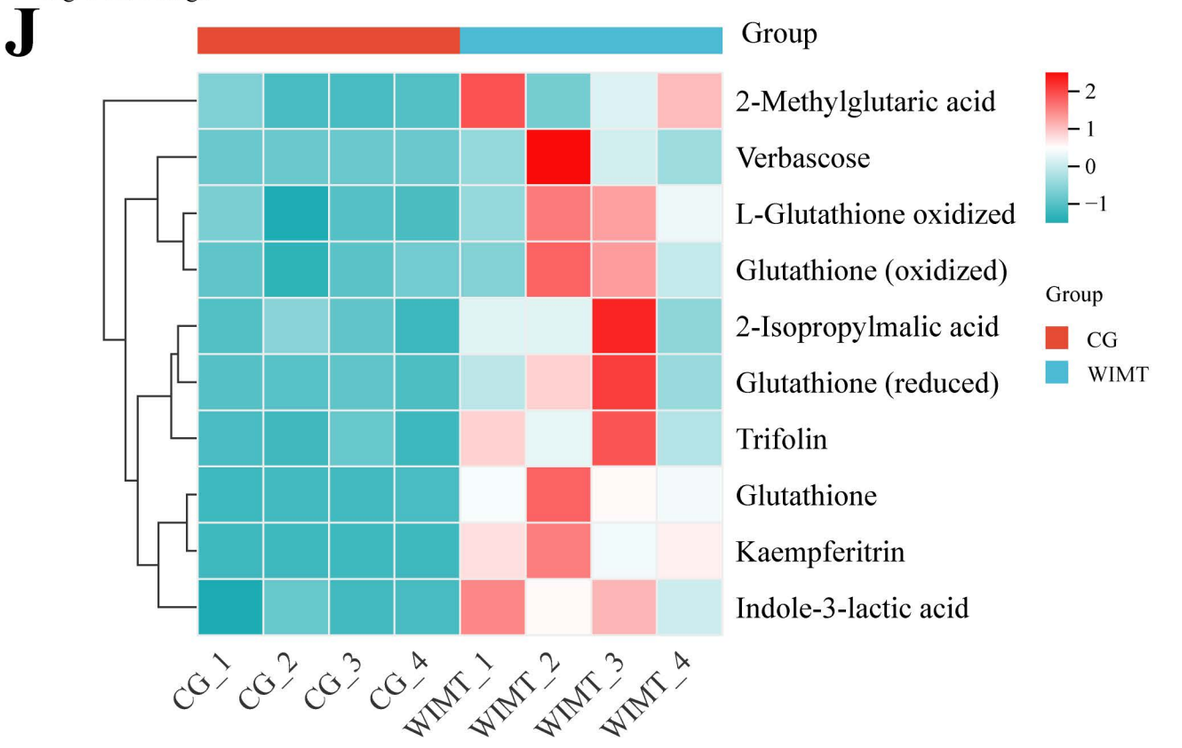
J
Group
2-Methylglutaric acid
Verbascose
L-Glutathione oxidized
Glutathione (oxidized)
2-Isopropylmalic acid
Glutathione (reduced)
Trifolin
Glutathione
Kaempferitrin
Indole-3-lactic acid
CG_1
CG_2
CG_3
CG_4
WIMT_1
WIMT_2
WIMT_3
WIMT_4

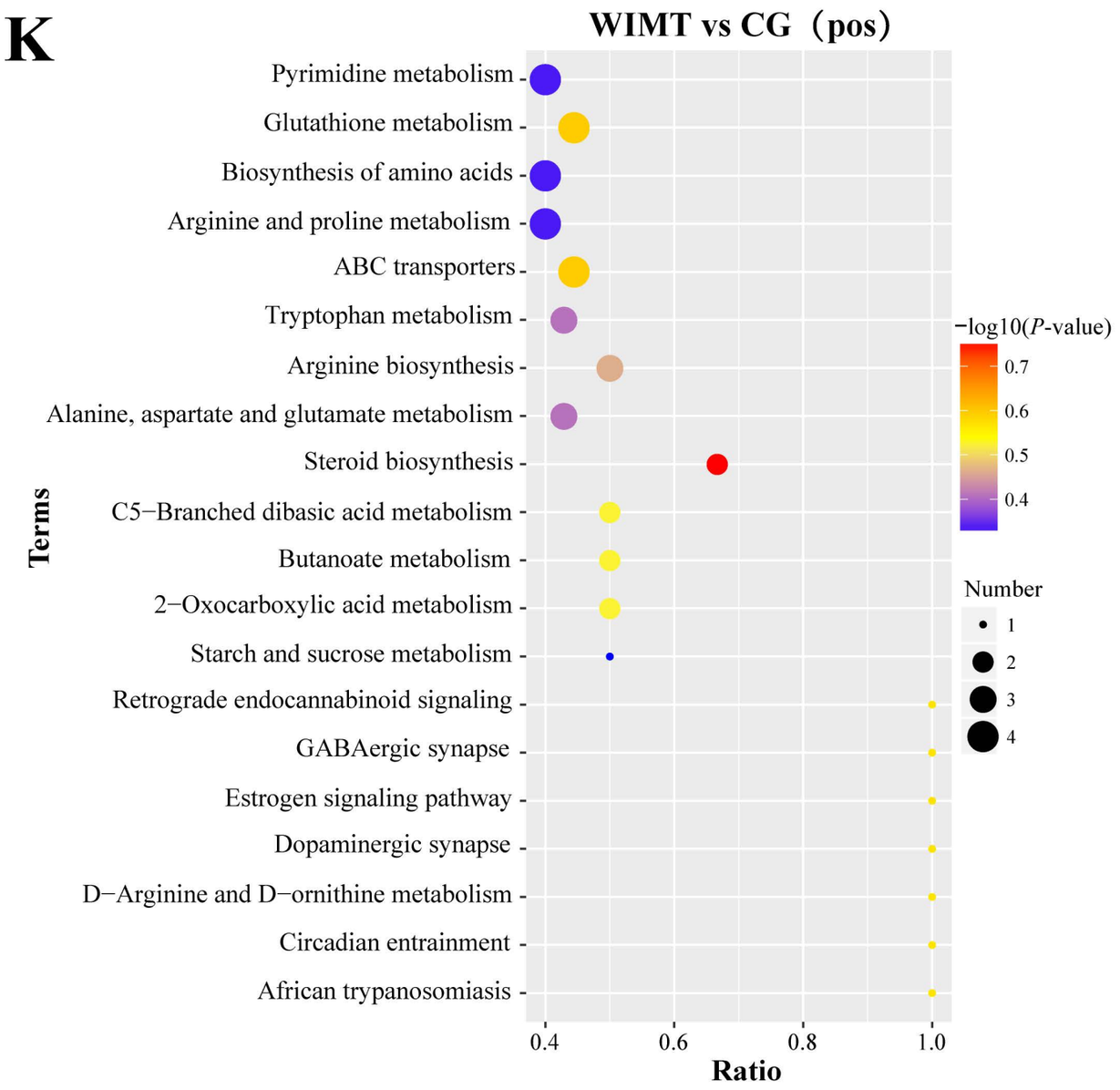
K
WIMT vs CG（pos）
Pyrimidine metabolism
Glutathione metabolism
Biosynthesis of amino acids
Arginine and proline metabolism
ABC transporters
Tryptophan metabolism
Arginine biosynthesis
Alanine, aspartate and glutamate metabolism
Steroid biosynthesis
C5−Branched dibasic acid metabolism
Butanoate metabolism
2−Oxocarboxylic acid metabolism
Starch and sucrose metabolism
Retrograde endocannabinoid signaling
GABAergic synapse
Estrogen signaling pathway
Dopaminergic synapse
D−Arginine and D−ornithine metabolism
Circadian entrainment
African trypanosomiasis
Terms
Ratio
−log10(P-value)
Number

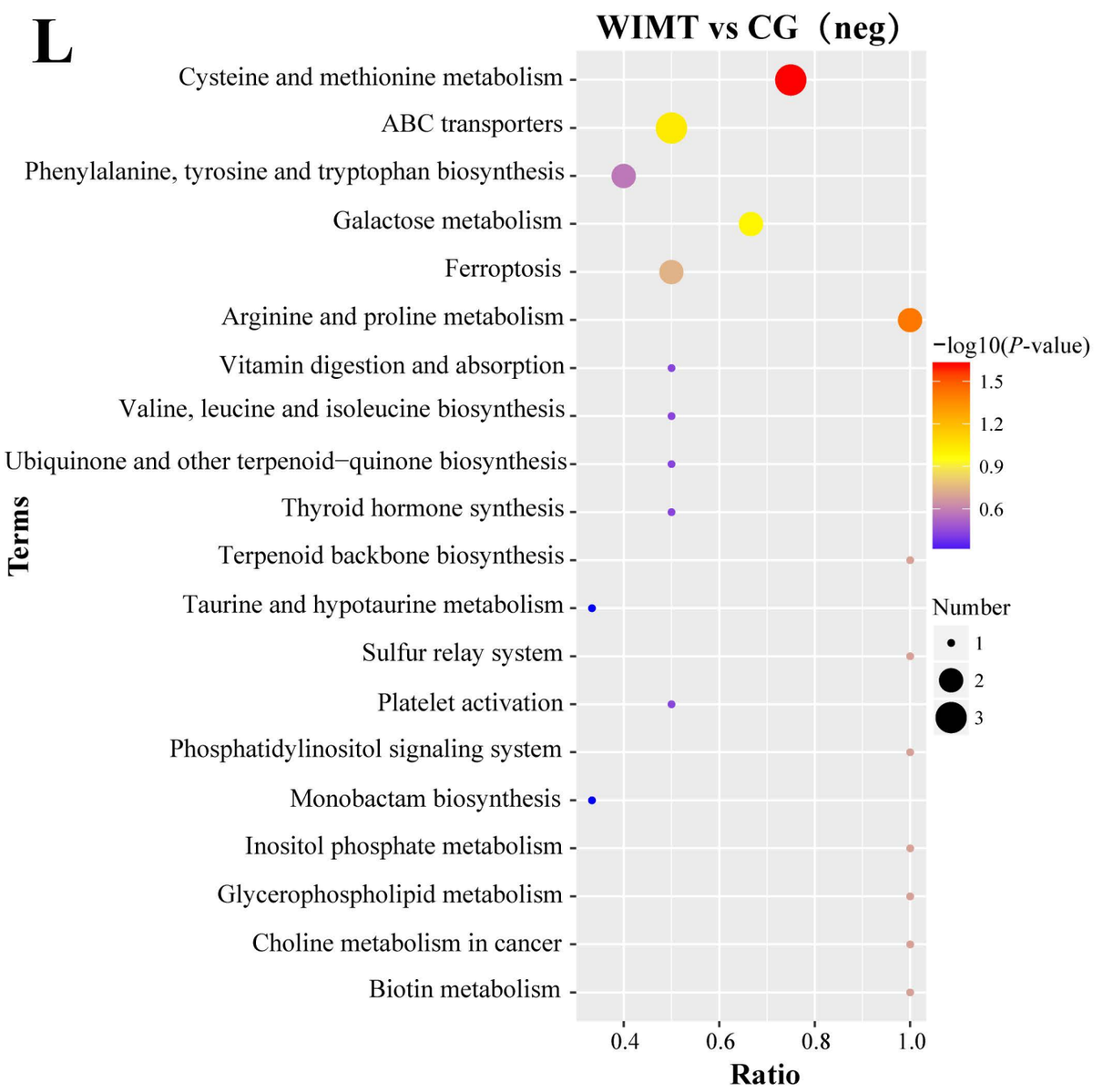
L
WIMT vs CG（neg）
Cysteine and methionine metabolism
ABC transporters
Phenylalanine, tyrosine and tryptophan biosynthesis
Galactose metabolism
Ferroptosis
Arginine and proline metabolism
Vitamin digestion and absorption
Valine, leucine and isoleucine biosynthesis
Ubiquinone and other terpenoid−quinone biosynthesis
Thyroid hormone synthesis
Terpenoid backbone biosynthesis
Taurine and hypotaurine metabolism
Sulfur relay system
Platelet activation
Phosphatidylinositol signaling system
Monobactam biosynthesis
Inositol phosphate metabolism
Glycerophospholipid metabolism
Choline metabolism in cancer
Biotin metabolism
Terms
Ratio
−log10(P-value)
Number

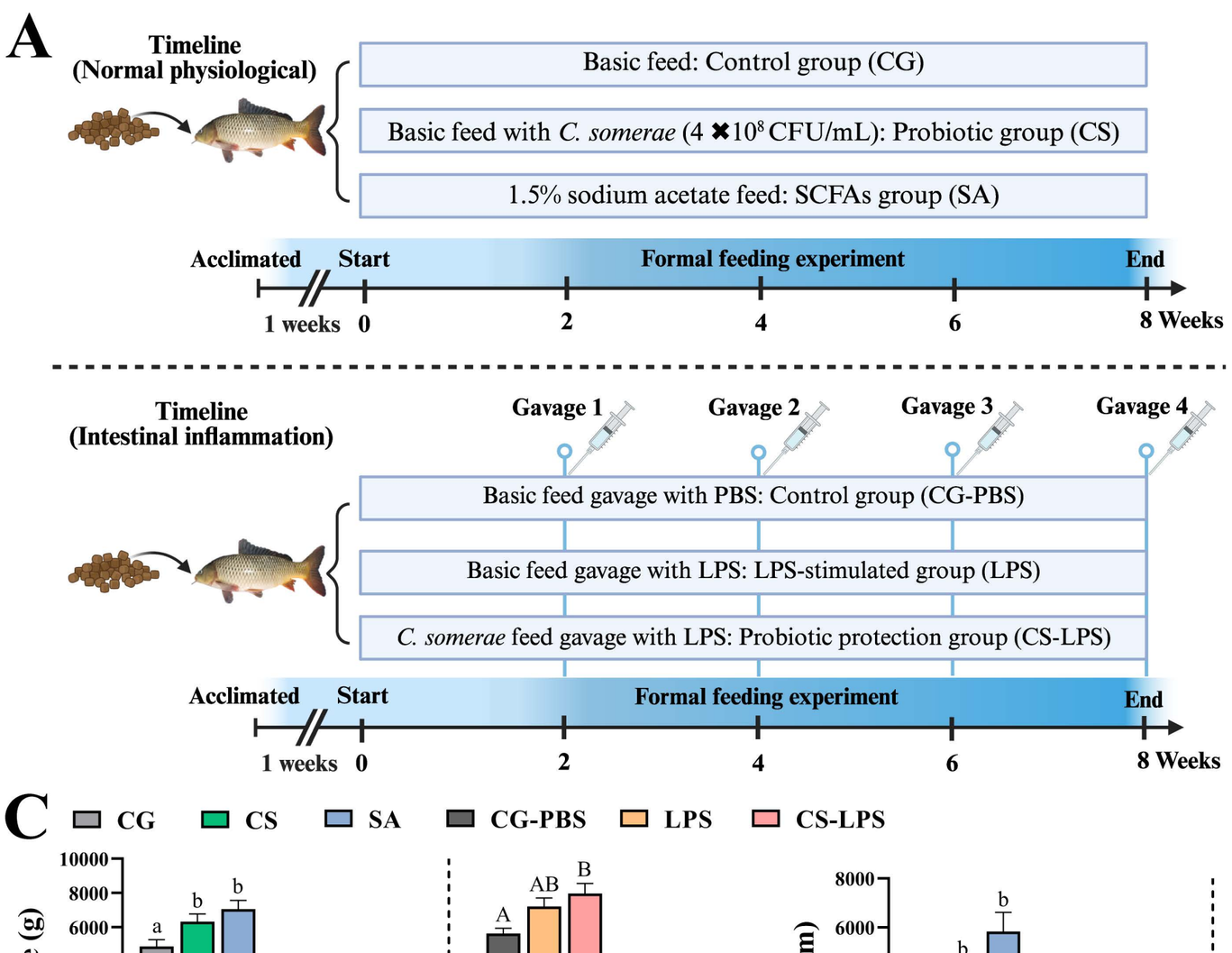
A
Timeline
(Normal physiological)
Basic feed: Control group (CG)
Basic feed with C. somerae (4 ✖10⁸ CFU/mL): Probiotic group (CS)
1.5% sodium acetate feed: SCFAs group (SA)
Acclimated
Start
Formal feeding experiment
End
1 weeks
0
2
4
6
8 Weeks
Timeline
(Intestinal inflammation)
Gavage 1
Gavage 2
Gavage 3
Gavage 4
Basic feed gavage with PBS: Control group (CG-PBS)
Basic feed gavage with LPS: LPS-stimulated group (LPS)
C. somerae feed gavage with LPS: Probiotic protection group (CS-LPS)
Acclimated
Start
Formal feeding experiment
End
1 weeks
0
2
4
6
8 Weeks

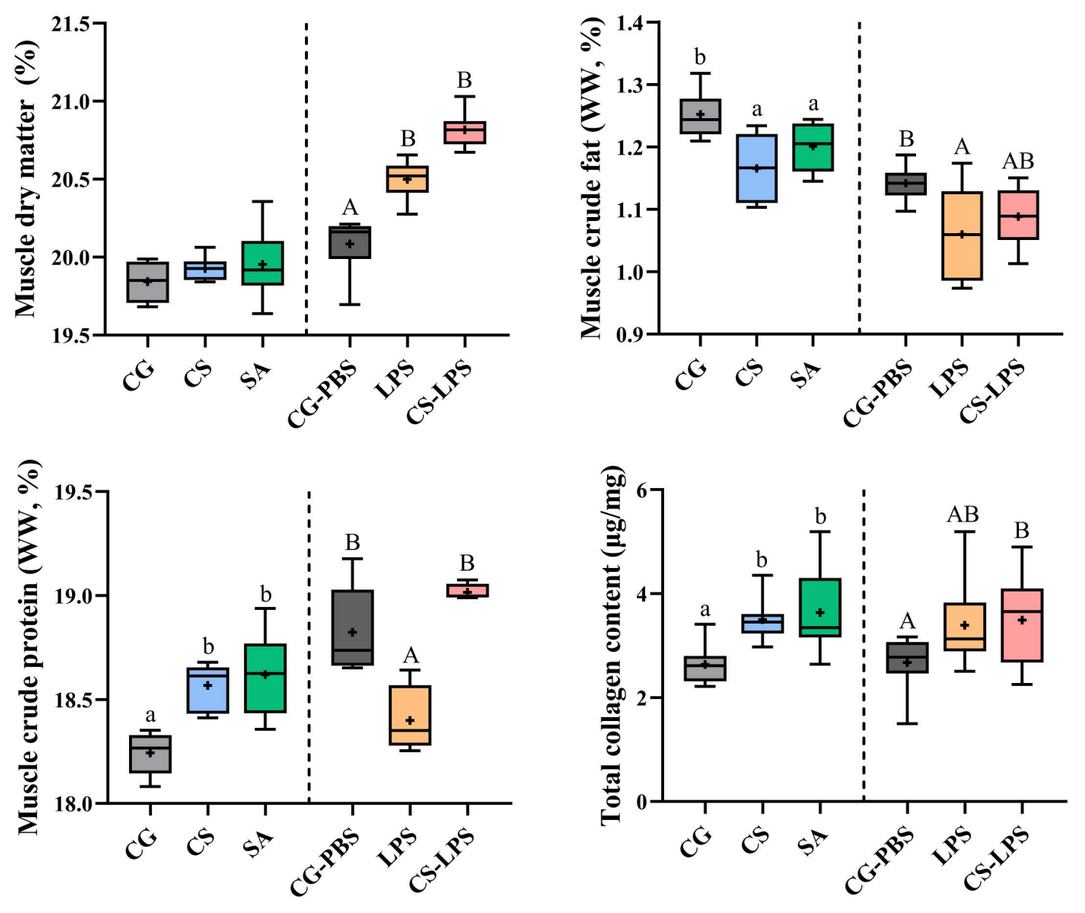
B
Muscle dry matter (%)
Muscle crude fat (WW, %)
Muscle crude protein (WW, %)
Total collagen content (μg/mg)
CG
CS
SA
CG-PBS
LPS
CS-LPS

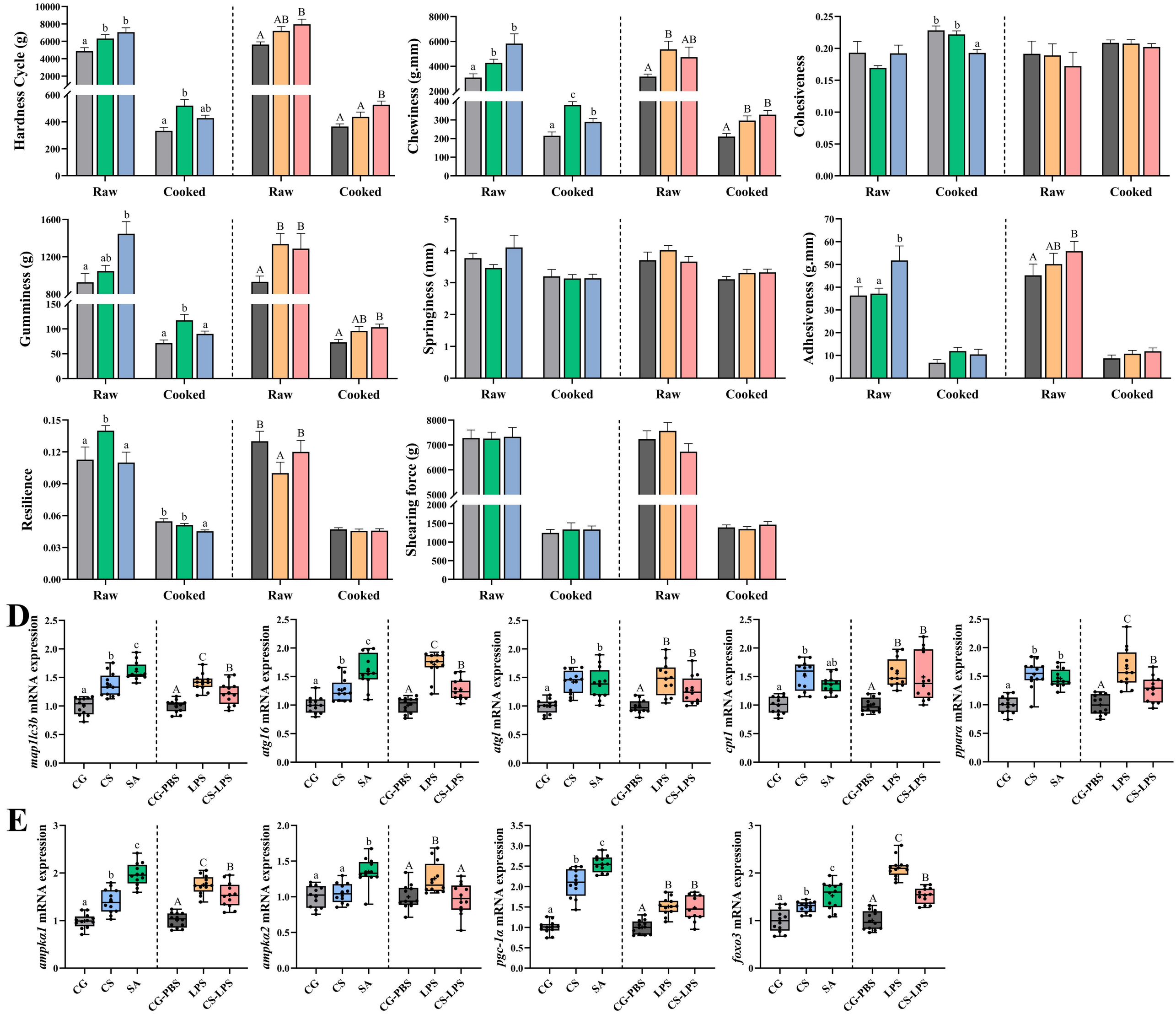
C
CG
CS
SA
CG-PBS
LPS
CS-LPS
Hardness Cycle (g)
Chewiness (g.mm)
Cohesiveness
Gumminess (g)
Springiness (mm)
Adhesiveness (g.mm)
Resilience
Shearing force (g)
Raw
Cooked

D
map1lc3b mRNA expression
atg16 mRNA expression
atgl mRNA expression
cpt1 mRNA expression
pparα mRNA expression
CG
CS
SA
CG-PBS
LPS
CS-LPS

E
ampkα1 mRNA expression
ampkα2 mRNA expression
pgc-1α mRNA expression
foxo3 mRNA expression
CG
CS
SA
CG-PBS
LPS
CS-LPS

(1) Establishment of a muscle quality difference model

Faba beans

Yellow River carp

Muscle

Gut microbiota

Muscle quality improved

- Texture properties ↑
- Small-diameter fibers ↑
- Collagen content ↑
- Crude fat ↓

Gut microbiota Modified

- *Cetobacterium* ↑
- *ZOR006* ↑
- *Aeromonas* ↑
- *Atopobium* ↑

Whole-intestinal bacterial suspension

WIMT

(2) Whole-intestinal microbiota transplantation (WIMT)

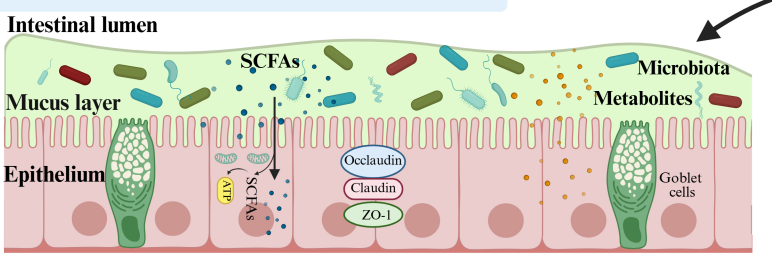

Normal intestinal morphology and structure

Microbiota: *Cetobacterium somerar* ↑

Metabolites:

SCFAs (**acetic acid**, propionic acid, butyric acid) ↑

Amino acids and derivatives ↑

Polyphenolic compounds ↑

Gut-muscle axis

AMPK-PGC-1α-FoxO signaling pathways

Muscle quality improved

- Texture properties ↑
- Small-diameter fibers ↑
- Collagen content ↑
- Crude fat ↓

(3) Functional validation

Cetobacterium somerar CFH_001

1.5% sodium acetate

4 ✖ 10^8 CFU/mL

LPS(1 mg/kg BW)

Normal physiological

Intestinal inflammation

Muscle quality improved

- Texture properties ↑
- Collagen content ↑
- Crude protein ↑
- Crude fat ↓
- AMPK-PGC-1α-FoxO ↑

(1) Establishment of a muscle quality difference model

Faba beans

Yellow River carp

Muscle

Gut microbiota

Muscle quality improved

- Texture properties ↑
- Small-diameter fibers ↑
- Collagen content ↑
- Crude fat ↓

Gut microbiota Modified

- *Cetobacterium* ↑
- *ZOR006* ↑
- *Aeromonas* ↑
- *Atopobium* ↑

Whole-intestinal bacterial suspension

WIMT

(2) Whole-intestinal microbiota transplantation (WIMT)

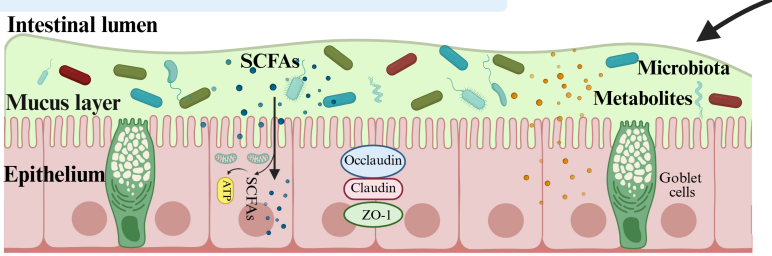

Normal intestinal morphology and structure

Microbiota: *Cetobacterium somerar* ↑

Metabolites:

SCFAs (**acetic acid**, propionic acid, butyric acid) ↑

Amino acids and derivatives ↑

Polyphenolic compounds ↑

Gut-muscle axis

AMPK-PGC-1α-FoxO signaling pathways

Muscle quality improved

- Texture properties ↑
- Small-diameter fibers ↑
- Collagen content ↑
- Crude fat ↓

(3) Functional validation

Cetobacterium somerar CFH_001

1.5% sodium acetate

4 ✖ 10^8 CFU/mL

LPS(1 mg/kg BW)

Normal physiological

Intestinal inflammation

Muscle quality improved

- Texture properties ↑
- Collagen content ↑
- Crude protein ↑
- Crude fat ↓
- AMPK-PGC-1α-FoxO ↑